Winter 12-2001

Fluorescence and Light Scattering Studies of Aromatic Polymers Near the Critical Concentration C*

M.Sean Healy
Seton Hall University

FLUORESCENCE AND LIGHT SCATTERING STUDIES OF AROMATIC POLYMERS NEAR THE CRITICAL CONCENTRATION C*

Thesis by

M. Sean Healy

In Partial Fulfillment of the Requirements

for the Degree of

Doctor of Philosophy

Seton Hall University

South Orange, New Jersey

2001

(Submitted December 14, 2001)

We certify that we have read this thesis and that in our opinion is adequate in scientific scope and quality as a dissertation for the degree of Doctor of Philosophy.

Approved

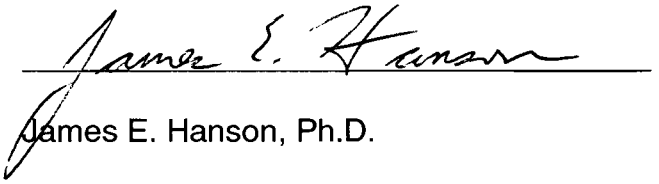

James E. Hanson, Ph.D.

Research Mentor

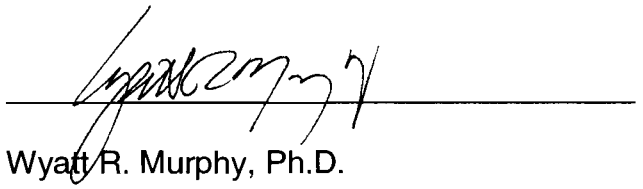

Wyatt R. Murphy, Ph.D.

Member of Dissertation Committee

Yuri Kazakevich, Ph.D.

Member of the Dissertation Committee

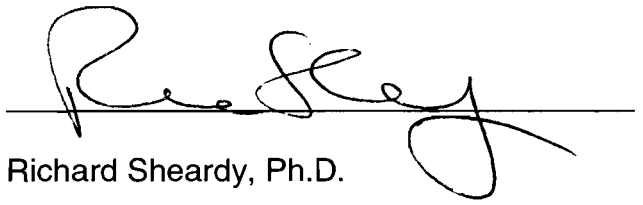

Richard Sheardy, Ph.D.

Chairperson, Department of Chemistry and Biochemistry

Acknowledgements

The author wishes to thank Dr. Hanson for his patience, understanding nature, and guidance as a mentor. I would also like to thank Dr. Murphy for the in-depth conversations pertaining to fluorescence and light scattering studies and his extensive availability for questions. I am very grateful to the members of my matriculation committee, Dr. Kazakevich, Dr. Sowa, and Dr. Sheardy, for the time and effort they expended helping me complete the Ph.D. requirements. I am also grateful to the members of the Hanson/Murphy research group for their friendship, help, and the ability to make the process bearable. I would also like to thank my family for their unending support over the many years it took to attain this goal. Last but not least, I would like to thank my wife, Marissa, for being so patient and understanding with the long hours required to complete this dissertation and supporting me through the nine-month residency.

Abstract

The phase diagram of polymer solutions has been of interest for many years. The boundary between the dilute and semi-dilute concentration regions is known as the critical concentration (c*) and is theoretically defined as the concentration where polymer-polymer interactions begin to occur. The critical concentration has historically been determined using scattering techniques, osmometry, and viscosity measurements. However, there are several disadvantages to each of these techniques. This phase boundary is related to the polymer radius, increasing the utility of determinations of c*.

The intent of this project was to develop a method of determining c* using common laboratory equipment that allows easier sample preparation than the currently accepted methods. These c* values were compared to results obtained using accepted methods. The critical concentration was determined from fluorescence excitation spectroscopy of four narrow molecular weight distribution samples of polystyrene (M_W = 225,000 D – 1,500,000 D) in decahydronapthalene and three broad molecular weight distribution samples of poly(bisphenol A) carbonate in dichloromethane. The polystyrene samples were studied at both 20°C and 30°C while the poly(bisphenol A) carbonate samples were studied at 25°C. A discontinuity in the plot of the corrected intensity of a dimer complex band in the excitation spectra vs. concentration allowed determination of the critical concentration.

To compare these results to an accepted method, light scattering studies were performed on both the polystyrene and polycarbonate samples. The light scattering data was fit to a Zimm plot using a Zimm treatment for the polystyrene samples and a Debye treatment for the polycarbonate samples to determine the radius of gyration (R_g) for each sample. The c* values were then calculated from R_g. The fluorescence excitation c* values were found to be in good agreement with the light scattering c* values for the polystyrene samples. However, due to the high polydispersity of the polycarbonate samples, neither the fluorescence excitation method nor the light scattering method was able determine c*.

The fluorescence excitation c* values were also compared to Mark-Houwink calculated c* values. The Mark-Houwink constants used for these calculations were obtained from literature. The fluorescence excitation c* values were also in good agreement with the Mark-Houwink calculated c* values for the polystyrene samples.

The results of these studies show that fluorescence excitation spectroscopy appears to be a convenient method for determining c* for polystyrene. It may also be possible to use this method to determine c* for polymers other than polystyrene if the polymer contains fluorophores and has a low polydispersity.

Table of Contents

List of Figures

Chapter 1.

Chapter 3.

Figure 12. Fluorescence emission spectra for several concentrations of polystyrene (M_w = 223,200 D) in decalin at 20°C with the excitation monochromator set to 250 nm. The band at 283 nm is due to monomer emission while the band at 332 nm is due to excimer emission.

Figure 13. Fluorescence excitation spectra for several concentrations of polystyrene (M_w = 223,200 D) in decalin at 20°C with the emission monochromator set to 332 nm. The band at 291 nm is due to dimmer complex excitation.

Figure 14. A plot of the uncorrected dimer complex intensity (I_{291}) vs. concentration for polystyrene (M_w = 223,200 D) in decalin at 20°C. The uncorrected dimer complex intensity increases with concentration but shows no change above the Mark-Houwink calculated c* value of 27.5 g/L. Measurement error is ± 9E+3 CPS.

Figure 15. Fluorescence emission spectra for several concentrations of polystyrene (M_w = 223,200 D) in decalin at 30°C with the excitation monochromator set to 250 nm. The band at 283 nm is due to monomer emission while the band at 332 nm is due to excimer emission.

Figure 16. Fluorescence excitation spectra for several concentrations of polystyrene (M_w = 223,200 D) in decalin at 30°C with the emission monochromator set to 332 nm. The band at 291 nm is due to dimer complex excitation.

Figure 17. A plot of the uncorrected dimer complex intensity (I_{291}) vs. concentration for polystyrene (M_w = 223,200 D) in decalin at 30°C. The uncorrected dimer complex intensity increases with concentration but shows no change above c*. Measurement error is ± 9E+3 CPS.

Figure 18. A plot of the corrected dimer complex intensity vs. concentration for polystyrene (M_w = 223,200 D) in decalin at 20°C and 30°C. c* is apparent between 30 and 35 g/L at 20°C and between 20 and 25 g/L at 30°C. Lines connecting points are for ease of interpretation only.

List of Tables

List of Schemes

Chapter 1

Introduction

A. Background

Polymers have become a mainstay in modern life from the tires on cars to life-saving synthetic heart valves. The advances in polymer chemistry which have made these developments possible arise from the increasing knowledge and understanding of polymers and their interactions in solution and the solid state.[1] Over the years, many studies of the properties of polymers have been performed. These studies have provided insight into the nature of polymers and have led to the development of new classes of polymers with unique properties.[2]

The study of polymer solution chemistry is one area that has aided in the understanding of polymers.[1,3,4] Solvent-polymer interactions, as well as intermolecular and intramolecular polymer-polymer interactions, are important for determining how polymers will perform under certain conditions such as in biological systems.[5] Also, these interactions will alert the polymer chemist to the potential for certain phenomena to occur such as weakening of a polymer by swelling or fracture.[1]

B. Polymers

Synthetic polymers are typically not a single molecular weight but contain a distribution of molecular weights. There are four common methods for calculating the average molecular weight; the number-average molecular weight, M_n; the weight-average molecular weight, M_w; the z-average molecular weight, M_z; and the viscosity-average molecular weight, M_η.[1]

When the contribution of each molecular weight is weighted according to the mole fraction within the polymer sample, the average is known as the number-average molecular weight and is defined by

$$M_n = \frac{\sum N_\sigma M_\sigma}{\sum N_\sigma} \tag{1.1}$$

where σ is the degree of polymerization, N_σ is the number of molecules in the sample with the degree of polymerization σ, and M_σ is the molecular weight of a chain with a degree of polymerization σ.[1]

If the contribution of each molecular weight is weighted according to the weight fraction, the average is known as the weight-average molecular weight and is defined as[1]

$$M_w = \frac{\sum N_\sigma M_\sigma^2}{\sum N_\sigma M_\sigma} \tag{1.2}$$

If another M_σ term is included in both the numerator and denominator of the expression for M_w, the result is the z-average molecular weight which is defined as[1]

$$M_z = \frac{\sum N_\sigma M_\sigma^3}{\sum N_\sigma M_\sigma^2} \tag{1.3}$$

When the values for M_n, M_w, and M_z are compared, they give information about how broad the distribution of molecular weights are for the polymer sample. In a polydisperse sample these averages follow the order of $M_n \leq M_w \leq M_z$ while for a monodisperse sample these averages are equal.[1]

Finally, the last way of averaging the molecular weight is the viscosity-average molecular weight which is related to the intrinsic viscosity and is defined as

$$M_v = \left[\frac{\sum N_\sigma M_\sigma^{a+1}}{\sum N_\sigma M_\sigma}\right]^{1/a} \tag{1.4}$$

where *a* is a constant for a particular polymer-solvent system at a particular temperature.[1] The summations in equations (1.1), (1.2), (1.3), and (1.4) are taken over all values of the degree of polymerization from $\sigma = 1$ to $\sigma = \infty$.

The distribution of molecular weights, known as the polydispersity, is defined as the ratio of the weight average molecular weight to the number average molecular weight (M_w/M_n).[1] If the molecular weights are all equal, the polydispersity is one and is the sample is termed monodisperse. Figure 1[3] is a

histogram (showing a Guassian distribution centered around the average) of the number (or mole fraction) of molecules with different molecular weights. The greater the polydispersity, the greater the width of the distribution curve while a polydispersity of one would yield a straight vertical line. Because polymer samples are composed of a distribution of molecular weights, they require more complex statistical treatments.[3]

Molecular weight can be determined by either absolute or relative measurements. Absolute measurements are based solely on theoretical considerations while relative methods must be calibrated using an absolute measurement.[1] Examples of relative methods include gel permeation chromatography (GPC) and intrinsic viscosity.[1] Absolute measurements for number-average molecular weight include osmometry and end-group analysis.[1] Absolute weight-average molecular weight and the z-average radius of gyration (R_g) can be obtained by light scattering, small angle neutron scattering studies (SANS), or x-ray scattering studies.[1] The radius of gyration is the root mean squared distance of all the polymer chains from the center of mass.[2]

C. Scattering Studies

Scattering studies, whether light, neutron, or x-ray scattering, all follow the same basic principles. Incident radiation is reflected when the object is larger

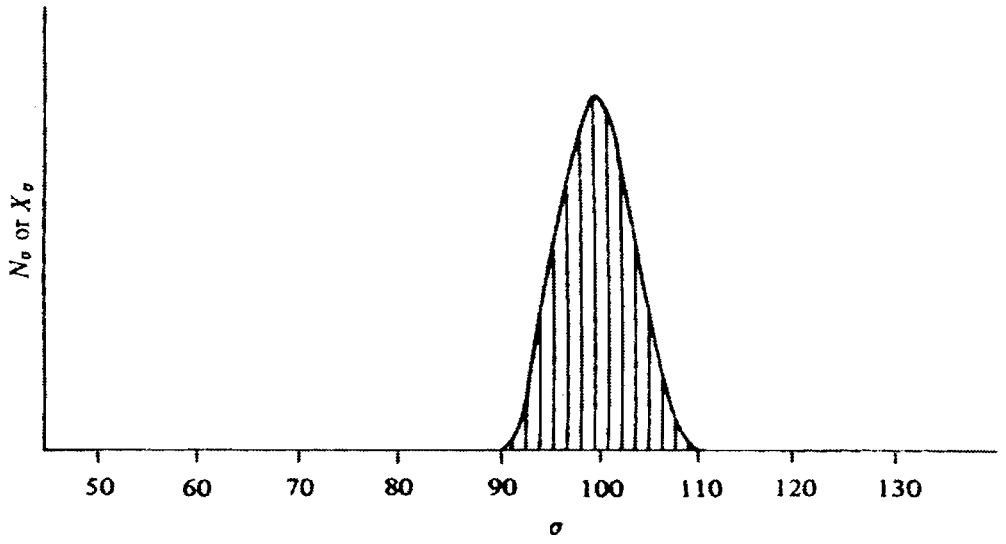

Figure 1. Molecular weight distribution. This histogram shows the number of molecules, N_a, (or their mole fractions, X_a) vs. the degrees of polymerization, σ.[3]

than the wavelength of the radiation but when the object is close to the size of the wavelength of the radiation, the radiation is scattered. This scattering has maximum intensity at certain angles depending on the size and shape of the object. At other angles the light waves cancel due to total destructive interference from the scattered radiation from the various parts of the object (see figure 2).[6] The intensity of the scattered light at various angles is characteristic of the size of the polymer. Therefore, observing the scattered light at various angles allows determination of the size of the object.[1]

If several concentrations are studied using light scattering techniques, the

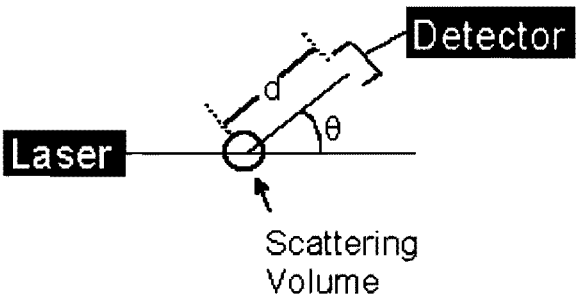

Figure 2. Schematic of the scattering phenomenon.[6] Laser light interacts with the scattering volume and is scattered at all angles. Detectors located at various angles observe the scattered light.

data can be plotted using a treatment known as a Zimm plot.[7,8] Other treatments such as the Debye[9] and Berry plots have also been developed which are similar to the Zimm plot and may offer a better fit to certain types of data. A great deal of information can be gathered from these plots including the weight-average molecular weight and the z-average radius of gyration. Figure 3 is an example of a typical Zimm plot.[10] The Zimm plot is a double extrapolation plot. Several different concentrations can be plotted on the Zimm plot and these concentrations are then extrapolated to a c = 0 line (where c is the concentration). The data gathered from the detectors located at several angles can also be plotted on the Zimm plot and the angle data can be extrapolated to a $\Theta = 0$ line (where Θ is the angle of the detector).

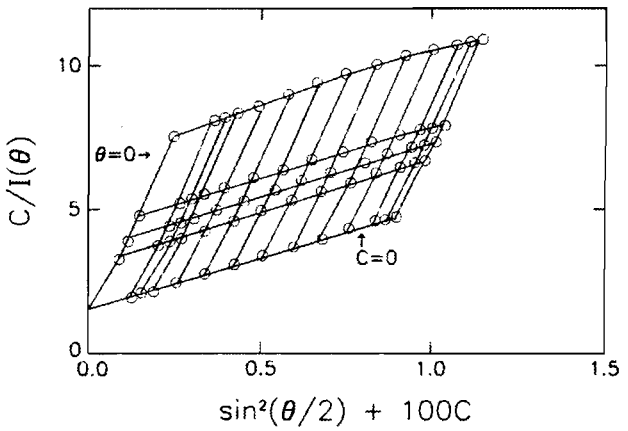

Figure 3. An example of the Zimm plot for a polyelectrolyte solution with an excess of added salt: sodium poly(styrenesulfonate) (M_w = 155,000 D).[10]

Using Zimm's formalism, the excess scattered light is related to the concentration and weight average molecular weight by

$$\frac{K^* c}{R(\Theta)} = \frac{1}{M_w P(\Theta)} + 2A_2 c \qquad (1.5)$$

where $R(\Theta)$ is the excess intensity of scattered light at angle Θ, c is the sample concentration, M_w is the weight-average molecular weight, A_2 is a second virial coefficient, K^* is an optical parameter equal to $4\pi^2 n^2 (dn/dc)^2 / (\lambda_o^4 N_A)$, n is the solvent refractive index, dn/dc is the refractive index increment, N_A is Avogadro's number, and λ_o is the wavelength of the scattered light in a vacuum.[6] Expansion of $1/ P(\Theta)$ to the first order gives

$$1/ P(\Theta) = 1 + (16\pi_2/3\lambda^2) \langle R_g^2 \rangle . \sin^2(\Theta/2) + f_4 \sin^4(\Theta/2) + \ldots \qquad (1.6)$$

where R_g is the z-average radius of gyration and f is a constant.[6]

When using a Zimm fit of the light scattering data, a plot of $K^*c/R(\Theta)$ vs. $\sin^2(\Theta/2)$ yields Mw from the intercept of the $\Theta = 0$ and $c = 0$ lines.[6] The radius of gyration can be obtained form the slope of the $\Theta = 0$ line.[6] When using a Debye fit of the light scattering data, a plot of $R(\Theta)/K^*c$ vs. $\sin^2(\Theta/2)$ yields Mw from the intercept of the $\Theta = 0$ and $c = 0$ lines.[6] The radius of gyration can be obtained form the slope of the $\Theta = 0$ line.[6]

The Flory temperature[11,12] or θ-temperature is the temperature where the polymer-polymer and polymer-solvent interactions are equal, in other words the polymer is considered to be unperturbed in solution.[1,13] At the Flory temperature, the solvent is considered to be a Flory solvent for a particular polymer/solvent system. [1,13] At temperatures above the Flory temperature, the polymer-solvent interactions are greater than the polymer-polymer interactions which causes the polymer to expand in solution.[1,13] Above the Flory temperature, the solvent is considered to behave like a "good" solvent for a particular polymer/solvent system. [1,13]

Large, non-rigid polymers, such as polystyrene, have been shown through light scattering techniques to adopt a random coil configuration when in solution.[11, 14] For most theoretical treatments, these random coils are assumed to be a solid sphere with a radius equal to the radius of gyration.[1]

D. Polymer Solution Phases

The behavior of a given polymer solution depends on temperature and concentration. Three different temperature and concentration regimes are considered polymer solution phases and can be represented in a phase diagram. Above the θ-temperature, polymer solutions are generally divided into three distinct regions[1,4,15] as shown in the phase diagram in Figure 4[16] and schematically in Figure 5.[17,18] The first region (Region I) is that of dilute solutions ($c<c^*$) and is defined by no intermolecular interactions between the polymers. The line separating Region I and Region II is known as the critical concentration, c^*, and is defined as the point where the polymer chains begin to have intermolecular interactions ($c=c^*$). The second region (Region II) is that of semi-dilute solutions ($c>c^*$) where the polymers are forced close enough to have intermolecular interactions. The third region (Region III) is that of concentrated solutions and is separated from Region II by a boundary designated c^{**}.[1]

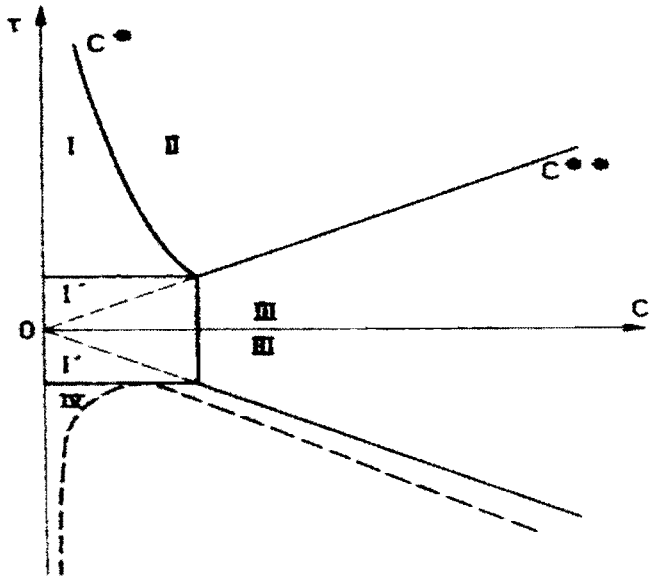

Figure 4. Phase diagram for a typical polymer solution. The quantity τ represents the reduced temperature, $(T - \theta) / \theta$, where θ is the Flory θ-temperature.[16]

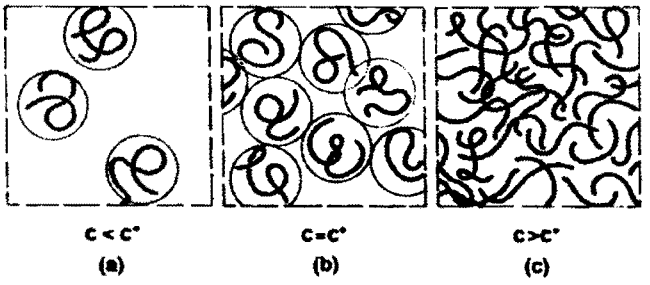

Figure 5. Relationship of polymer chains in solution at different concentrations and solvents.[17,18] (a) The dilute region is characterized by no polymer-polymer interactions. (b) The critical concentration is the concentration when the polymers begin to have interactions. (c) The semi-dilute concentration is characterized by polymer-polymer interactions.

Historically, techniques such as scattering experiments (light, x-ray, neutron) and osmometry have been used to measure the radius of gyration (R_g) and c*, respectively.[1] Osmometry can be used to determine c* directly by noting the upward curve in the plot of (π/c) vs. c where π is the osmotic pressure and c is the concentration (see Figure 6).[1] Light scattering can be used to determine the radius of gyration of the polymer. The radius of gyration is related to c* by

$$c^* = \frac{M}{(4/3)\pi R_g^3 N_A} \tag{1.7}$$

where M is the weight-average molecular weight and N_A is Avogadro's number.[19] Higher temperatures cause the radius of gyration of a polymer to increase due to increased polymer-solvent interactions.[1,2] As the radius of gyration increases, there is more crowding within the solution and hence c* occurs at a lower concentration.

Several difficulties are inherent with these types of studies. First, both osmometry and scattering techniques require rigorous dust-free conditions to give accurate results. Samples must be filtered through 0.02 to 0.2 μm filters to remove dust or any other contaminants, which can prove difficult for higher molecular weight and higher concentration samples. All glassware must be

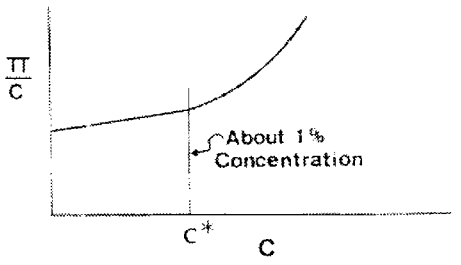

Figure 6. Schematic illustration of the dependence of osmotic pressure on concentration.[1]

clean and dust free so as not to introduce dust back into the filtered samples. Second, scattering instruments and osmometers are expensive instruments that are not common to most laboratories. Therefore, most research groups are not able to determine c* or R_g. Third, osmometers typically require 24 hours to reach equilibrium which means it takes several days to acquire data from just a few samples.[1] Therefore, it would be beneficial to find a more convenient method to measure c* and R_g with less sample preparation, shorter operational time, and using more common instrumentation.

E. Fluorescence

When a molecule absorbs energy, it is promoted from the ground state to an excited state. This excitation energy can come from a variety of sources such as an electrical discharge, ionizing radiation, thermal activation or the result of a

chemical reaction.[20] However, for spectroscopic purposes the most common excitation method is the absorption of light. Because the excited molecule is not stable, it can remain in an excited state for only a short time ($<10^{-7}$s for most organic molecules in solution)[20] and it must return to the ground state by emitting energy. Figure 7[20] shows the several decay paths available to excited state molecules.

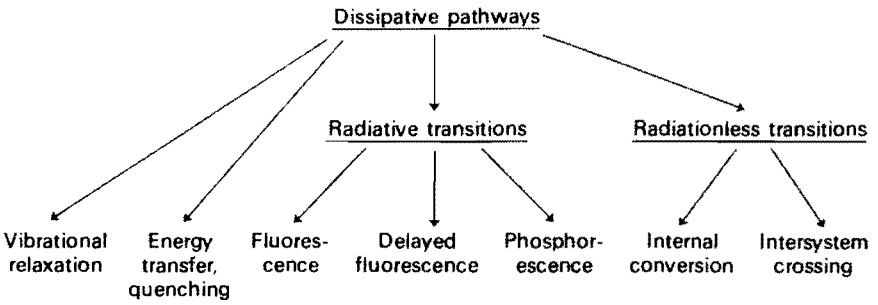

Figure 7. Physical pathways for the dissipation of electronic energy.[20]

Fluorescence is one possible radiative pathway for an excited molecule. Figure 8[20] shows that when a molecule absorbs a photon, it causes the molecule to go from the ground state (S_o) to an excited state (S_n where $n \geq 1$). If the absorption causes the molecule to go to a state above S_1, then the molecule will typically undergo rapid vibrational relaxation to reach S_1. From the S_1 state, the molecule can follow one of several different pathways. It can undergo internal conversion to the higher vibrational bands of S_o which will result in vibrational

relaxation to the ground state. Intersystem crossing to the triplet state is possible which can yield phosphorescence or decay non-radiatively. It can also emit a photon to lose energy and reach the ground state, which is known as fluorescence. However, phosphorescence is rare in compounds with atoms of the second period.[21]

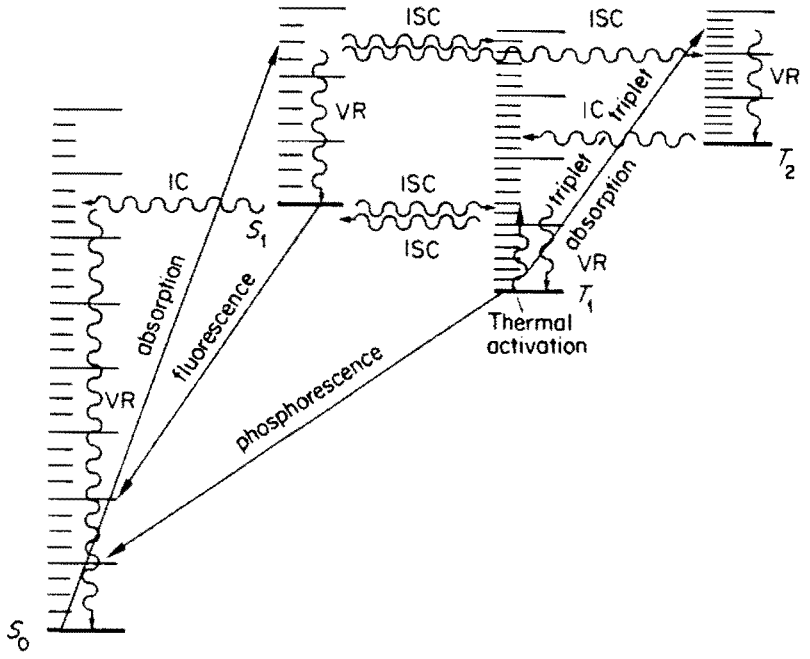

Figure 8. A Jablonski diagram showing some of the radiative and non-radiative pathways available to molecules. (VR = vibrational relaxation, IC = internal conversion, ISC = intersystem crossing).[20]

Fluorescence spectroscopy is a versatile tool that is capable of excellent sensitivity. Fluorimeters are also fairly common instruments that are accessible

to most research groups. These two facts make fluorescence spectroscopy a desirable method for the study of molecules which contain fluorophores.

As shown in Figure 9,[20] it is interesting to note that typically the fluorescence excitation spectrum of dilute solutions is similar in appearance to the corresponding absorbance spectrum. When the excitation light is scanned using fluorescence spectroscopy, the molecules absorb at the characteristic wavelengths for that particular molecule as in absorbance spectroscopy. One pathway for these molecules (if they contain chromophores) to return to the ground state is by the emission of light. Therefore, for each absorbance band there must be a corresponding fluorescence excitation band which results in a fluorescence spectrum that is similar in appearance to the absorbance spectrum.[20]

The main advantage of fluorescence spectroscopy over absorbance spectroscopy is enhanced sensitivity. This enhanced sensitivity results from the direct observation, amplification, and measuring of fluorescence while absorption spectroscopy relies on the difference between the incident and transmitted light intensities.[20] In addition, when the fluorescence is measured from the front face of the cell, the self-absorbance effects of concentrated solutions are minimized thereby allowing the spectra of highly concentrated solutions to be measured.

The intensity of fluoresced light is proportional to the intensity of exciting light.[22] The optical density (OD) is defined as $OD = I_o/I$ where I_o is the intensity of the light incident on the cuvette and I is the intensity of the light at the center of the cuvette.[22] Solutions that are considered optically dilute have low optical

densities while solutions that are optically concentrated have high optical densities. When measuring the fluorescence of optically concentrated solutions, the apparent fluorescence yield is typically less than that observed for an infinitely dilute solution. This phenomenon is known as an inner filter effect.[22] Inner filter effects can cause a decrease in the intensity of the excitation light at the point of observation, especially if the fluoresced light is observed at 90° or 180° from the incident light. It can also cause a direct decrease in the intensity of the fluoresced light. Both of these decreases in intensity cause a decrease in the apparent fluorescence yield. By measuring fluorescence from the front-face of the cuvette, these inner filter effects can be minimized.[23]

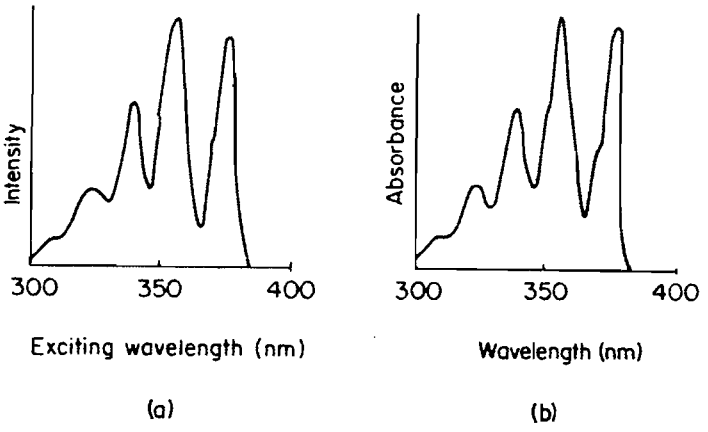

Figure 9. (a) Corrected fluorescence excitation spectrum, and (b) absorption spectrum, of anthracene.[20]

Excimers are formed by the interaction of a ground state species with an excited state species[24] as shown in Scheme 1.[20] If the ground state and the

excited state species are different, the complex is known as an exciplex. Aromatic molecules, such as those containing benzene rings, are known to form excimers[1,25-31] when the benzene rings are arranged in a stacked conformation and are 3.0 to 3.7 Å apart.[29,32] Exciton resonance as well as charge-transfer resonance contribute to the formation of excimers as shown in Scheme 2.[20] If the chromophores have interactions in the ground state and are excited together, as a single entity, this species is known as an exciton.[20] When the transfer of an electron occurs between excited state species, it is known as a charge-transfer complex.[20]

$$\mathrm{M} + h\nu \underset{\text{monomer fluorescence}}{\longleftrightarrow} {}^1\mathrm{M}^* \overset{\mathrm{M}}{\rightleftarrows} \underset{\text{excimer}}{{}^1(\mathrm{MM})^*} \xrightarrow[\text{fluorescence}]{\text{excimer}} \mathrm{M} + \mathrm{M} + h\nu'$$

Scheme 1. Scheme showing formation and emission of excimers.[20]

$$\psi_{\text{excimer}} = a\psi_{\mathrm{MM}^*} + b\psi_{\mathrm{M}^*\mathrm{M}} + c\psi_{\mathrm{M}^-\mathrm{M}^+} + d\psi_{\mathrm{M}^+\mathrm{M}^-}$$

Scheme 2. The excimer wavefunction is combination of exciton resonance [$MM^* \leftrightarrow M^*M$] as well as charge-transfer resonance [$M^-M^+ \leftrightarrow M^+M^-$].[20]

It is clear from the energy diagram in Figure 10[33] that the energy of the excimer is lower relative to the total energy of the excited species plus the ground state species. This energy difference is manifested in fluorescence

emission spectroscopy with the excimer band being structureless and at a lower energy than the individual, unassociated components. Excimers are known to form through both intermolecular and intramolecular interactions of molecules. [1,25-31]

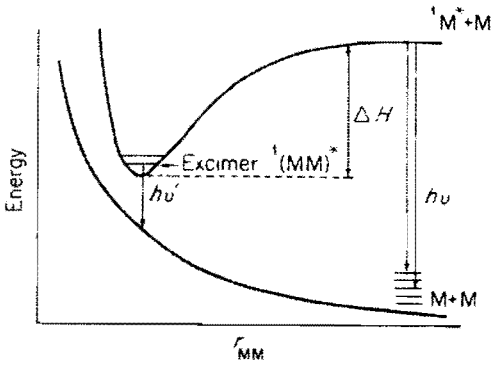

Figure 10. Schematic energy surfaces showing excimer formation and emission. The emission to the ground state is structureless.[33]

F. Previous Work

Several exhaustive literature and internet searches were performed. Previous work in this area of research is limited and most papers were at least 10 years old. One possible reason for this may be because fluorescence emission spectroscopy was found not to be able to determine c* for polymer solutions.[28] It is also possible that papers studying the critical concentration have not been published recently because the accepted methods of determining c* use equipment not common to most laboratories and the sample preparation is difficult and time consuming. A more convenient method may increase

researcher's interest in studying c* and allow more research groups to determine R_g.

One of the first polymers to be studied using fluorescence was polystyrene.[25] Vala et al.[26] conducted studies of polystyrene, ethylbenzene, and several bibenzyl compounds. Their results resembled Figure 11[28] and they attributed the polystyrene fluorescence peak at 280 nm was due to monomer emission while the peak at 335 nm was attributed to excimer emission. These findings were the basis of several studies that followed.

In the same paper, Vala et al.[26] also studied absorption spectroscopy of paracyclophanes under dilute concentrations. Paracyclophanes are interesting molecules because they are able to form ground state dimer complexes that are reinforced through covalent bonding. In other words, the benzene rings of these compounds are held, through covalent bonding, in an orientation where they are close enough to interact in the ground state. The authors observed a shift in the absorbance spectra between 280 nm and 320 nm which they attributed to these dimer complexes.

Hirayama[27] studied intramolecular excimer fluorescence of several diphenyl and triphenyl alkanes as well as toluene, ethylbenzene and several substituted toluene derivatives. These studies were conducted in dilute solutions to minimize intermolecular interactions thereby ensuring the excimers observed are only intramolecular interactions. No excimer formation was observed for the benzene derivatives. For the diphenyl and triphenyl alkanes, varying the carbon chains between the chromophores altered the ability to form excimers. They

concluded that these intramolecular excimers can form only if the chromophores are separated by three carbons which they named the "n = 3 rule". The "n = 3 rule" was also found to apply to naphthalene, adenine, and carbazole substituents.[30,31]

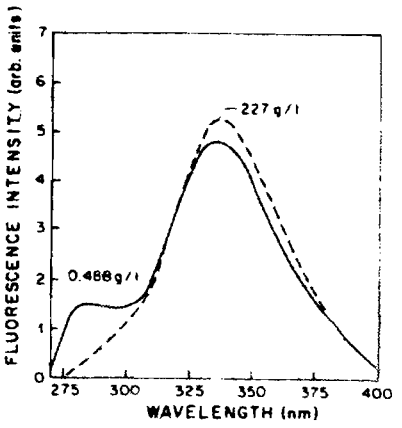

Figure 11. Fluorescence excitation spectra of polystyrene (M_w = 100,000 D) in 1,2-dichloroethane.[28] The monomer peak is at 283 nm and the excimer peak is at 335 nm.[26-32,34-36]

In another study, Torkelson et al.[28] studied intramolecular excimer formation using dilute solutions of polystyrene in various solvents using fluorescence emission spectroscopy. They concluded that intramolecular excimer formation is the result of nearest neighbor chromophores and not due to remote chromophores on the polymer chain. These findings were similar to the conclusions presented in a separate paper by Lindsell et al.[34] which was published at approximately the same time.

Others have studied intermolecular excimer formation using fluorescence emission spectroscopy with conflicting results. Nishihara and Kaneko[35] have

shown that increasing the concentration of polystyrene caused an increase in the ratio of excimer to monomer intensity (I_E/I_M) even under dilute concentrations. This was in direct contradiction to an earlier study by Vala et al.[26] who reported little change in the I_E/I_M ratio for dilute solutions of polystyrene. Contradiction of results of previous publications seems prevalent in these types of studies.

Later, Roots and Nystrom,[36] who also studied polystyrene using fluorescence emission spectroscopy, noted an upward curve in the I_E/I_M vs. concentration plot. They concluded this curvature was due to the transition between the dilute and semi-dilute concentrations and hence was a measurement of the critical concentration or c*.

Torkelson et al.[37] performed similar experiments to Root and Nystrom[36] and determined the curvature of the I_E/I_M vs. concentration plot was due to self-absorbance of these highly concentrated polymer solutions and not c*. When these plots of I_E/I_M vs. concentration were corrected for this self-absorbance, the plot was linear up to very high concentrations. Therefore, Roots and Nystrom[36] were not able to determine c* using fluorescence emission spectroscopy.

In another paper by Roots and Nystrom,[38] they studied the effects of pressure on intramolecular excimer formation of polystyrene in a good solvent (1,2-dichloroethane) and a theta solvent (trans-decalin). Fluorescence emission spectroscopy was performed on both of these polymer/solvent systems at pressures ranging from atmospheric pressure to 250 MPa. These studies were conducted at dilute concentrations to rninimize intermolecular excimer formation. They found that I_E/I_M decreased with increasing pressure for both systems. They

attributed this decrease in I_E/I_M to the increase the solution viscosity that occurs at high pressures. They concluded the increased viscosity would hinder the mobility of the polymer chains thereby hindering the ability of the chromophores to move close enough to interact and form excimers.

Nicolai and Brown[39] published a study of the effects of temperature on semi-dilute concentrations of polystyrene in cyclohexane using light scattering. These studies were performed between 35°C (θ-temperature) and 65°C on polystyrene (M_w = 3,800,000 D) at concentrations ranging from 3% to 12.6%. Even though they concluded their results were in good agreement with theory, they were unable to distinguish the transition from a poor solvent to a good under the conditions tested.

Lee et al.[40] performed ultraviolet absorption spectroscopy of poly(oxyethylene) in water and poly(vinyl acetate) in acetonitrile at dilute and semi-dilute concentrations. They obtained absorbance spectra for these polymer/solvent systems using two spectrophotometers and two different path lengths. They found when they plotted this absorbance data as a function of concentration, there was a discontinuity in the plot. However, they also noted the discontinuity was at a different concentration for each of the two different path lengths. Therefore, they concluded this discontinuity was due to an instrument artifact and not to a concentration transition such as c*. This work disputed earlier work performed by Destor et al.[41] who studied the same polymer/solvent systems and concluded they were able to measure c* through a discontinuity in

absorbance vs. concentration plots. However, based on the work performed by Lee et al.,[40] this discontinuity was due to instrument artifacts and not c*.

Yeung and Frank[42] performed fluorescence emission spectroscopy of miscible blends of polystyrene and poly(vinyl methyl ether) in heptane solution and dodecane solution. They were able to determine the critical micelle temperature by observing the changes in the ratio of the excimer band intensity to the monomer band intensity (I_D/I_M). Below the critical micelle temperature, the I_D/I_M ratio remained steady with temperature. As the temperature surpassed the critical micelle temperature, the I_D/I_M ratio decreased with temperature. The authors concluded the decrease in the I_D/I_M ratio with temperatures above the critical micelle temperature was due to breakup of polymer aggregates in the dispersed phase. Below the critical micelle temperature, the polymers are dispersed in the solvent and polymer aggregates may form. Above the critical micelle temperature, micelles can form which would cause the aggregates to break-up. This break-up of the aggregates caused a decrease in excimer formation.

Pethrick[43] studied the fluorescence emission of isotactic polystyrene in the gel state. They determined that as the polystyrene gel annealed at 318K as a function of time, the monomer band at 283 nm decreased in intensity and the excimer band at 335 nm increased in intensity. They attributed this increase in excimer formation to the increase in intermolecular and intramolecular interactions that occurred as the gel annealed.

The idea of determining c* by studying fluorescence is intriguing. Theoretically, because c* occurs at the concentration where the polymer chains are forced into contact with each other, it should be measurable using fluorescence by observing changes in the excimer band. It was determined that it is not possible to measure c* using fluorescence emission spectroscopy,[37] but this dissertation will show that it is possible using fluorescence excitation spectroscopy.

Chapter 2

Experimental Section

Materials

Spectroscopic-grade decahydronapthalene and dichloromethane (Aldrich Chemical Co.) were used without further purification. All polymer samples were manufactured by Scientific Polymer Products, Inc of Ontario, NY. The polystyrene samples were narrow molecular weight distribution primary standards. The molecular weights and polydispersities were: M_w = 223,200 D, M_w/M_n = 1.11; M_w = 560,900 D, M_w/M_n = 1.04; M_w = 1,015,000 D, M_w/M_n = 1.03; and M_w = 1,571,000 D, M_w/M_n = 1.03. The poly(bisphenol A) carbonate samples were secondary standards. The molecular weights and polydispersities are: M_w = 24,400 D, M_w/M_n = 1.88; M_w = 30,900 D, M_w/M_n = 1.68; M_w = 36,600 D, M_w/M_n = 1.67.

For each polymer studied, a stock solution of the highest concentration measured (approximately two times the calculated value for c*) was prepared in a 50 mL volumetric flask and aliquots transferred using graduated pipettes into 10 mL volumetric flasks and diluted to the mark with solvent.

Fluorescence Measurements

All fluorescence measurements were performed on a Jobin-Yvon Spex Tau-2 (FL1T11) Spectrofluorimeter consisting of a 450W ozone-free xenon lamp, a single grating excitation monochromator, a single grating emission monochromator and a T-box sampling module. All spectra were measured using front-face sampling (15° from incident light) and collected on a room temperature Hamamatsu R928 red-sensitive photomultiplier tube with a low-energy cut off of 930 nm. The fluorescence excitation spectra for polystyrene in decalin were scanned from 240 nm to 320 nm with the emission monochromator set to 332 nm and for poly(bisphenol A) carbonate in dichloromethane from 260 nm to 345 nm with the emission monochromator set to 360 nm. The fluorescence emission spectra were scanned from 265 nm to 400 nm with the excitation monochromator set to 250 nm for both the polystyrene in decalin samples and the poly(bisphenol A) carbonate in dichloromethane samples. All spectra were corrected for source intensity variation by Rhodamine B. The emission spectra were not corrected for detector response. All spectra were an average of two separate scans to reduce noise. Error in the fluorescence measurements was determined by running multiple scans and noting the variability. Cell temperatures were maintained using a constant temperature bath containing a 50/50 water/ethylene glycol mixture which was circulated through the cell holder. The cells were allowed to equilibrate to the correct temperature for at least 30 minutes and checked using a mercury thermometer before the measurements were taken. Far UV quartz

(Spectrosil®) 1-cm path length UV-Vis cells were used for all measurements. The cells were equipped with stoppers to prevent solvent evaporation. Slit widths used were 0.5 mm for the polystyrene in decalin samples and 0.3 mm for the poly(bisphenol A) carbonate in dichloromethane samples.

Light Scattering

Light scattering data were gathered using a Wyatt Technologies Corporation Dawn EOS (Enhanced Optical System) Light Scattering Detector (SN 249-E) equipped for scintillation vials. The output data was analyzed using Astra for Windows software version 4.73.04. This system utilizes a 30 mW linearly polarized GaAs laser (690.0 nm) and collects the scattered light with eighteen diodes ranging from 23° to 147°. The samples were transferred to a scintillation vial using a syringe equipped with a 0.02 μm filter for solvents and 0.2 μm filter for solvent/polymer samples and the first 1 mL passed through each filter was discarded to remove any dust from inside the filter. The temperature of the scintillation vial was maintained by an integrated Peltier Heater/Cooler controlled by a Watlow thermocontroller. The scintillation vials containing the polymer/solvent mixture were allowed to equilibrate for 30 minutes before any measurements were taken. Data were obtained over one second intervals for a two minute acquisition period thereby giving 120 data points for each sample tested. Spectroscopic-grade toluene was used as a calibration standard and a

narrow molecular weight polystyrene (M_w = 32,200) in decalin was used as the normalization standard. The dn/dc values are 0.110 mL/g for the polystyrene in decalin and 0.164 mL/g for the poly(bisphenol A) carbonate in dichloromethane.[44]

Chapter 3

Results Section

A. Fluorescence of Polystyrene in Decalin

Figure 12 shows the fluorescence emission spectra of several concentrations of polystyrene (M_w = 223,200 D) in decalin at 20°C with the excitation monochromator set to 250 nm. The emission spectra were gathered to determine the correct wavelength of the monomer and excimer bands. The band at 283 nm is attributed to monomer emission while the band at 332 nm is attributed to excimer emission. Above 0.5 g/L the overall intensity decreases significantly but I_E/I_M still increases with concentration. This decrease in intensity is attributed to a decrease in fluorescence at 250 nm as noted in the fluorescence excitation spectra in Figure 13. This decrease in intensity was noted for all four molecular weights of polystyrene in decalin tested.

Figure 13 shows the fluorescence excitation spectra for polystyrene (Mw = 223,200 D) in decalin from 0.1 g/L to 40 g/L at 20°C while detecting the emission of the excimer band (332 nm). The band that grows in at higher concentrations at 291 nm is attributed to excimer emission resulting from dimer complex formation.

Using the Mark-Houwink equation (equation 4.1 – see Discussion Section) for polystyrene (M_w = 223,200 D) in decalin at 18°C, the calculated c* value is 27.5 g/L. When the dimer complex emission intensity, I_{291}, is plotted vs. concentration as shown in Figure 14, the intensity increases with concentration approaching c*, then shows

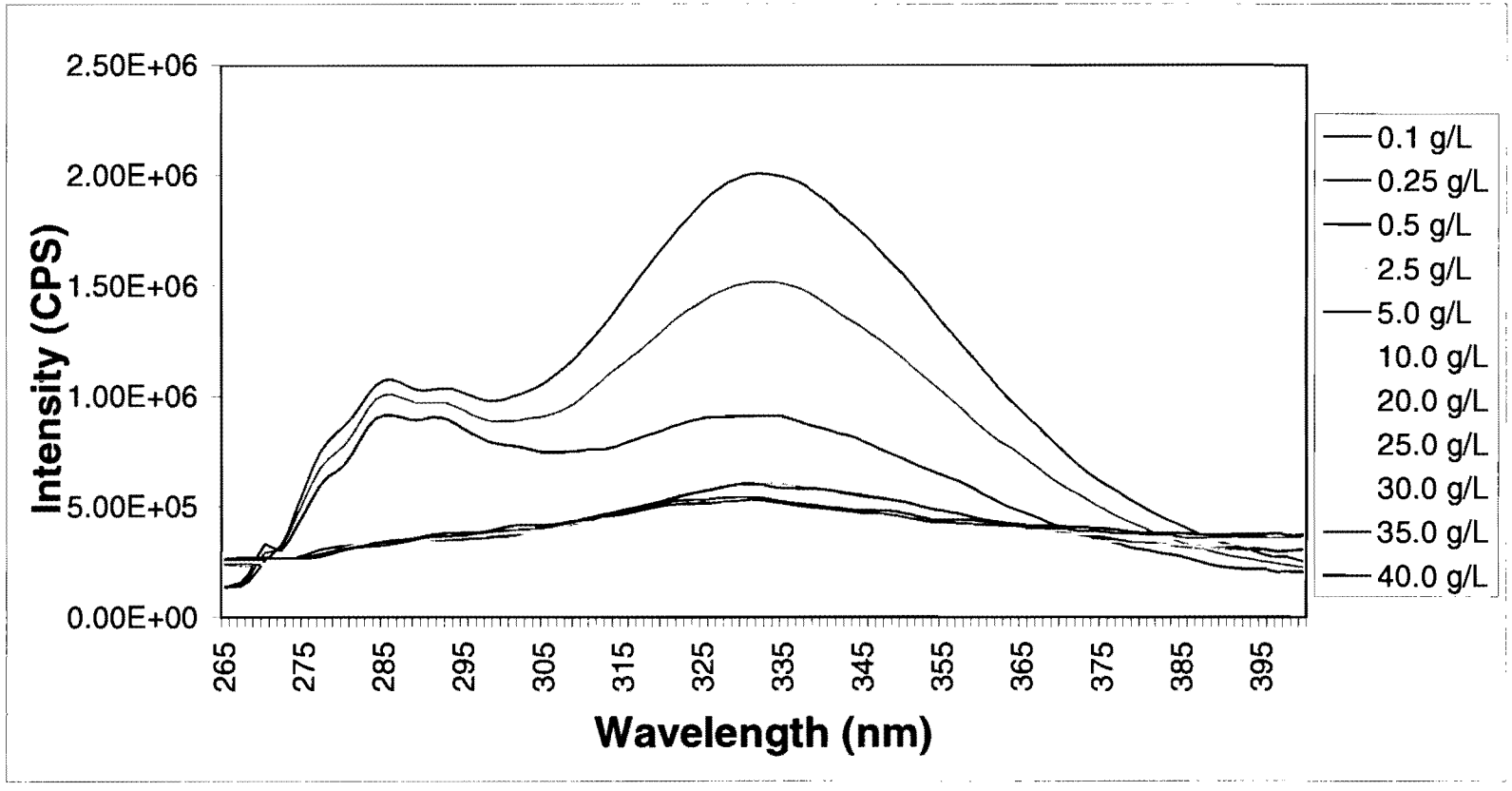

Figure 12. Fluorescence emission spectra for several concentrations of polystyrene (M_w = 223,200 D) in decalin at 20°C with the excitation monochromator set to 250 nm. The band at 283 nm is due to monomer emission while the band at 332 nm is due to excimer emission.

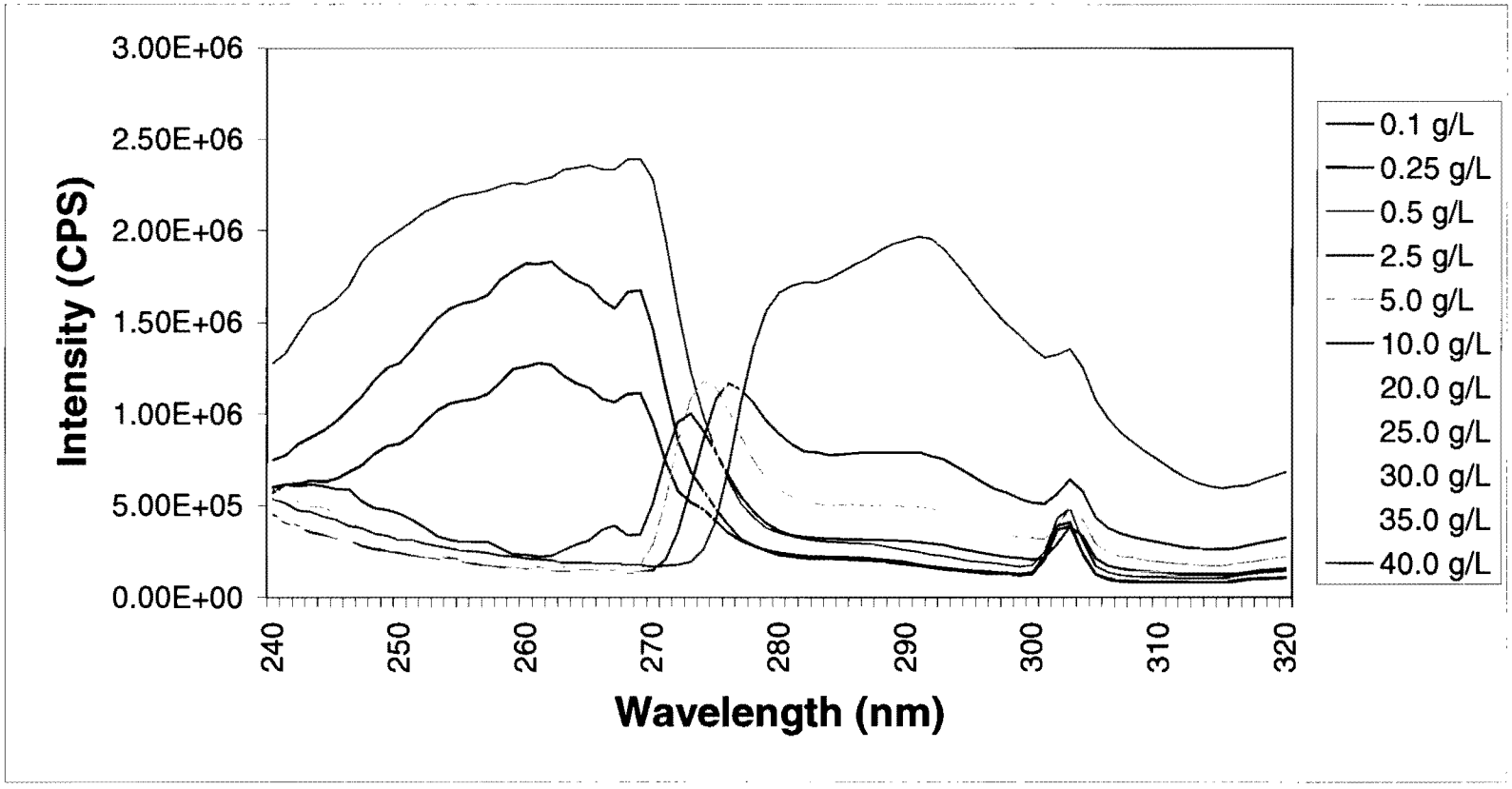

Figure 13. Fluorescence excitation spectra for several concentrations of polystyrene (M_w = 223,200 D) in decalin at 20°C with the emission monochromator set to 332 nm. The band at 291 nm is due to dimmer complex excitation.

only a small change above c*. (The error bars shown in all graphs presented in this dissertation were determined by running multiple fluorescence scans at different concentrations for each molecular weight. Variability in the measurement at the wavelength of interest was noted and the largest measured error within each polymer/solvent system was determined to be the error.)

However, the change in I_{291} as a function of concentration can be seen more dramatically when corrected for scattering. As the concentration of a dissolved substance is increased, there is an increase in Rayleigh light scattering. Scattering also increases with particle size so it is more intense for polymer solutions. Scattering was noted in all of the polystyrene fluorescence excitation spectra as an increase in the baseline. The intensity at 314 nm was used as a reference wavelength for scattering in the excitation spectra of all polystyrene in decalin samples tested. This wavelength was chosen because there is little fluorescence due to polystyrene absorbance at that wavelength and therefore the increases in intensity are mainly due to scattering.

Fluorescence emission and excitation spectra for polystyrene (M_w = 223,200 D) in decalin at 30°C are shown in Figure 15 and 16, respectively. These results are similar to the 20°C results except the excimer and dimer complex bands begin to appear at lower concentrations. The plot of I_{291} vs. concentration at 30°C (Figure 17) shows similar results to the 20°C results with increasing ground state dimer emission intensity and little change above c*. Unfortunately, there are no constants for the Mark-Houwink equation for polystyrene in decalin at 30°C.

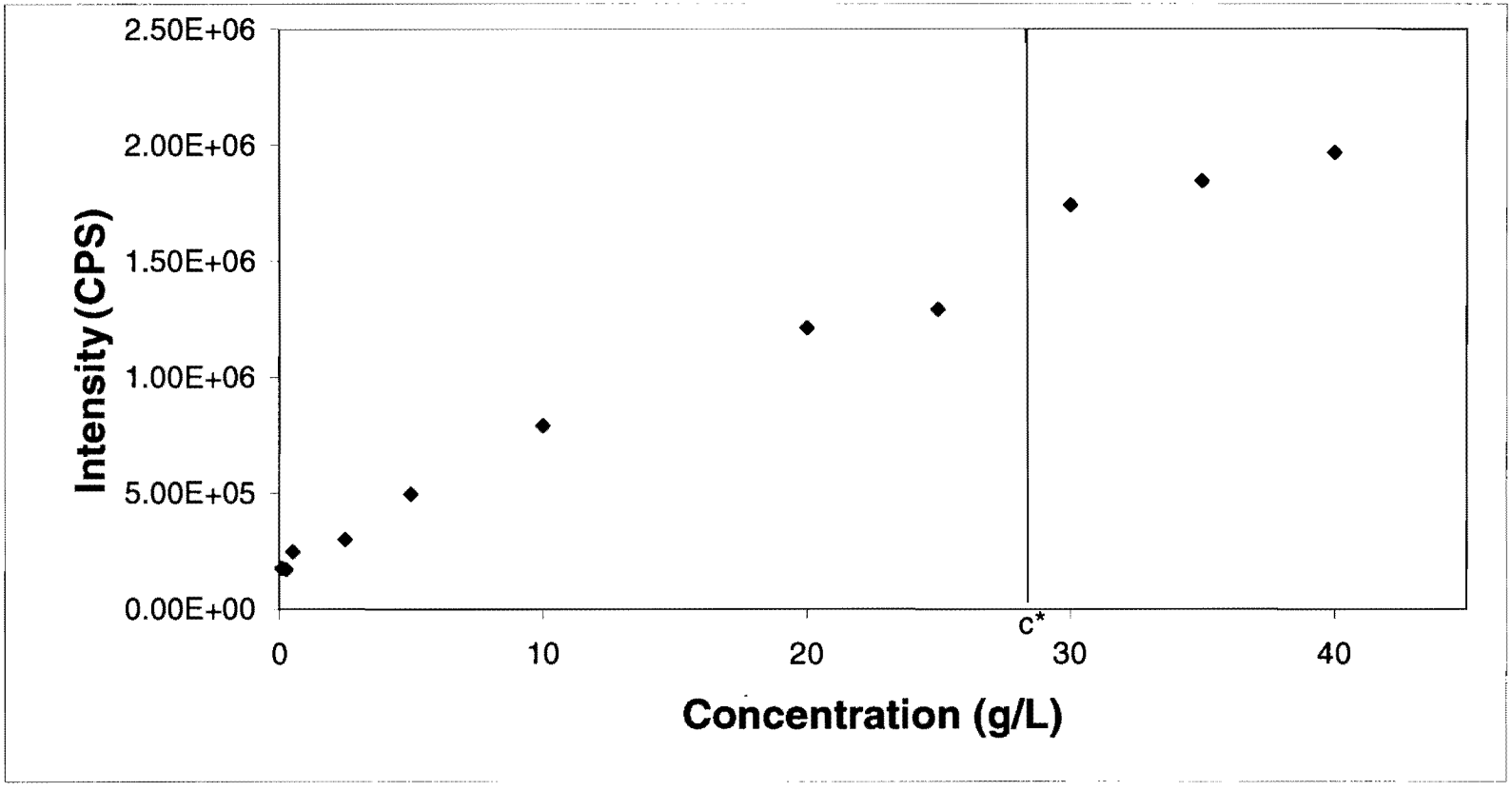

Figure 14. A plot of the uncorrected dimer complex intensity (I_{291}) vs. concentration for polystyrene (M_w = 223,200 D) in decalin at 20°C. The uncorrected dimer complex intensity increases with concentration but shows no change above the Mark-Houwink calculated c* value of 27.5 g/L. Measurement error is ± 9E+3 CPS.

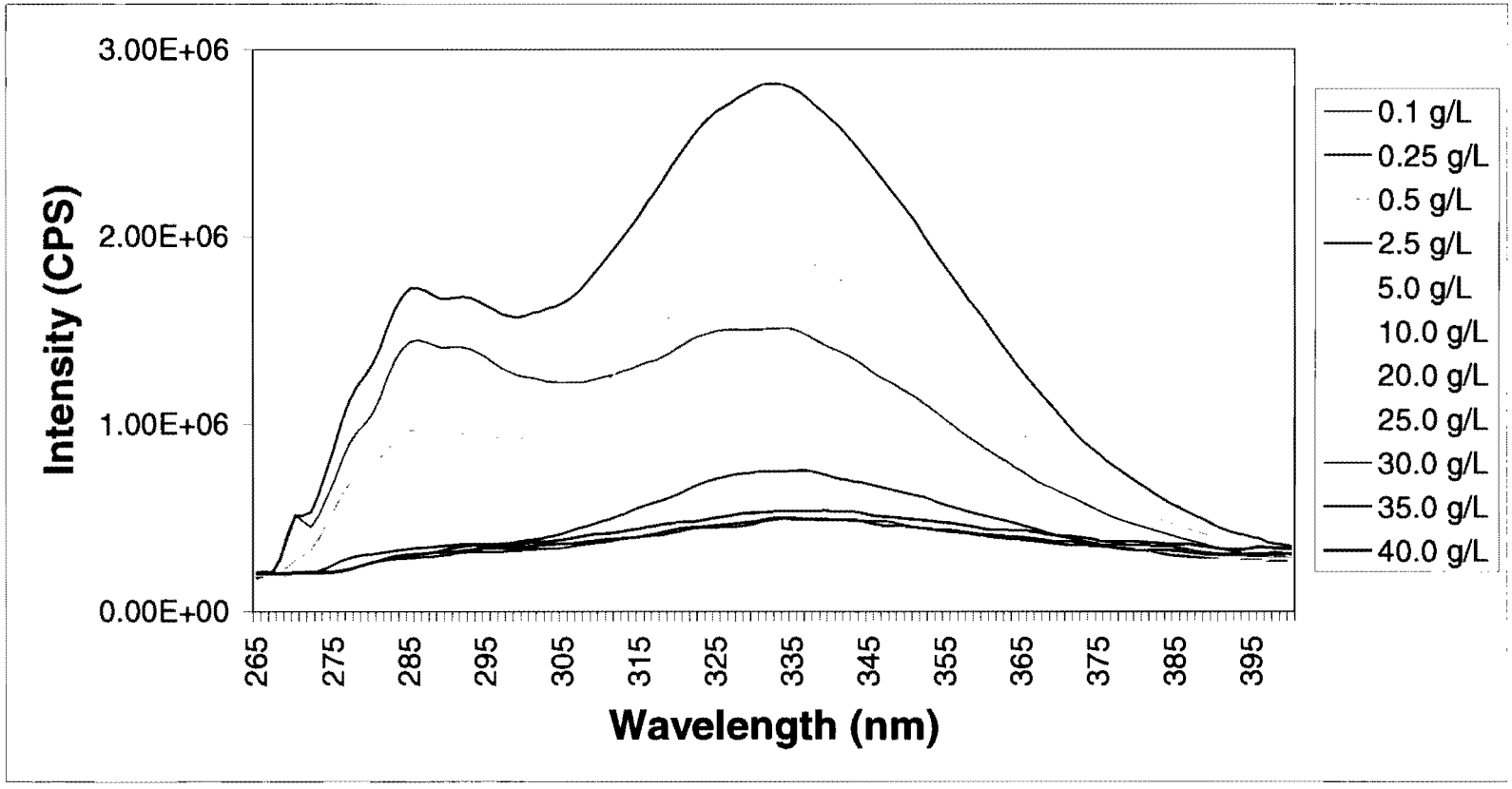

Figure 15. Fluorescence emission spectra for several concentrations of polystyrene (M_w = 223,200 D) in decalin at 30°C with the excitation monochromator set to 250 nm. The band at 283 nm is due to monomer emission while the band at 332 nm is due to excimer emission.

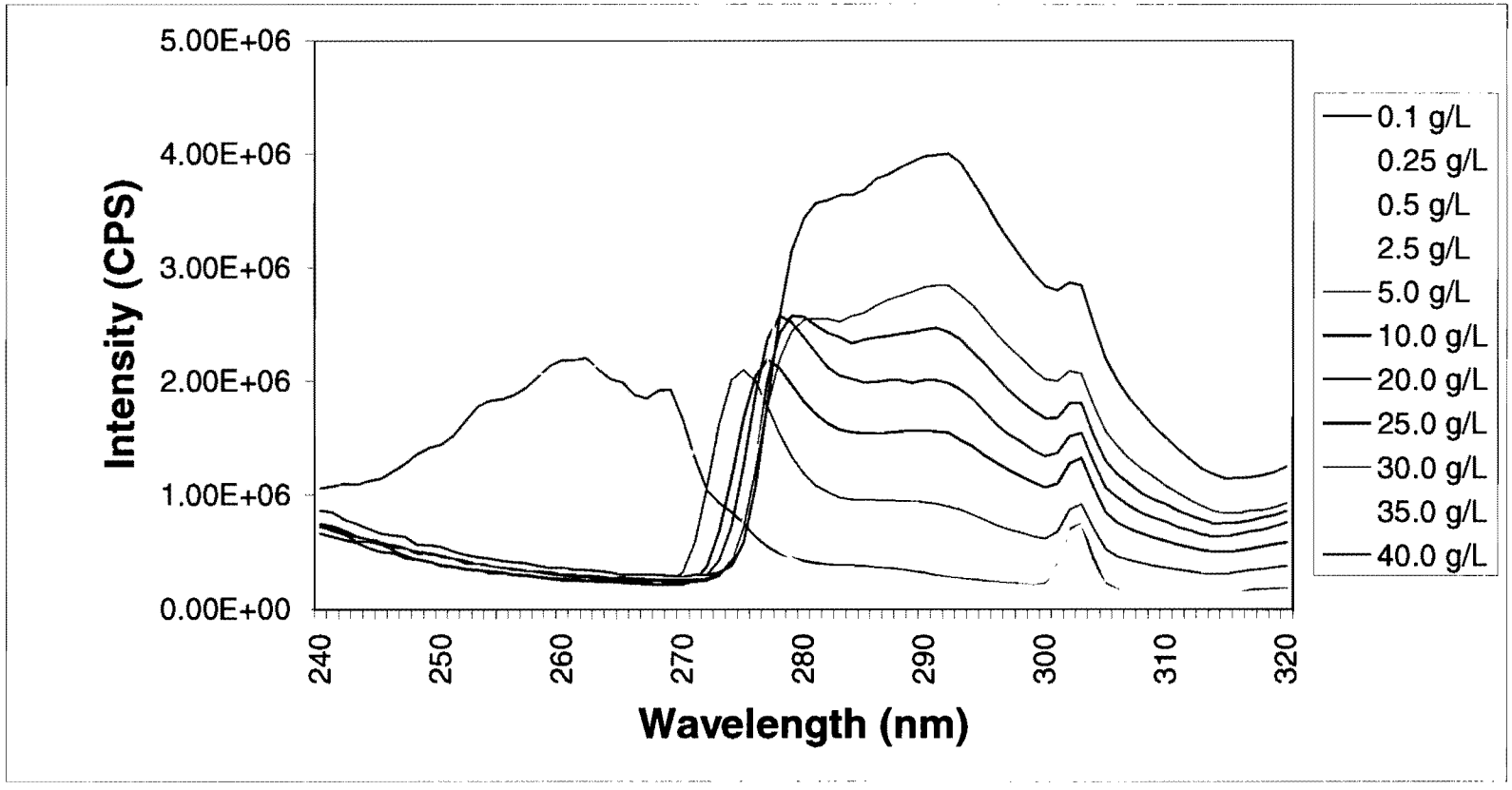

Figure 16. Fluorescence excitation spectra for several concentrations of polystyrene (M_w = 223,200 D) in decalin at 30°C with the emission monochromator set to 332 nm. The band at 291 nm is due to dimer complex excitation.

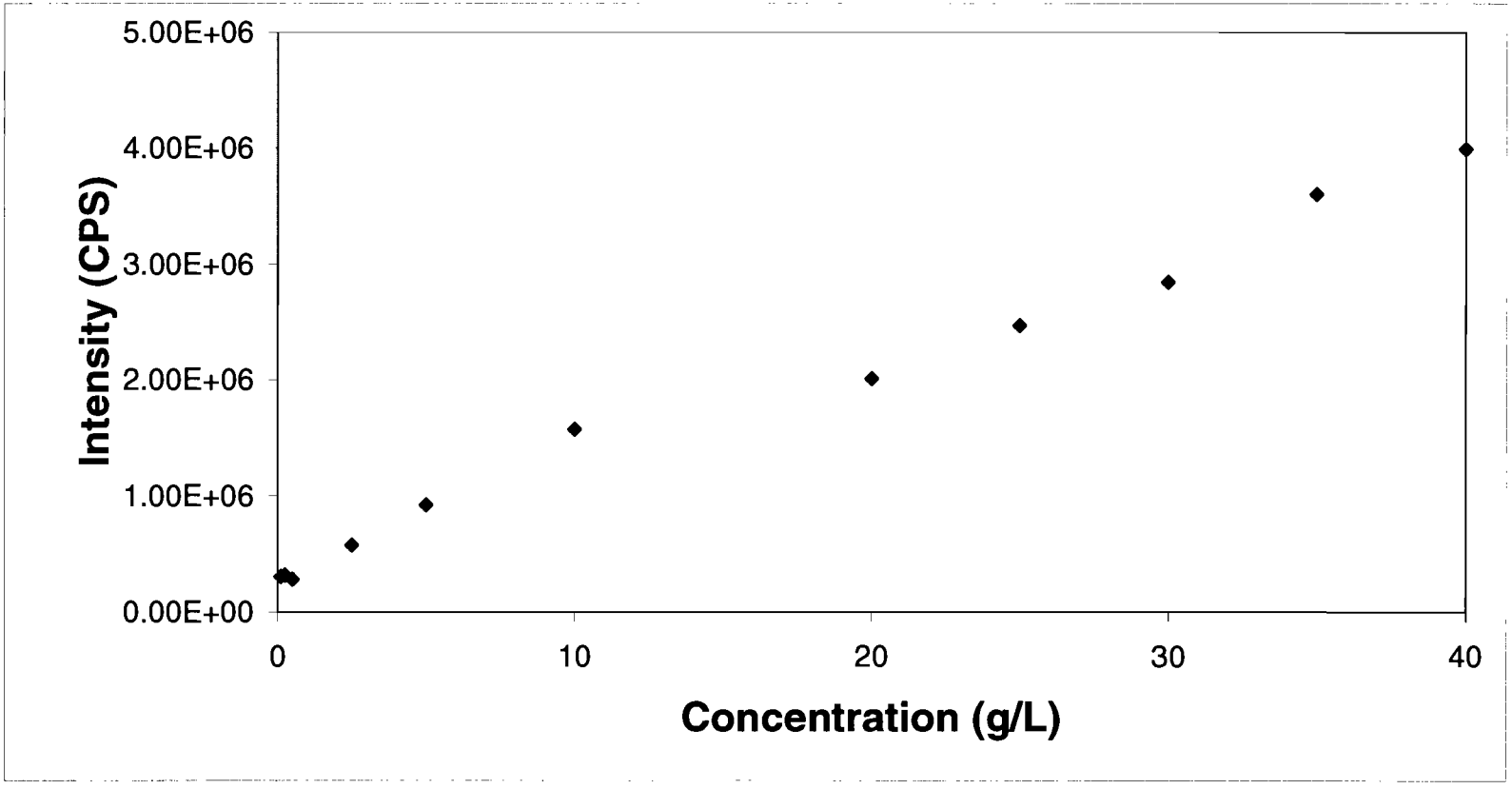

Figure 17. A plot of the uncorrected dimer complex intensity (I_{291}) vs. concentration for polystyrene (M_w = 223,200 D) in decalin at 30°C. The uncorrected dimer complex intensity increases with concentration but shows no change above c*. Measurement error is ± 9E+3 CPS.

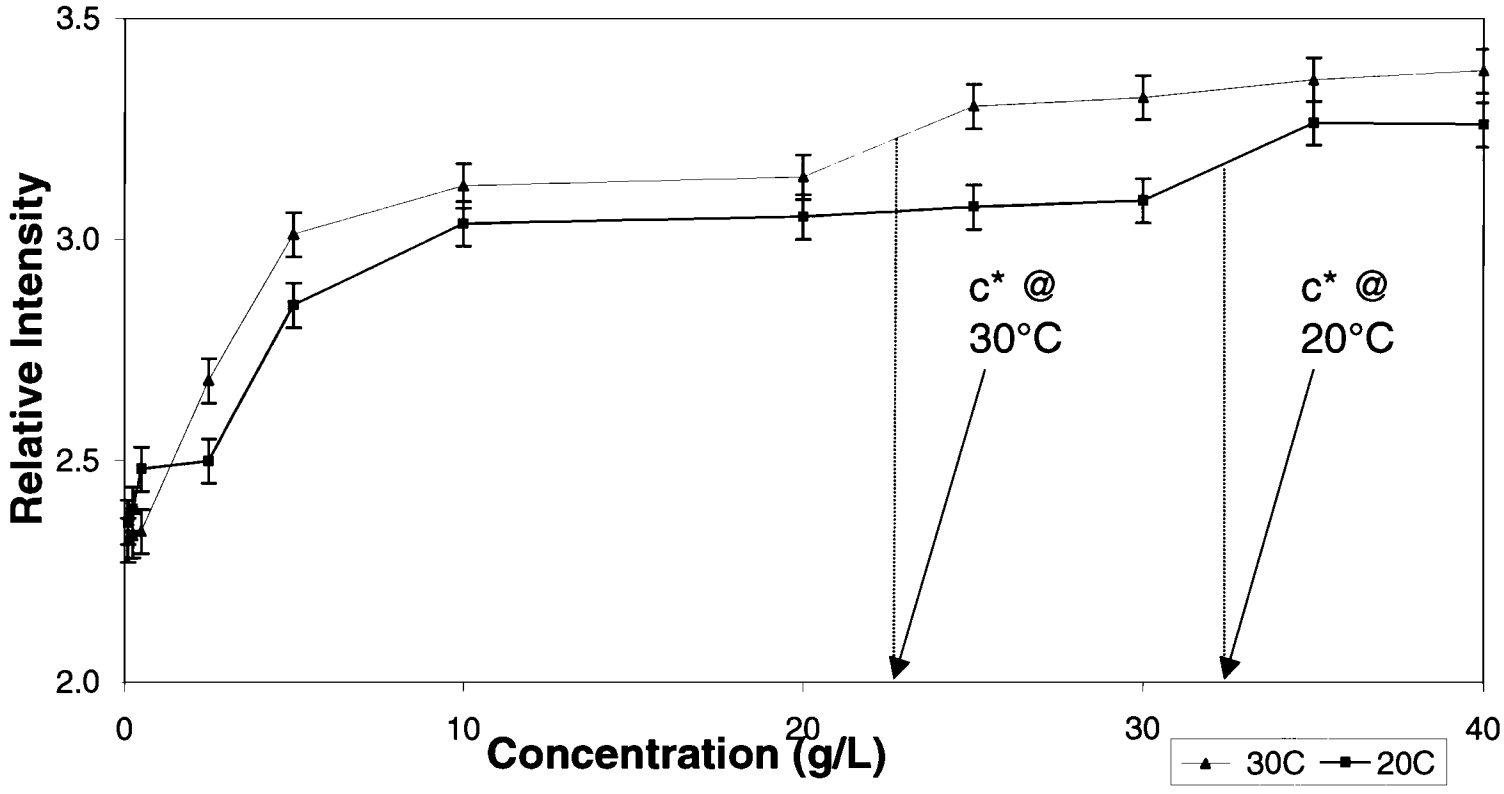

Figure 18. A plot of the corrected dimer complex intensity vs. concentration for polystyrene (M_w = 223,200 D) in decalin at 20°C and 30°C. c* is apparent between 30 and 35 g/L at 20°C and between 20 and 25 g/L at 30°C. Lines connecting points are for ease of interpretation only.

To correct for scattering, I_{291} was divided by I_{314} and plotted against concentration. Figure 18 shows a plot of I_{291}/I_{314} vs. concentration for polystyrene in decalin at 20°C and 30°C. As the concentration increases, the corrected intensity shows a sharp increase at lower concentrations followed by a plateau. The corrected intensity shows little increase with concentration until it makes a sharp increase between 30 and 35 g/L for the 20°C samples and between 20 and 25 g/L for the 30°C samples. This increase is assigned to the sharp increase in intramolecular and intermolecular interactions due to crowding of the polymer chains that is associated with the transition from dilute to semi-dilute solution phases also known as the critical concentration (c*). Therefore at 20°C, c* is shown to occur between 30 and 35 g/L and at 30°C, c* is shown to occur between 20 and 25 g/L. This decrease in c* with increased temperature is expected due to expansion of the polymer chains with increased thermal energy and polymer-solvent interactions.

It is expected that as the molecular weight of a polymer is increased, c* will decrease. This occurs because as the polymer becomes larger, the radius of gyration also increases which causes polymer chains to be in contact at lower concentrations, hence c* decreases. To test this theory and to extend the scope of this method, higher molecular weight samples of polystyrene were tested.

The fluorescence emission and excitation spectra for polystyrene (M_w = 560,900 D) in decalin at several concentrations are shown in Figures 19 and 20 at 20°C and Figures 21 and 22 at 30°C, respectively. These spectra are similar in appearance to the M_w = 223,200 D spectra except the excimer and dimer

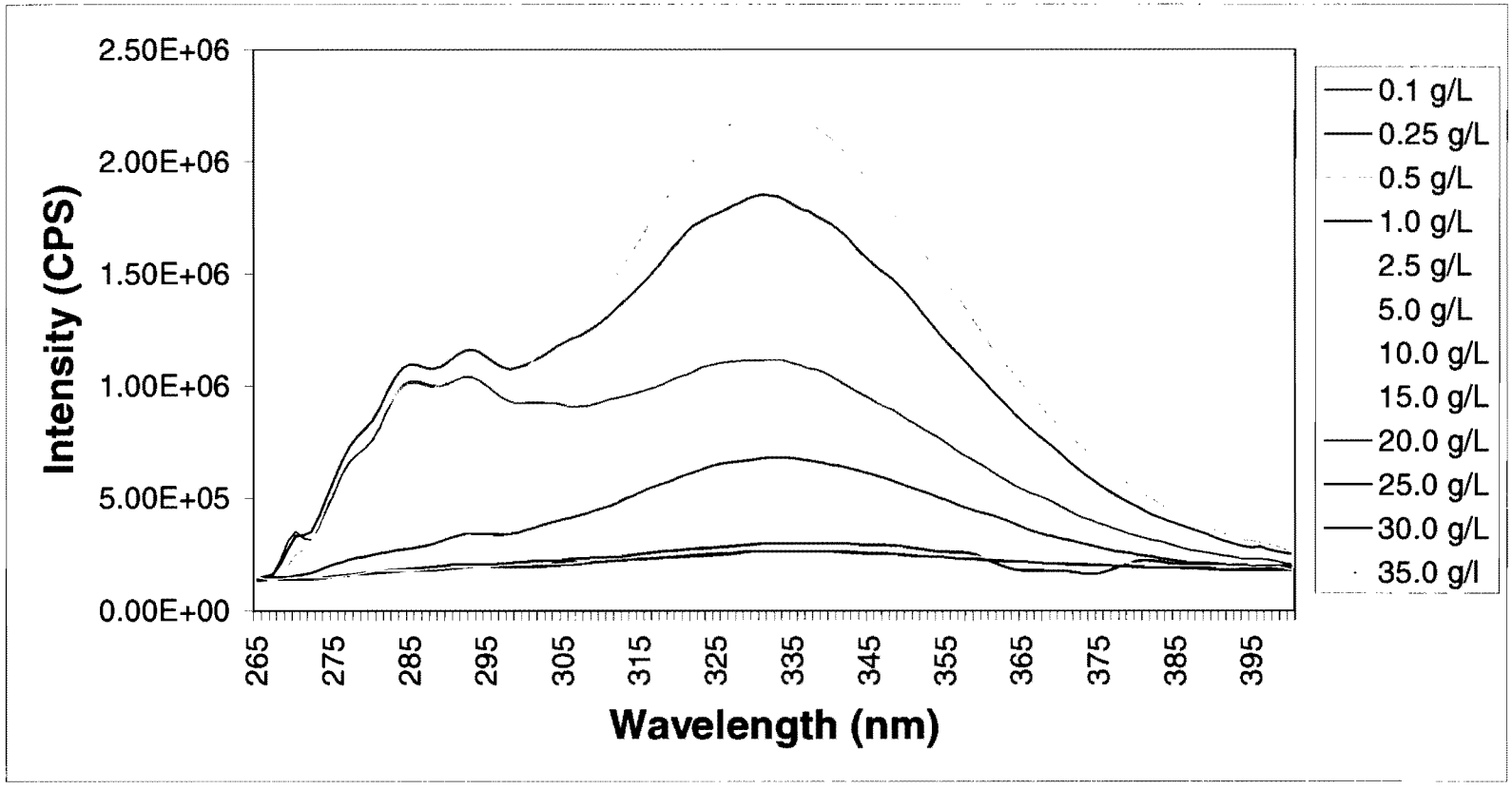

Figure 19. Fluorescence emission spectra for several concentrations of polystyrene (M_w = 560,900 D) in decalin at 20°C with the excitation monochromator set to 250 nm. The band at 283 nm is due to monomer emission while the band at 332 nm is due to excimer emission.

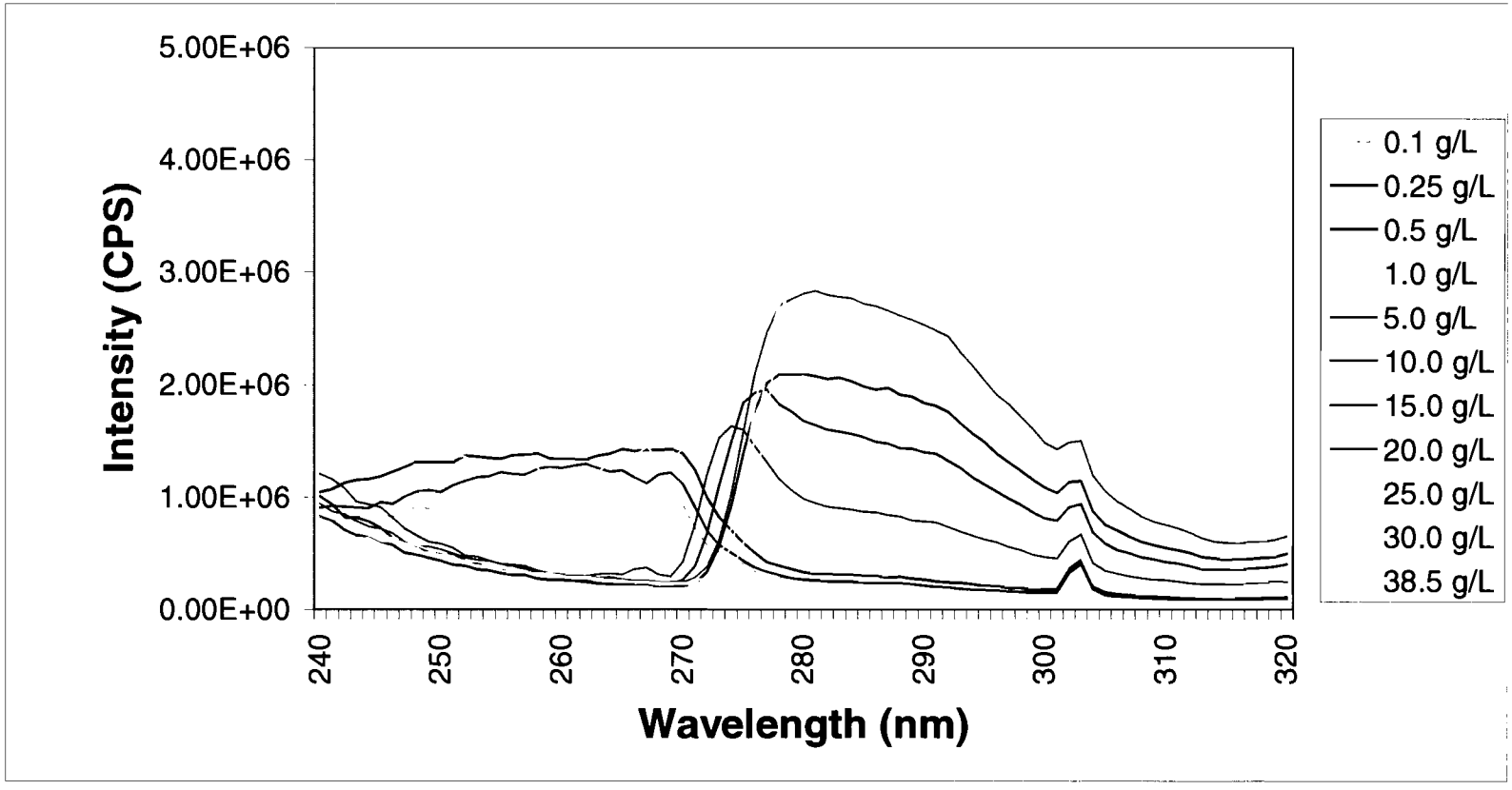

Figure 20. Fluorescence excitation spectra for several concentrations of polystyrene (M_w = 560,900 D) in decalin at 20°C with the emission monochromator set to 332 nm. The band at 291 nm is due to dimer complex excitation.

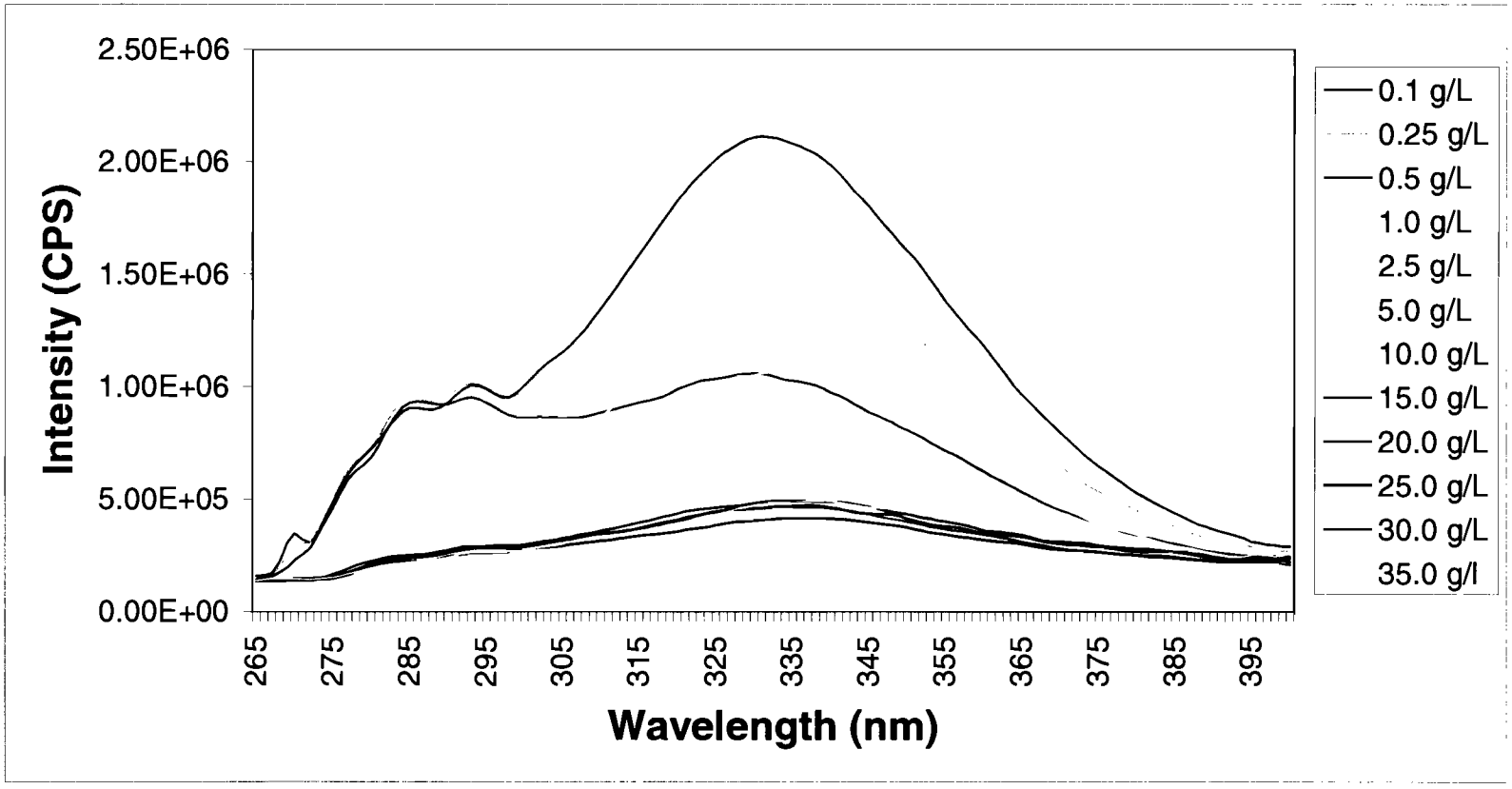

Figure 21. Fluorescence emission spectra for several concentrations of polystyrene (M_w = 560,900 D) in decalin at 30°C with the excitation monochromator set to 250 nm. The band at 283 nm is due to monomer emission while the band at 332 nm is due to excimer emission.

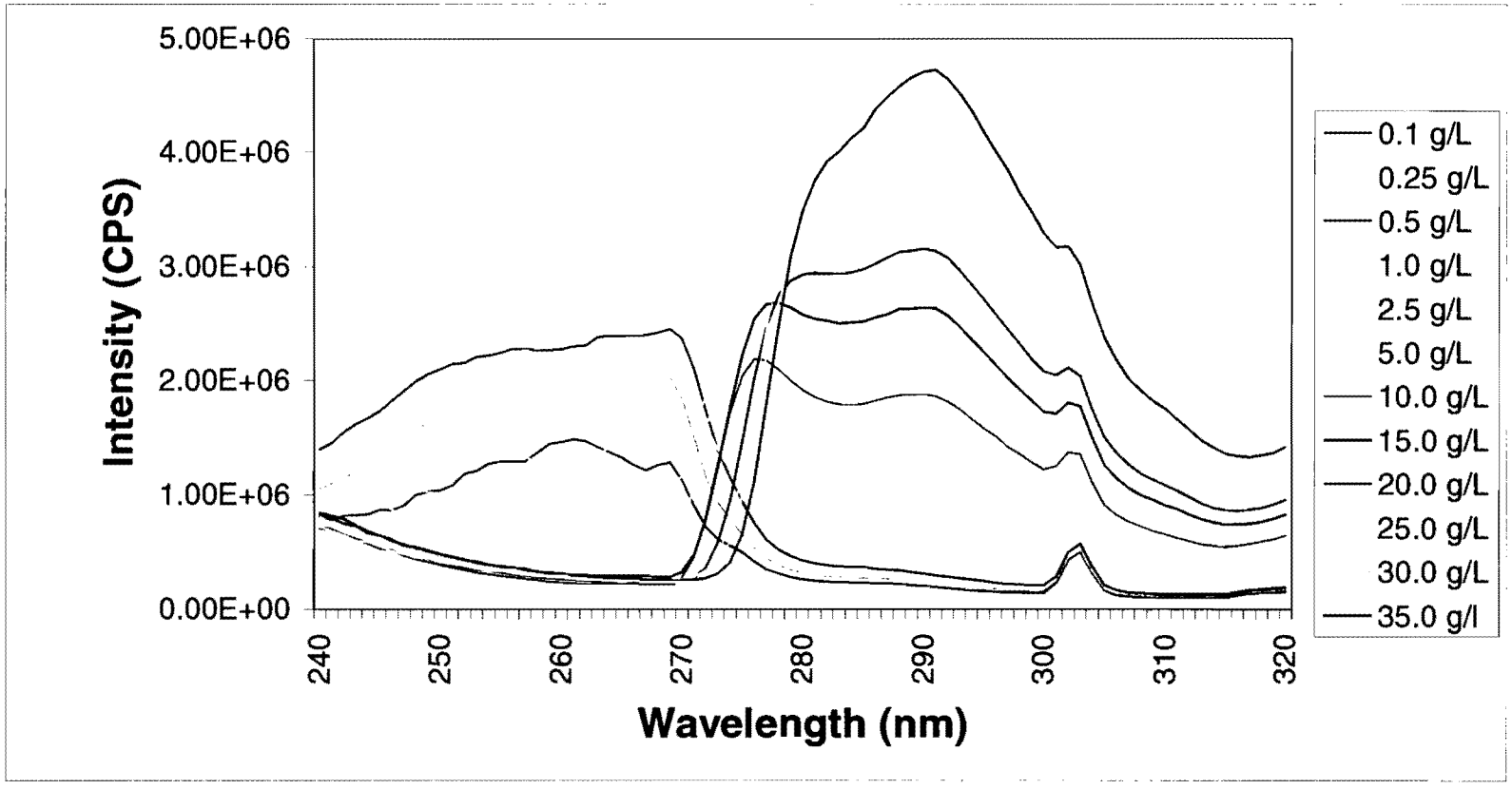

Figure 22. Fluorescence excitation spectra for several concentrations of polystyrene (M_w = 560,900 D) in decalin at 30°C with the emission monochromator set to 332 nm. The band at 291 nm is due to dimer complex excitation.

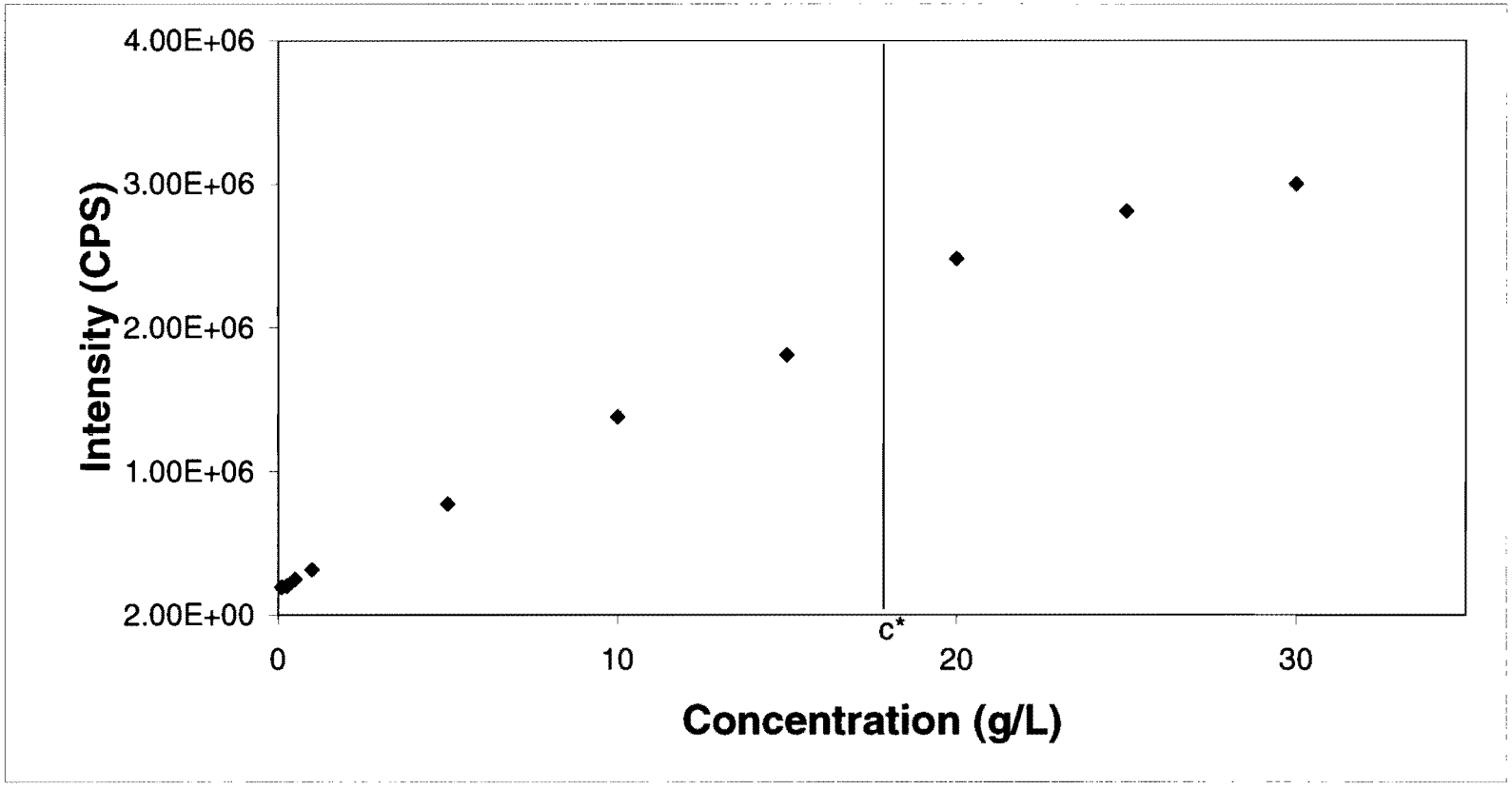

Figure 23. A plot of the uncorrected dimer complex intensity (I_{291}) vs. concentration for polystyrene (M_w = 560,900 D) in decalin at 20°C. The uncorrected dimer complex intensity increases with concentration but shows no change above the Mark-Houwink calculated c* value of 17.3 g/L. Measurement error is ± 9E+3 CPS.

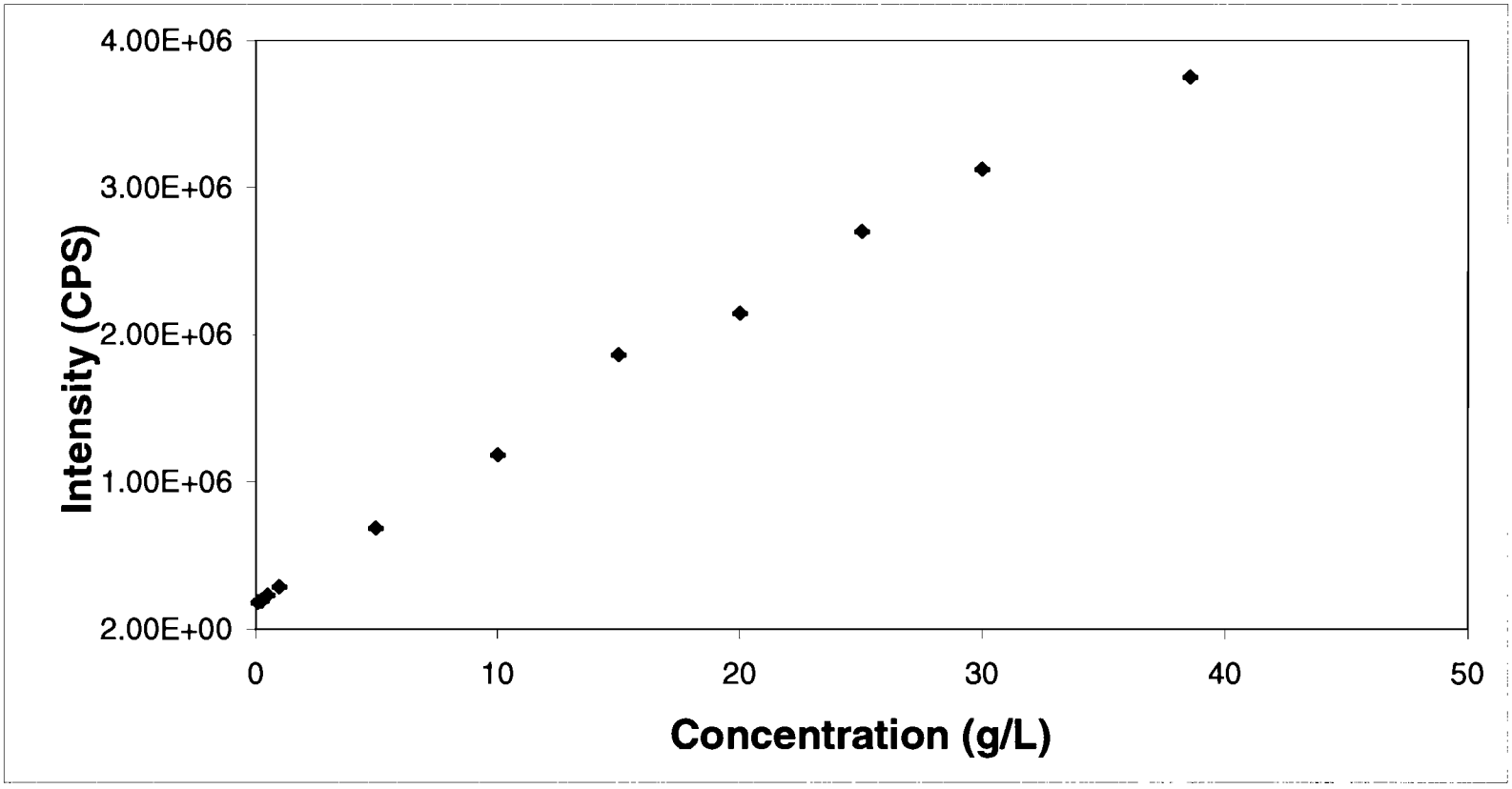

Figure 24. A plot of the uncorrected dimer complex intensity (I_{291}) vs. concentration for polystyrene (M_w = 560,900 D) in decalin at 30°C. The uncorrected dimer complex intensity increases with concentration but shows no change above c*. Measurement error is ± 9E+3 CPS.

complex bands begin to appear at lower concentrations. The I_{291} vs. concentration plot is shown in Figure 23 for 20°C and in Figure 24 for 30°C. As previously noted for the M_w = 223,200 D plot, these plots shows increasing dimer complex intensity with concentration with no distinction at the Mark-Houwink calculated c* value of 17.3 g/L at 18°C.

The I_{291}/I_{314} vs. concentration plots for polystyrene (Mw = 560,900 D) in decalin at 20°C and 30°C are shown in Figure 25. It is apparent that c* falls between 15 and 20 g/L at 20°C and between 10 and 15 g/L at 30°C. It was noted that the transition from the dilute region to the semi-dilute region becomes less obvious with higher molecular weights of polystyrene in decalin at higher temperatures. This may be because c* is not observed as a sharp transition but by a transition range. Within a dilute solution there can be localized areas where the polymer chains are in contact and in these areas the concentration is more closely resembles semi-dilute than dilute. In the case of polystyrene or other aromatic polymers, this would cause the benzene rings on adjacent polymers within these regions to be close enough to interact and to cause dimer complexes to form at a lower concentration than is expected.

The fluorescence emission spectra and excitation spectra for polystyrene (M_w = 1,015,000 D) in decalin are shown in Figure 26 and 27 at 20°C and Figure 28 and 29 at 30°C, respectively. If these spectra are compared with the lower molecular weight spectra presented earlier, the threshold for the formation of excimers and dimer complexes appear at lower concentrations for higher molecular weights. This is expected since a larger radius of gyration will be

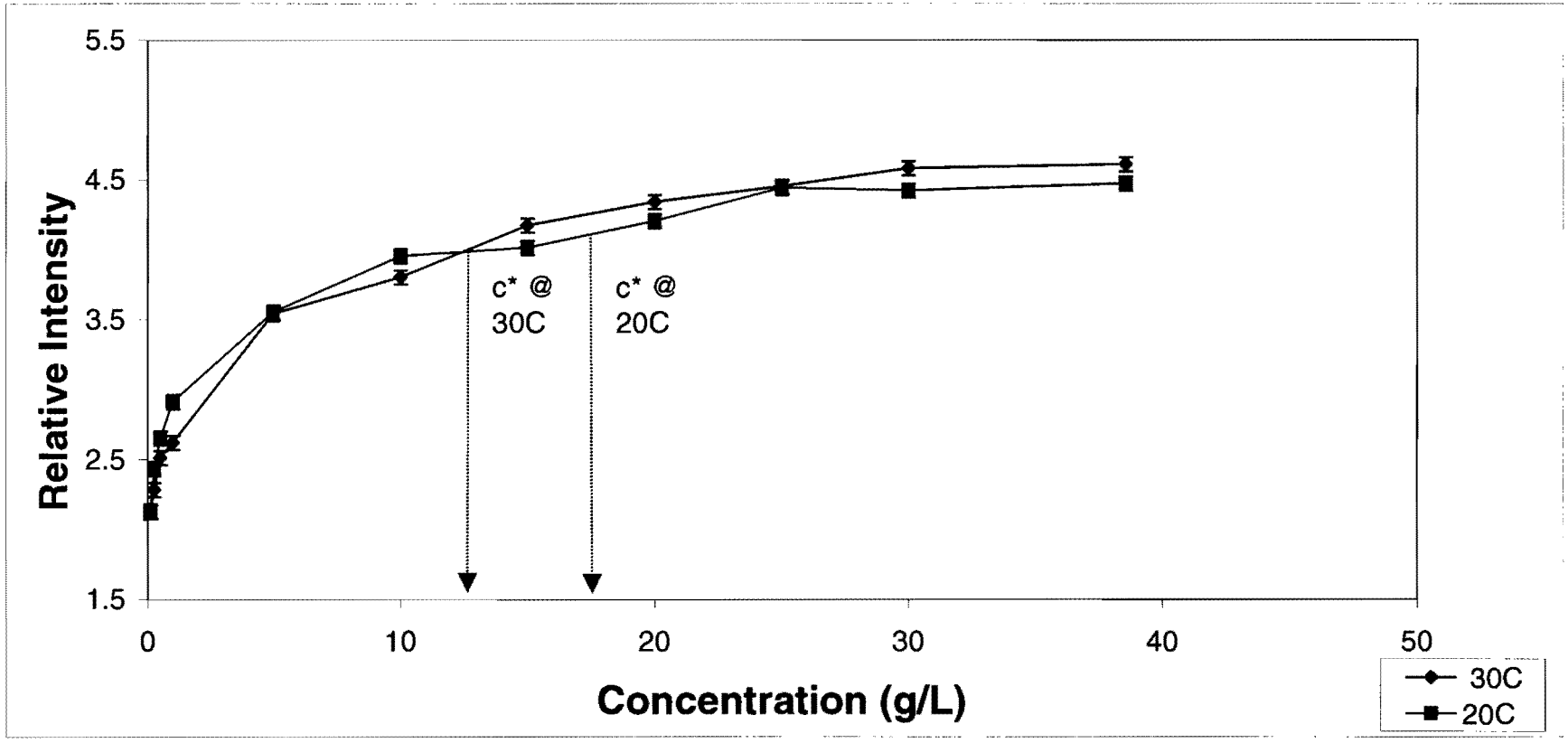

Figure 25. A plot of the corrected dimer complex intensity vs. concentration for polystyrene (M_w = 560,900 D) in decalin at 20°C and 30°C. c* is apparent between 15 and 20 g/L at 20°C and between 10 and 15 g/L at 30°C. With higher molecular weight samples at higher temperature, c* may be more difficult to determine. Lines connecting points are for ease of interpretation only.

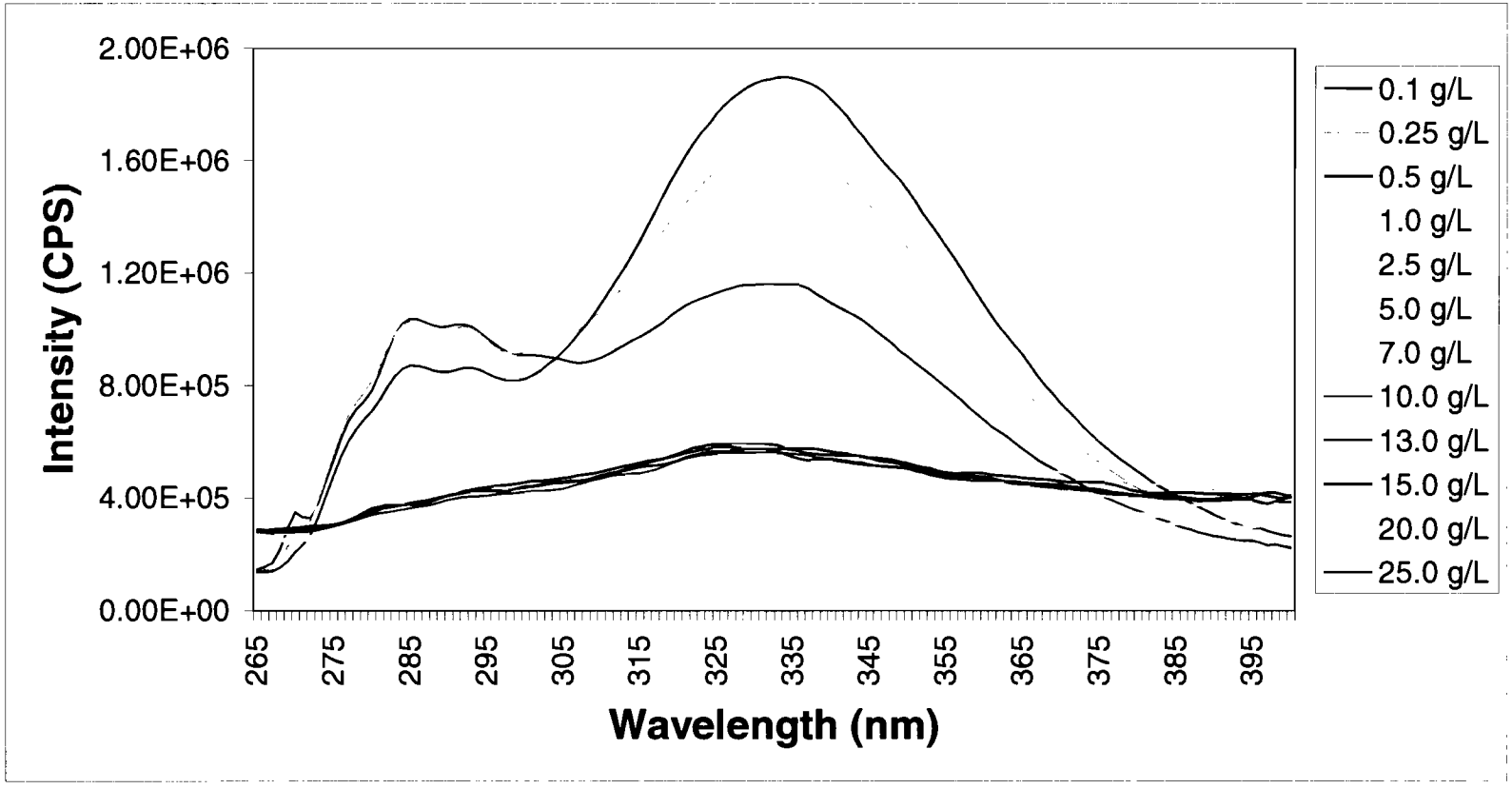

Figure 26. Fluorescence emission spectra for several concentrations of polystyrene (M_w = 1,015,000 D) in decalin at 20°C with the excitation monochromator set to 250 nm. The band at 283 nm is due to monomer emission while the band at 332 nm is due to excimer emission.

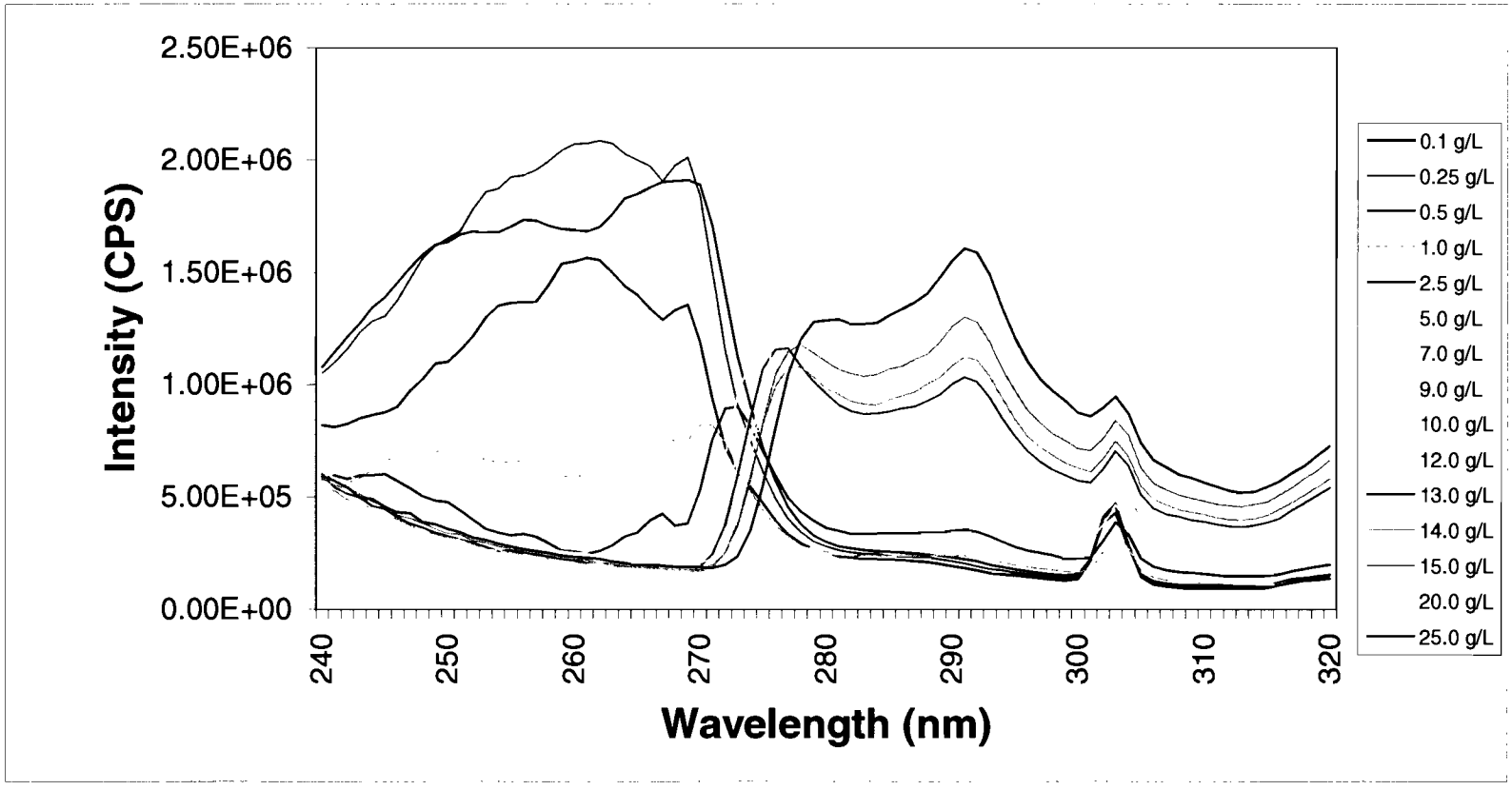

Figure 27. Fluorescence excitation spectra for several concentrations of polystyrene (M_w = 1,015,000 D) in decalin at 20°C with the emission monochromator set to 332 nm. The band at 291 nm is due to dimer complex excitation.

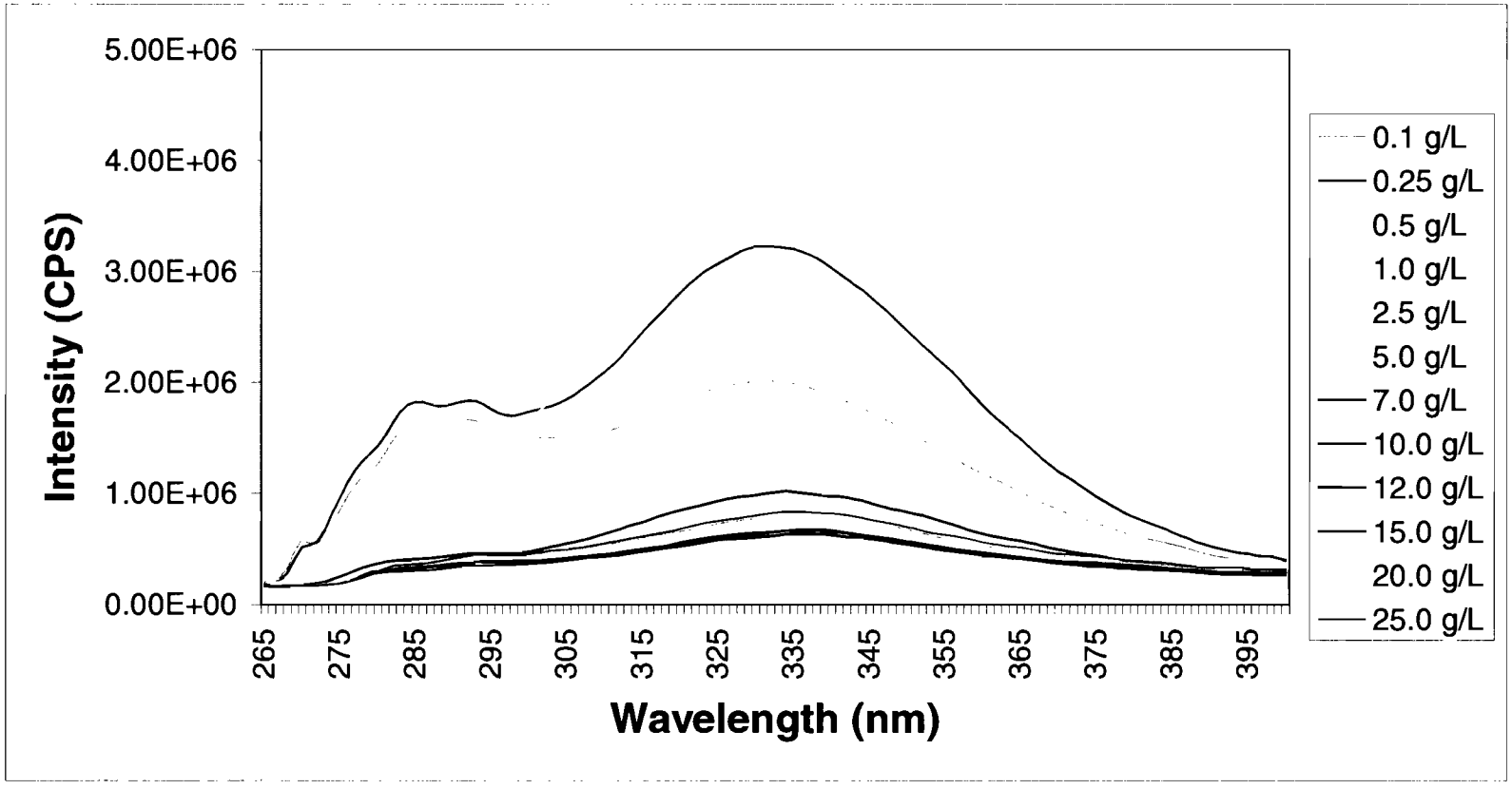

Figure 28. Fluorescence emission spectra for several concentrations of polystyrene (M_w = 1,015,000 D) in decalin at 30°C with the excitation monochromator set to 250 nm. The band at 283 nm is due to monomer emission while the band at 332 nm is due to excimer emission.

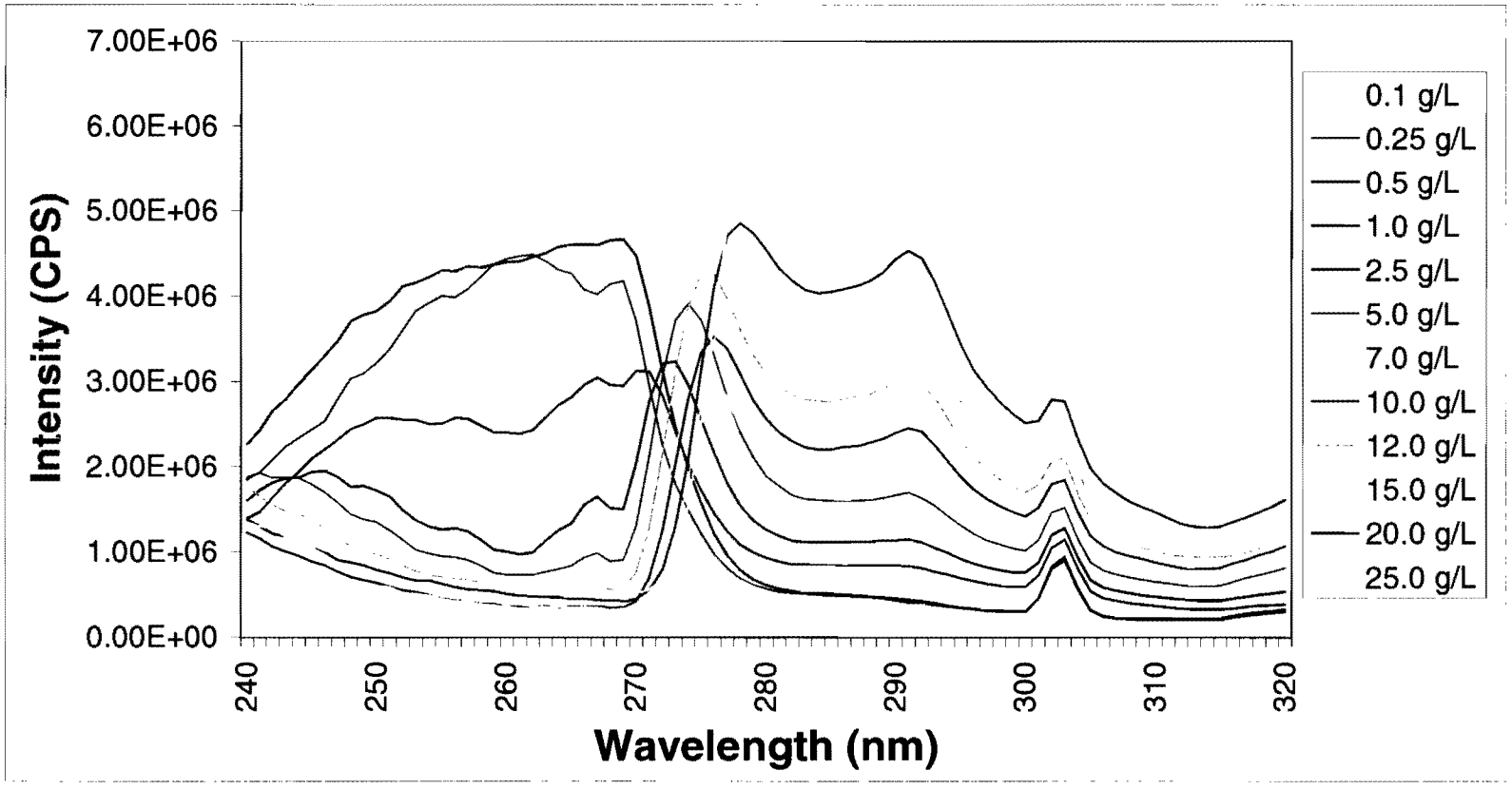

Figure 29. Fluorescence excitation spectra for several concentrations of polystyrene (M_w = 1,015,000 D) in decalin at 30°C with the emission monochromator set to 332 nm. The band at 291 nm is due to dimer complex excitation.

found for the higher molecular weight. As the radius of gyration increases, fewer polymers are needed to completely fill the solvent. Therefore, interactions between polymers begin at lower concentrations which is observed by the formation of excimers and dimer complexes at lower concentrations.

The I_{291} vs. concentration plot for polystyrene (M_w = 1,015,000 D) in decalin is shown in Figure 30 for 20°C and in Figure 31 for 30°C. As previously noted for the lower molecular weight plots, these plots shows increasing dimer complex intensity with concentration and little distinction above the Mark-Houwink calculated c* value of 12.9 g/L at 18°C.

Figure 32 shows the corrected ground state dimer emission vs. concentration for polystyrene (M_w = 1,015,000 D) in decalin at 20°C and 30°C. It is apparent that c* falls between 12 and 13 g/L at 20°C and between 10 and 12 g/L at 30°C. As noted previously for the higher molecular weights it becomes more difficult to determine c* at higher temperatures.

The fluorescence emission spectra and excitation spectra for polystyrene (M_w = 1,571,000 D) in decalin are shown in Figure 33 and 34 at 20°C and Figure 35 and 36 at 30°C, respectively. These results are similar to the lower molecular weights of polystyrene in decalin that were reported earlier except the excimer and dimer complex bands appear at a lower concentration.

Figure 37 and 38 show the uncorrected dimer complex intensity as a function of concentration for polystyrene (M_w = 1,571,000 D) in decalin at 20°C and 30°C, respectively. The Mark-Houwink calculated c* value for this molecular weight is 10.4 g/L at 18°C. Both plots show increasing dimer complex intensity

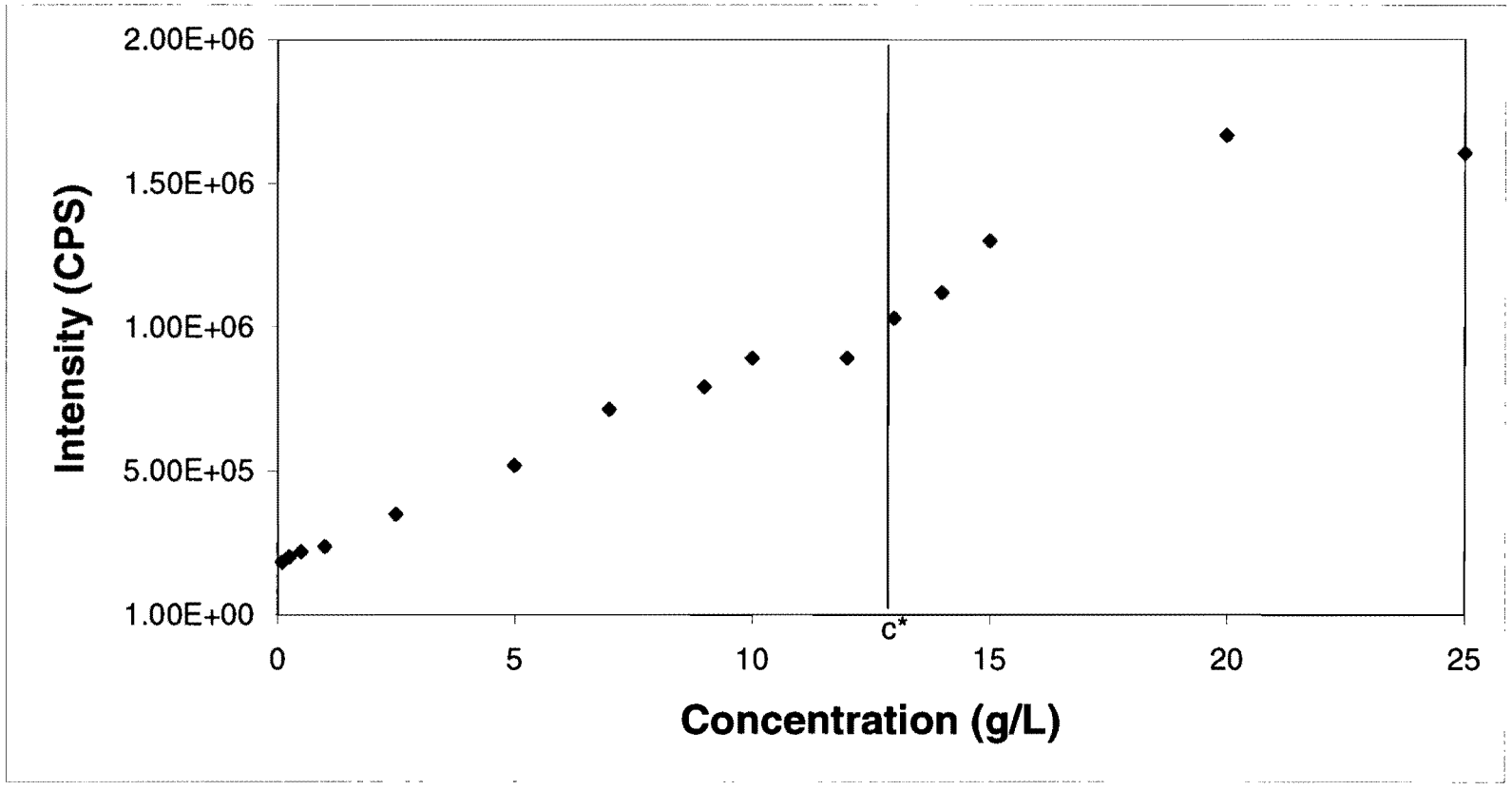

Figure 30. A plot of the uncorrected dimer complex intensity (I_{291}) vs. concentration for polystyrene (M_w = 1,015,000 D) in decalin at 20°C. The uncorrected dimer complex intensity increases with concentration but shows no change above the Mark-Houwink calculated c* value of 12.9 g/L. Measurement error is ± 9E+3 CPS.

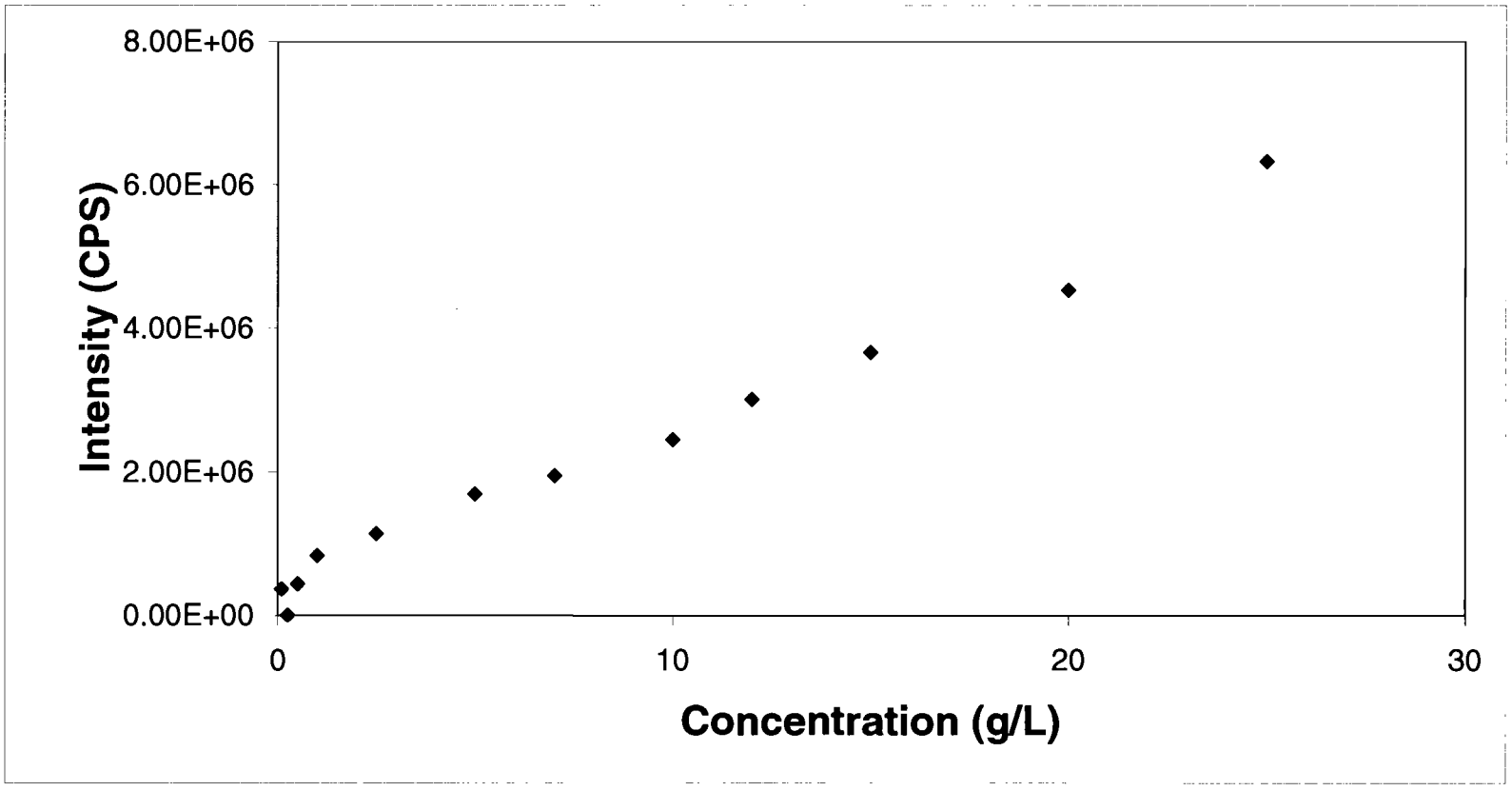

Figure 31. A plot of the uncorrected dimer complex intensity (I_{291}) vs. concentration for polystyrene (M_w = 1,015,000 D) in decalin at 30°C. The uncorrected dimer complex intensity increases with concentration but shows no change above c*. Measurement error is ± 9E+3 CPS.

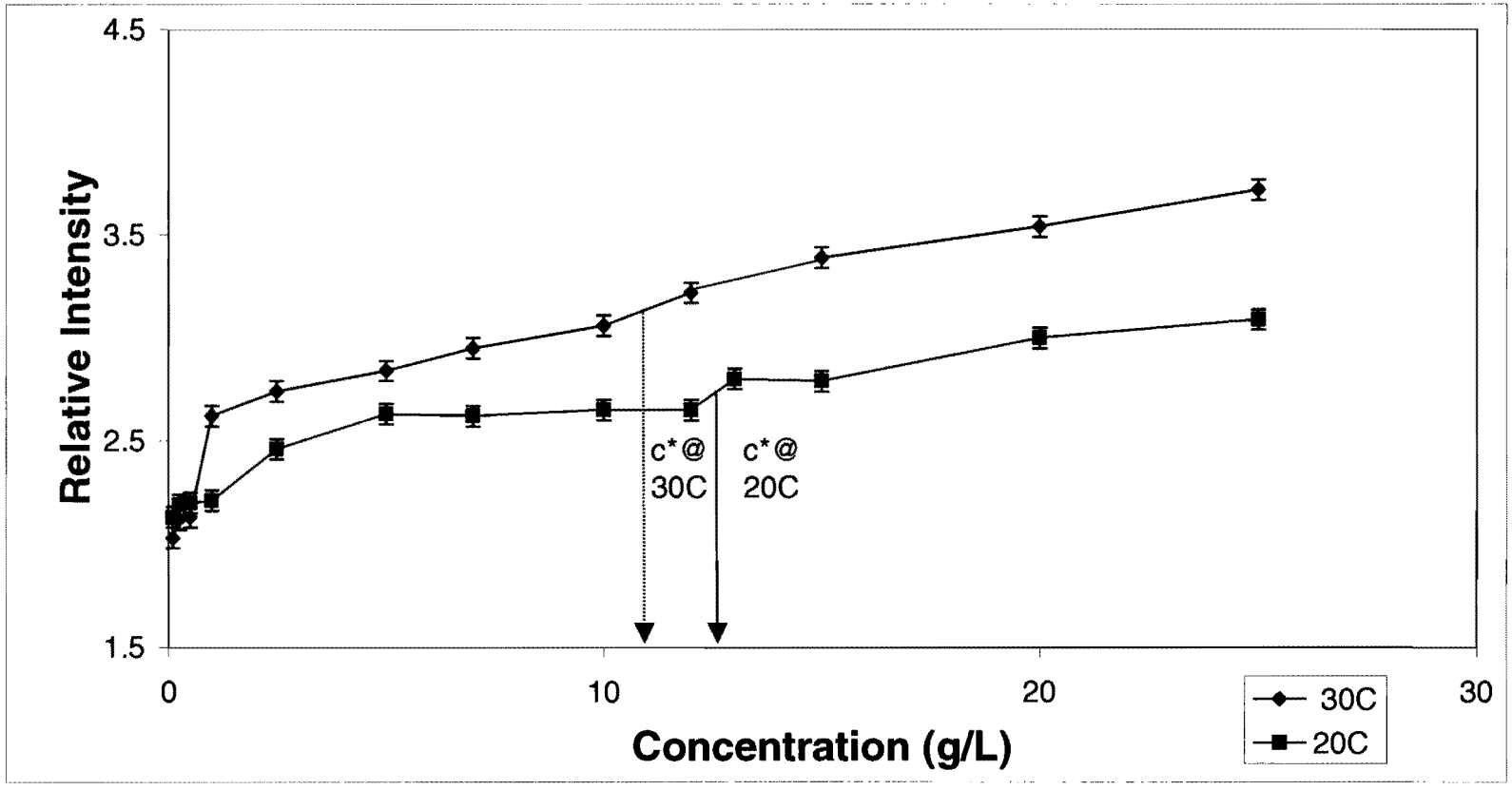

Figure 32. A plot of the corrected dimer complex intensity vs. concentration for polystyrene (M_w = 1,015,000 D) in decalin at 20°C and 30°C. c* is apparent between 12 and 13 g/L at 20°C and between 10 and 12 g/L at 30°C. With higher molecular weight samples at higher temperature, c* may be more difficult to determine. Lines connecting points are for ease of interpretation only.

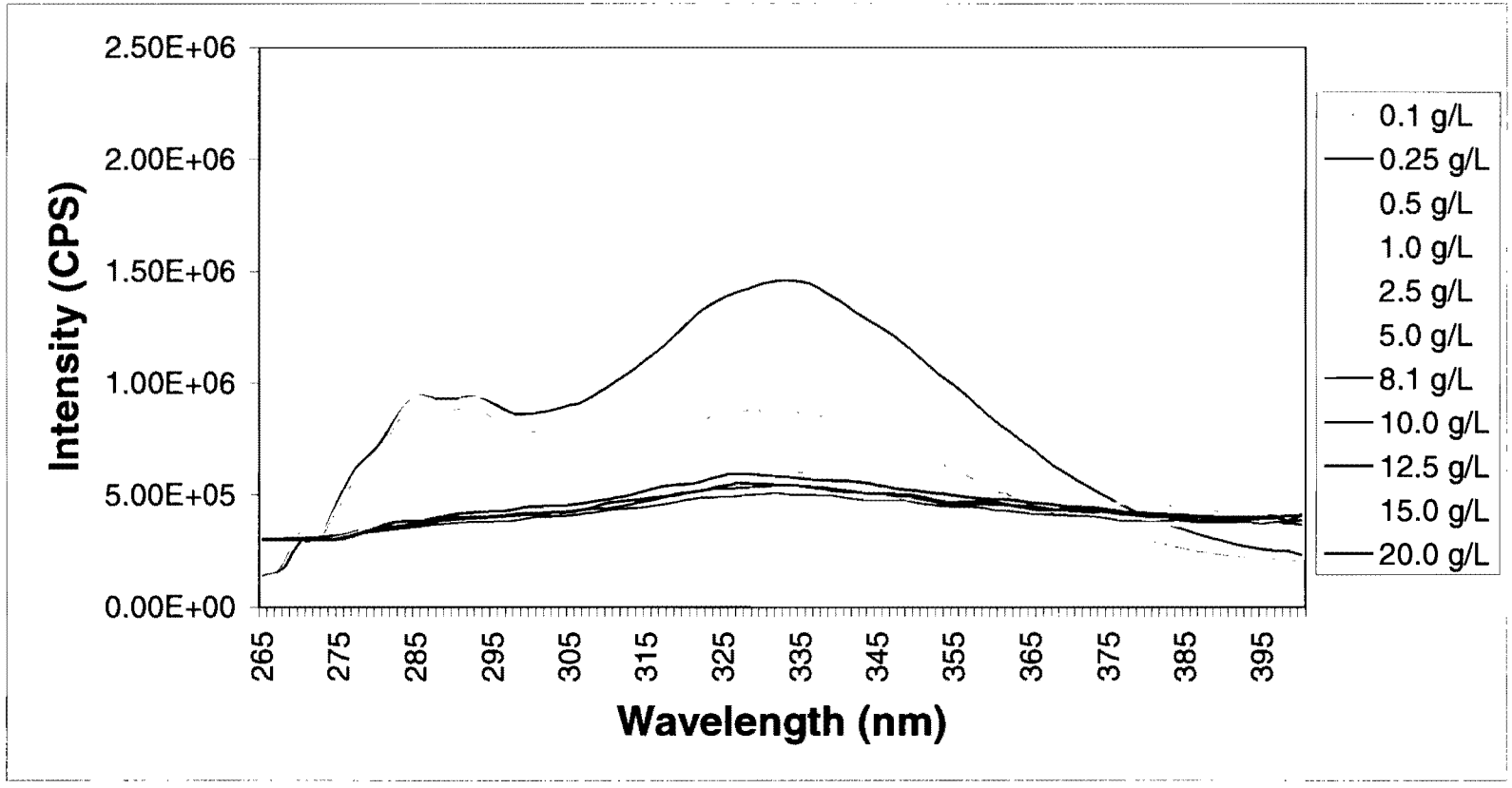

Figure 33. Fluorescence emission spectra for several concentrations of polystyrene (M_w = 1,571,000 D) in decalin at 20°C with the excitation monochromator set to 250 nm. The band at 283 nm is due to monomer emission while the band at 332 nm is due to excimer emission.

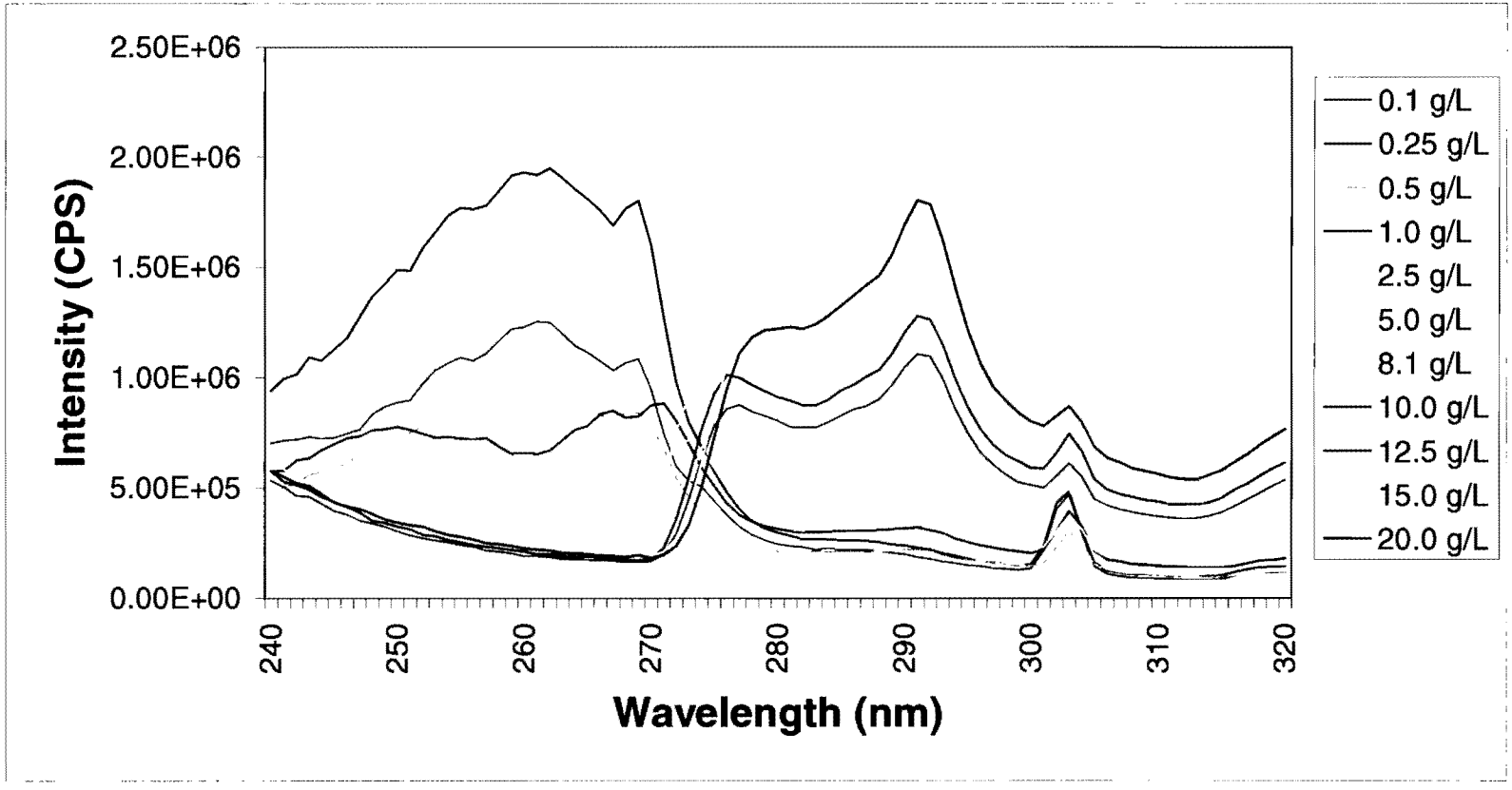

Figure 34. Fluorescence excitation spectra for several concentrations of polystyrene (M_w = 1,571,000 D) in decalin at 20°C with the emission monochromator set to 332 nm. The band at 291 nm is due to dimer complex excitation.

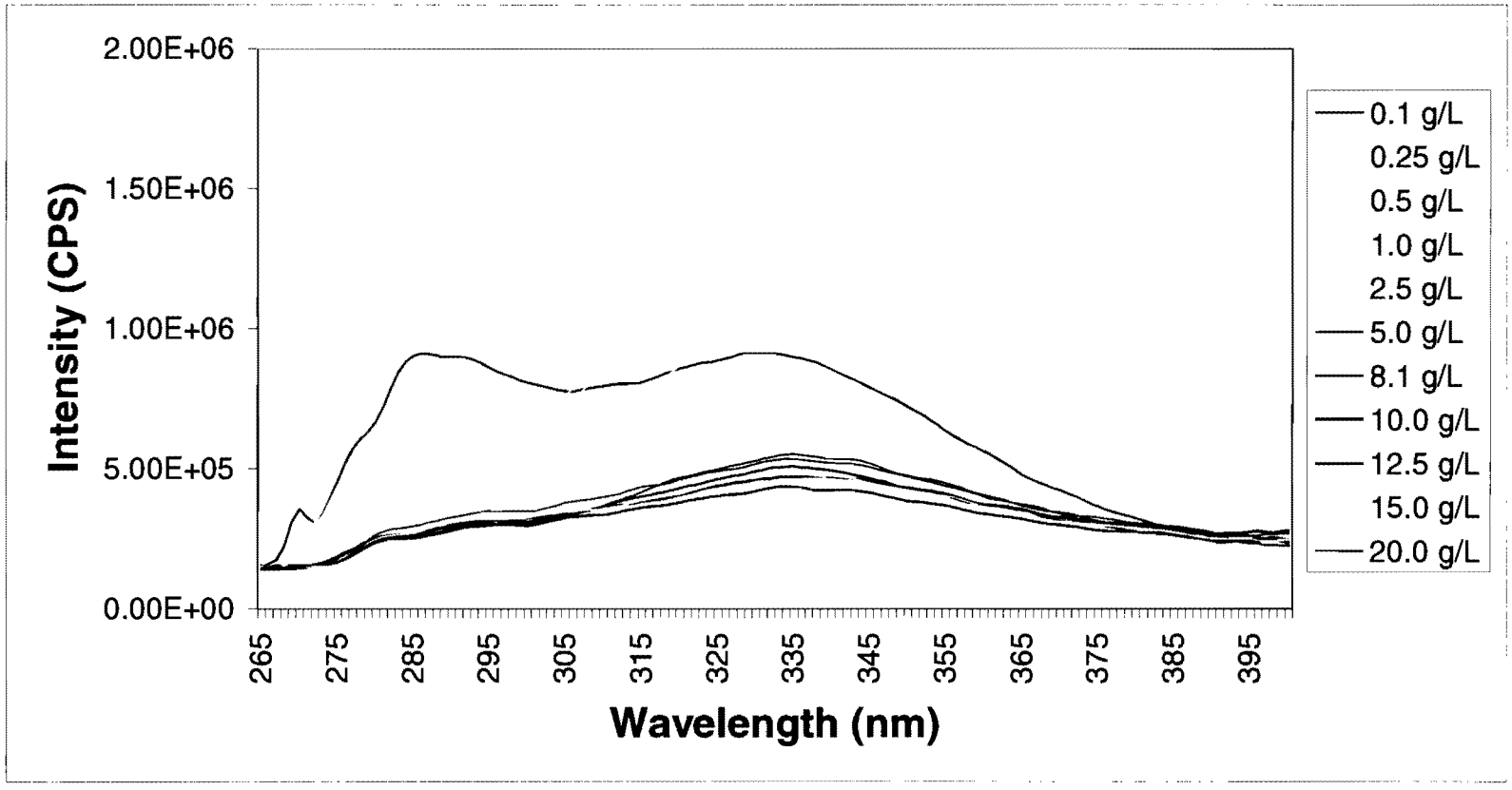

Figure 35. Fluorescence emission spectra for several concentrations of polystyrene (M_w = 1,571,000 D) in decalin at 30°C with the excitation monochromator set to 250 nm. The band at 283 nm is due to monomer emission while the band at 332 nm is due to excimer emission.

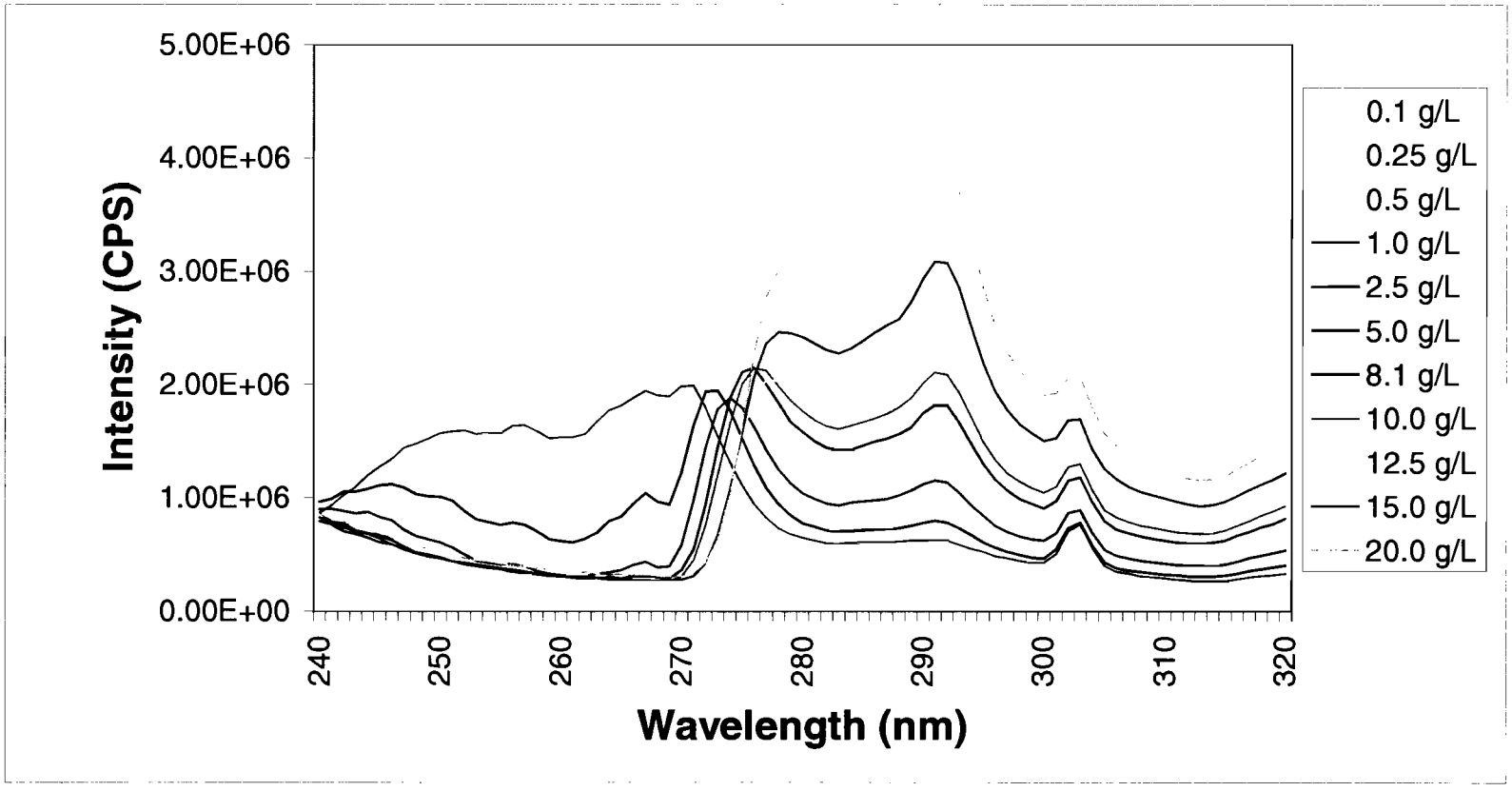

Figure 36. Fluorescence excitation spectra for several concentrations of polystyrene (M_w = 1,571,000 D) in decalin at 30°C with the emission monochromator set to 332 nm. The band at 291 nm is due to dimer complex excitation.

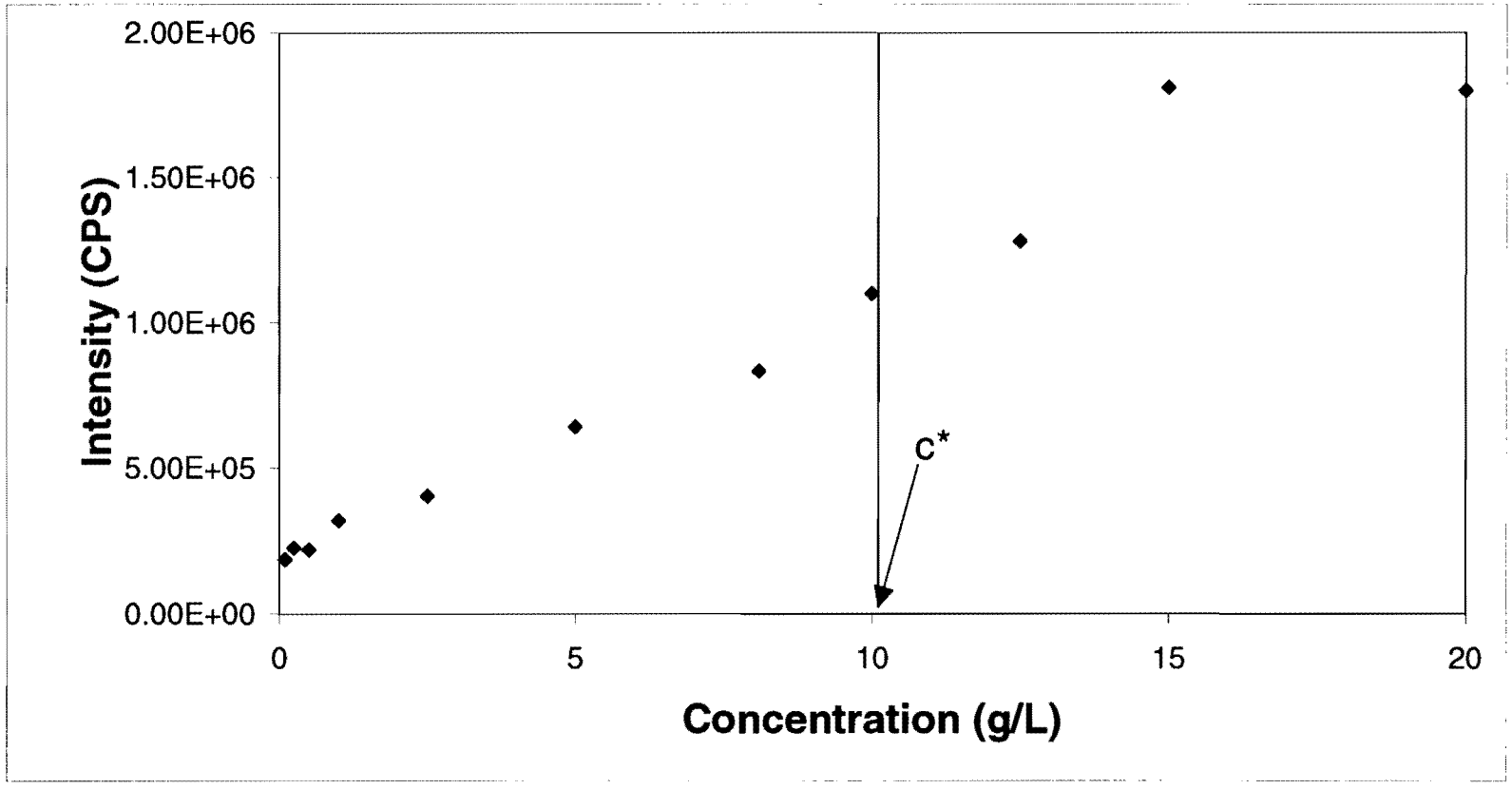

Figure 37. A plot of the uncorrected dimer complex intensity (I_{291}) vs. concentration for polystyrene (M_w = 1,571,000 D) in decalin at 20°C. The uncorrected dimer complex intensity increases with concentration but shows no change above the Mark-Houwink calculated c* value of 10.4 g/L. Measurement error is ± 9E+3 CPS.

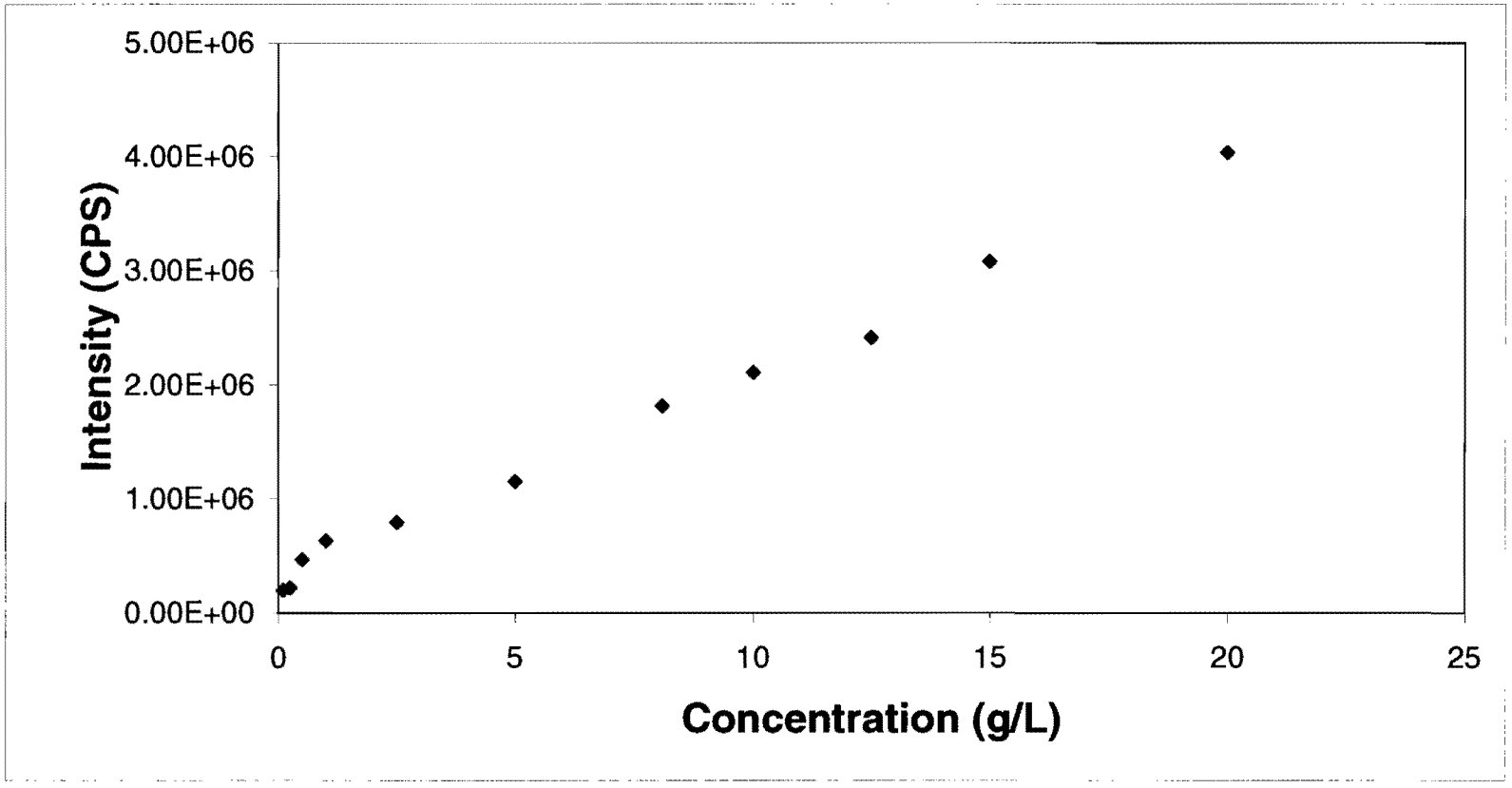

Figure 38. A plot of the uncorrected dimer complex intensity (I_{291}) vs. concentration for polystyrene (M_w = 1,571,000 D) in decalin at 30°C. The uncorrected dimer complex intensity increases with concentration but shows no change above c*. Measurement error is ± 9E+3 CPS.

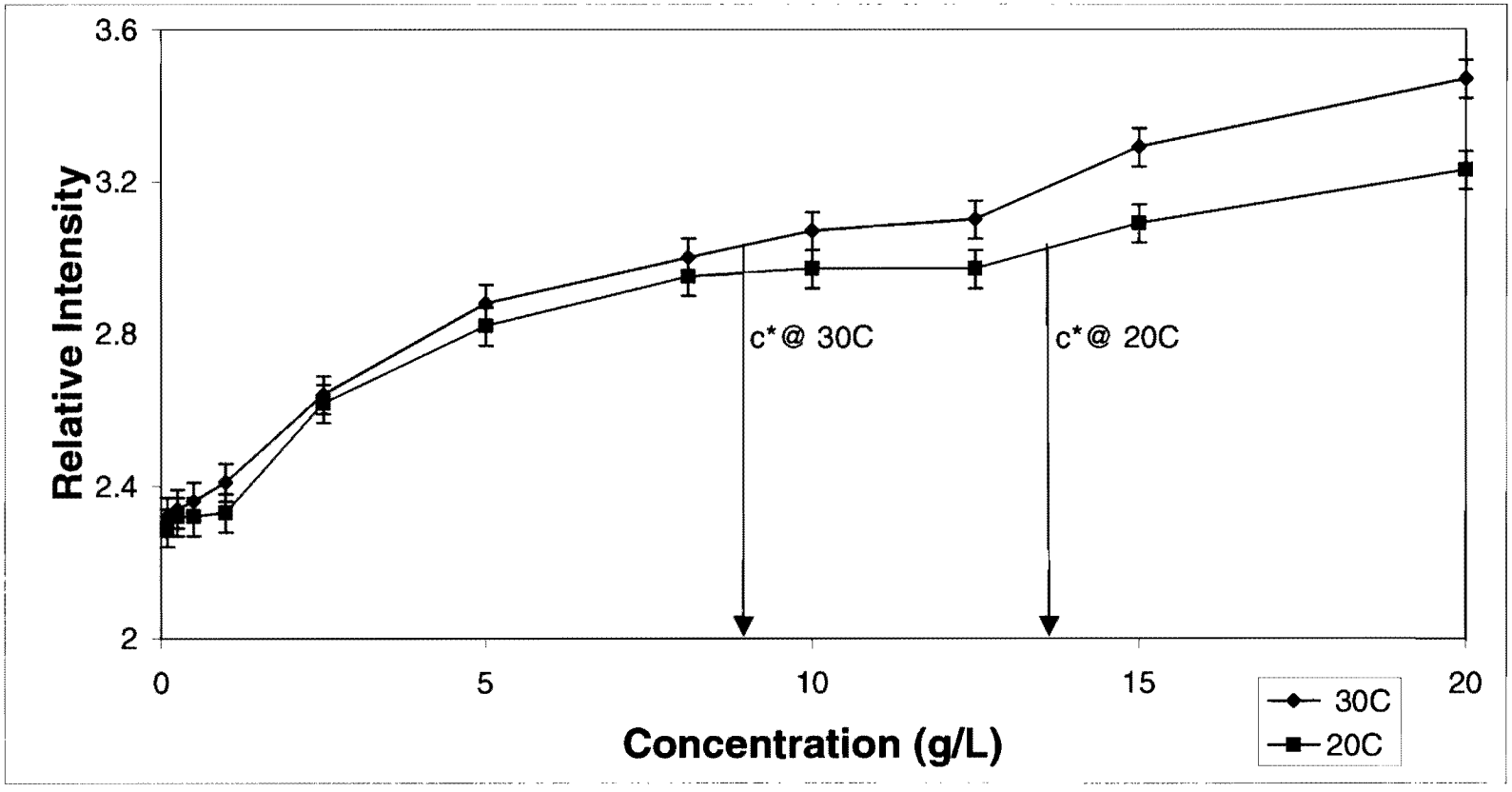

Figure 39. A plot of the corrected dimer complex intensity vs. concentration for polystyrene (M_w = 1,571,000 D) in decalin at 20°C and 30°C. c* is apparent between 12.5 and 15 g/L at 20°C and between 8 and 10 g/L at 30°C. With higher molecular weight samples at higher temperature, c* may be more difficult to determine. Lines connecting points are for ease of interpretation only.

with concentration with little change above c*. Figure 39 shows the corrected dimer complex intensity as a function of concentration for polystyrene (M_w = 1,571,000 D) in decalin at 20°C and 30°C. These plots show a similar shape to the smaller molecular weight polystyrene samples discussed earlier. At 20°C, c* is apparent between 12.5 and 15 g/L. At 30°C, the results are more difficult to read (as noted with the previous results) with c* apparent between 8 and 10 g/L.

B. Fluorescence of Controls

To prove the validity of the fluorescence results, control samples were evaluated. The positive control should be capable of forming excimers. Ethylbenzene was chosen as the positive control because polystyrene is a polymer comprised of repeating units of ethylbenzene. Benzene and its derivatives are known to form excimers at high concentrations which are detectable using fluorescence.[19] Therefore, at high concentrations ethylbenzene should be capable of forming both excimers and fluorescence emission due to ground state dimer formation which are detectable using fluorescence.

The fluorescence emission spectra for ethylbenzene in decalin at 20°C is shown in Figure 40. The results are similar to the polystyrene in decalin results with the emission due to monomer fluorescence at 285 nm and the excimer fluorescence emission at 332 nm. Because the monomer band is so intense at lower concentrations, Figure 40 does not display an intense excimer band. Even

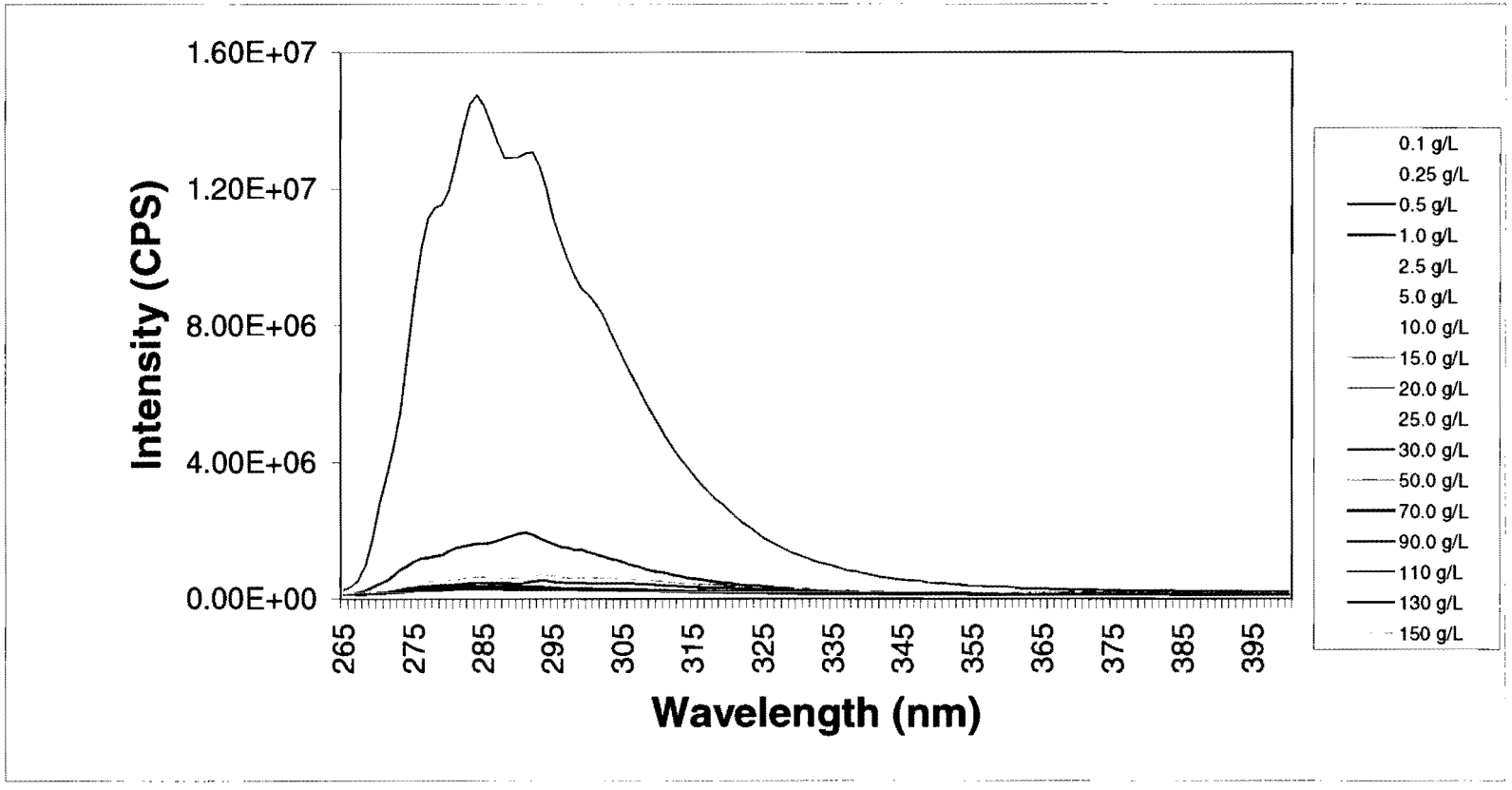

Figure 40. Fluorescence emission spectra for several concentrations of ethylbenzene in decalin at 20°C with the excitation monochromator set to 250 nm. The band at 285 nm is due to monomer emission while the band at 332 nm is due to excimer emission.

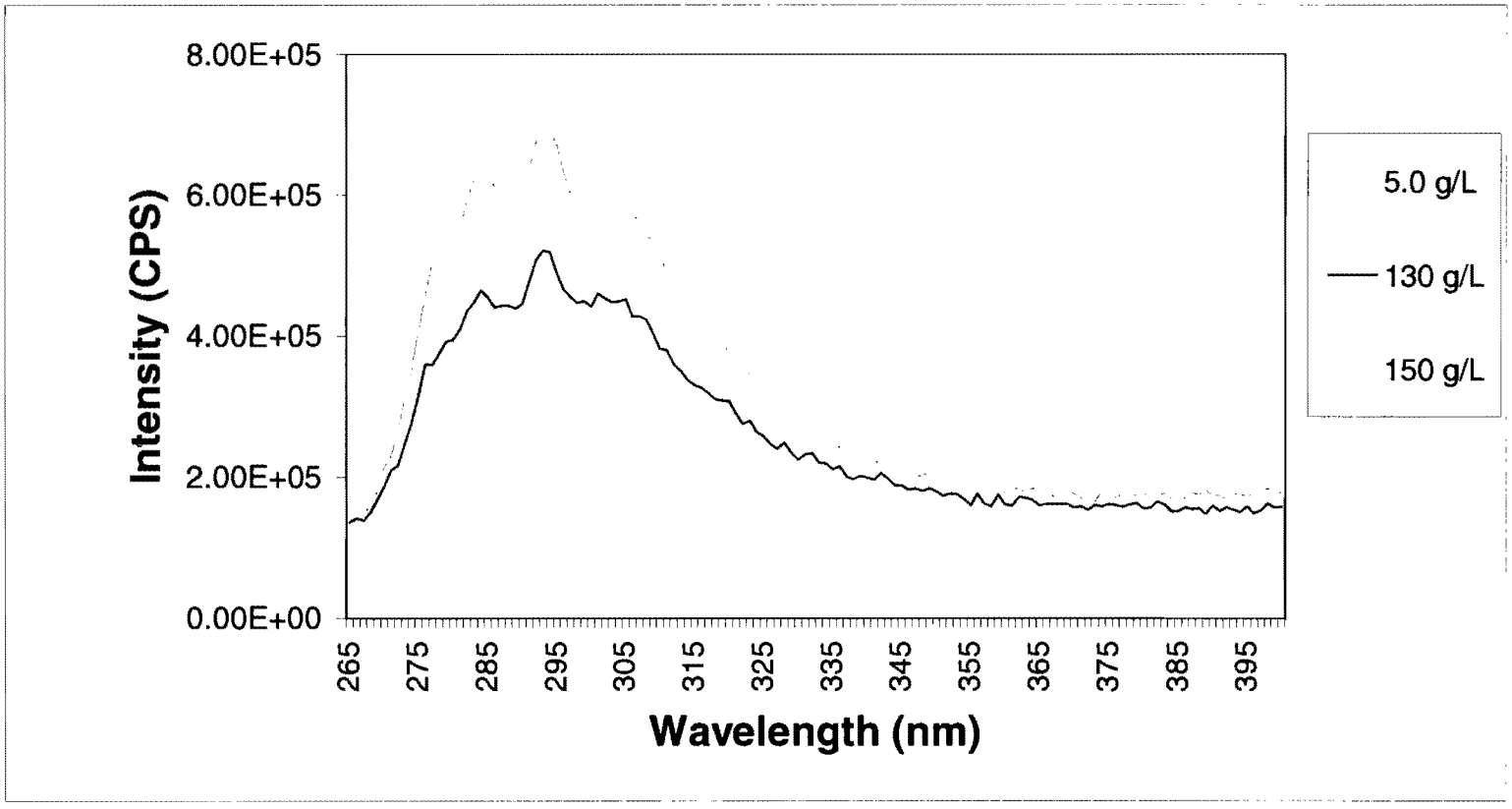

Figure 41. Fluorescence emission spectra for the higher concentrations of ethylbenzene in decalin at 20°C with the excitation monochromator set to 250 nm. The band at 285 nm is due to monomer emission while the band at 332 nm is due to excimer emission. The monomer band is very intense for ethylbenzene and obscures the excimer band.

when only high concentrations are observed (Figure 41), the excimer band is obscured by the very intense monomer band. Therefore, the excimer band was assumed to be at 332 nm as noted with the polystyrene samples.

Figure 42 shows fluorescence excitation spectra for ethylbenzene in decalin at 20°C with the emission monochromator set to the excimer wavelength of 332 nm. The dimer complex band appears at higher concentrations at 291 nm. A significant increase in intensity at 291 nm occurs at the two highest concentrations (130 and 150 g/L). This can be explained by the inability of ethylbenzene to form intramolecular excimers like polymers such as polystyrene can, only intermolecular interactions can occur. At dilute concentrations, intermolecular interactions between the benzene rings are minimal. When the concentration is such that the benzene rings are forced into contact (analogous to c* for polymers), the formation of excimers relative to concentration occurs rapidly. Also, because more dimers are present in the semi-dilute region and scattering is a function of particle size, these dimers will scatter more light and cause an increase in the fluorescence baseline. As a result, the transition from dilute concentrations to semi-dilute concentrations is more pronounced with ethylbenzene relative to polystyrene.

Figure 43 shows the uncorrected dimer complex intensity vs. concentration for ethylbenzene in decalin at 20°C. These results are similar to the polystyrene in decalin results showing I_{291} increasing with concentration. At higher concentrations (above 110 g/L), the intensity increases dramatically. However, it is interesting to note the shape of the corrected intensity vs.

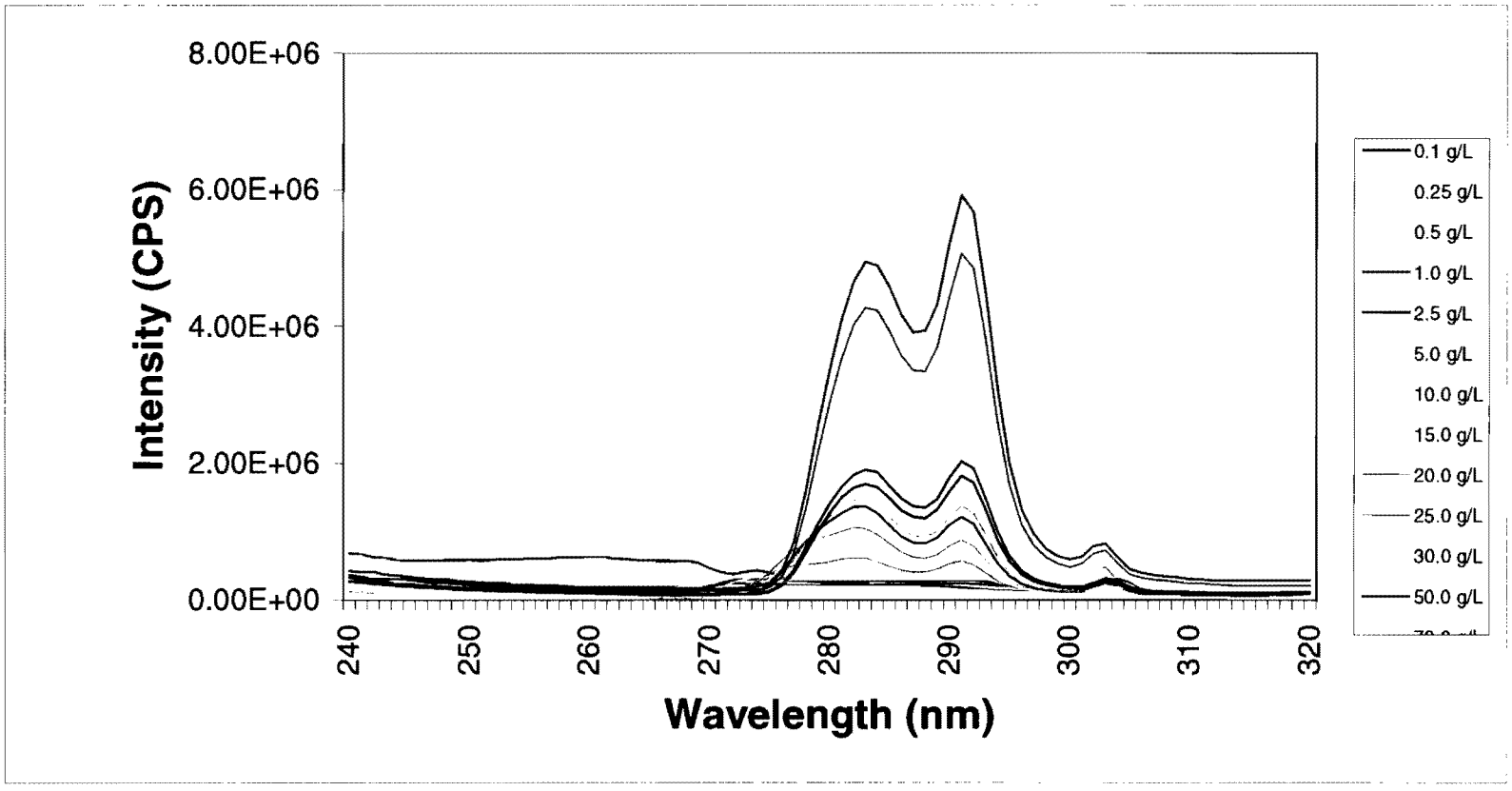

Figure 42. Fluorescence excitation spectra for several concentrations of ethylbenzene in decalin at 20°C with the emission monochromator set to 332 nm. The band at 291 nm is due to dimer complex excitation.

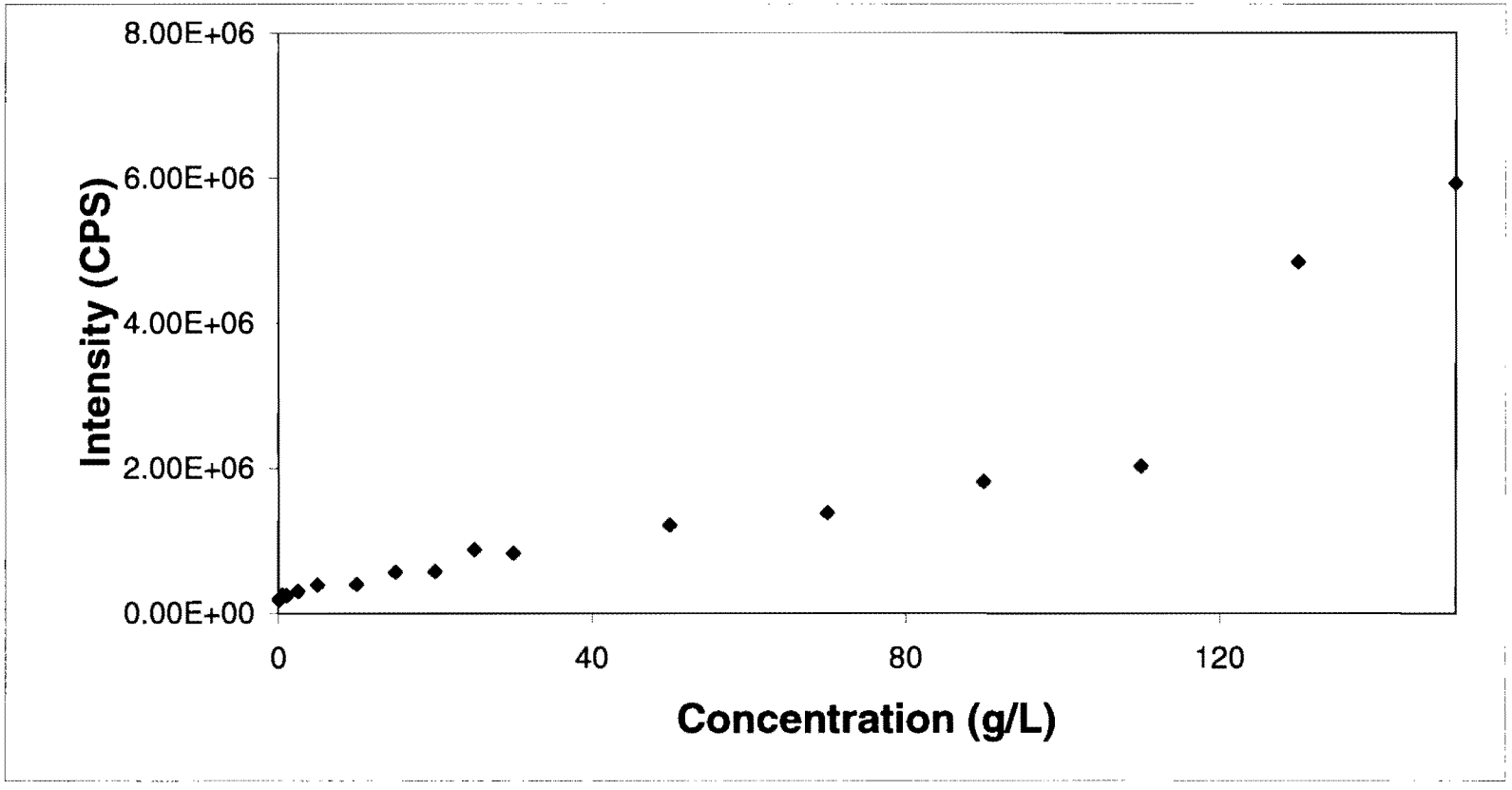

Figure 43. A plot of the uncorrected dimer complex intensity (I_{291}) vs. concentration for ethylbenzene in decalin at 20°C. The uncorrected dimer complex intensity increases with concentration up to high concentrations. Measurement error is approximately equal to the size of the point. The increase in uncorrected dimer complex intensity above 120 g/L is due to excessive scattering from the ground state dimers.

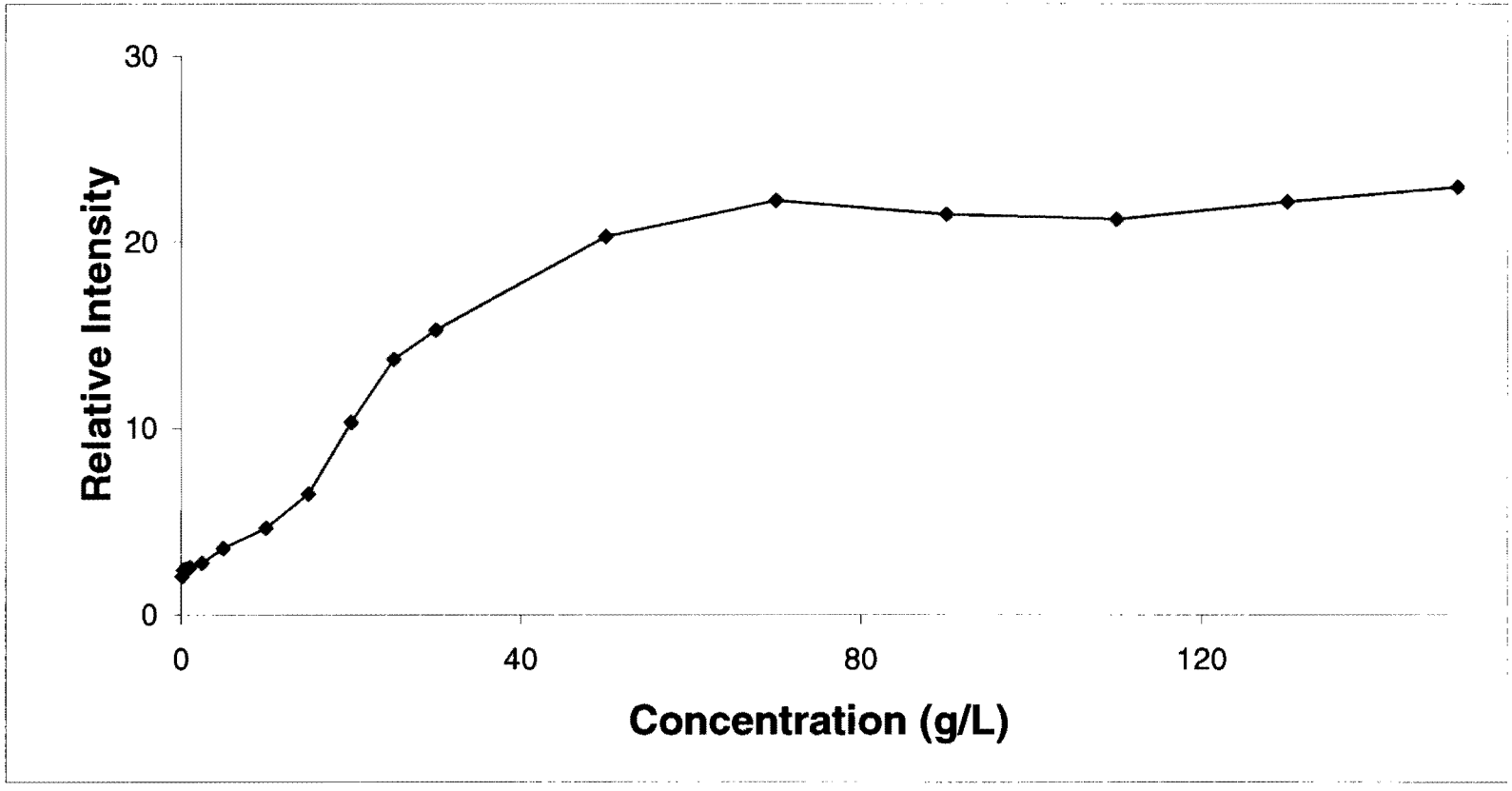

Figure 44. A plot of the corrected dimer complex intensity vs. concentration for ethylbenzene in decalin at 20°. The increase in corrected dimer complex intensity above 110 g/L is attributed to the transition between dilute and semi-dilute concentrations. Line connecting points are for ease of interpretation only.

concentration plot (Figure 44) appears similar to the polystyrene in decalin results, with no excessive deviations at higher concentrations. Because these results are corrected for scattering, it confirms the significant increases in dimer complex intensity noted in Figures 42 and 43 at high concentrations are the result of scattering due to the formation of dimers.

A good negative control for these fluorescence experiments would eliminate the ability of the benzene rings to interact and form dimer complexes or excimers. By attaching bulky groups to a benzene ring, it would be more difficult for the rings to get close enough to form excimers or dimer complexes due to steric hindrance. 1,3,5 tri-t-butyl benzene was chosen because the t-butyl groups are in the 1, 3, and 5 positions should provide enough steric hindrance to separate the benzene rings thereby providing resistance to interactions between rings.

Figure 45 shows the fluorescence emission spectra for 1,3,5 tri-t-butyl benzene in decalin for several concentrations at 20°C with the excitation monochromator set to 250 nm. The band at 295 nm is attributed to monomer emission and the band at 350 nm is attributed to excimer emission.

The fluorescence excitation spectra for 1,3,5 tri-t-butyl benzene in decalin for several concentrations at 20°C with the emission monochromator set to 350 nm showed excessive fluorescence at high concentrations. This excessive fluorescence intensity caused the photon counter to saturate as the intensity exceeded 1×10^6 cps. When the photon counter becomes saturated, the response is no longer linear and therefore the results were not reliable so a

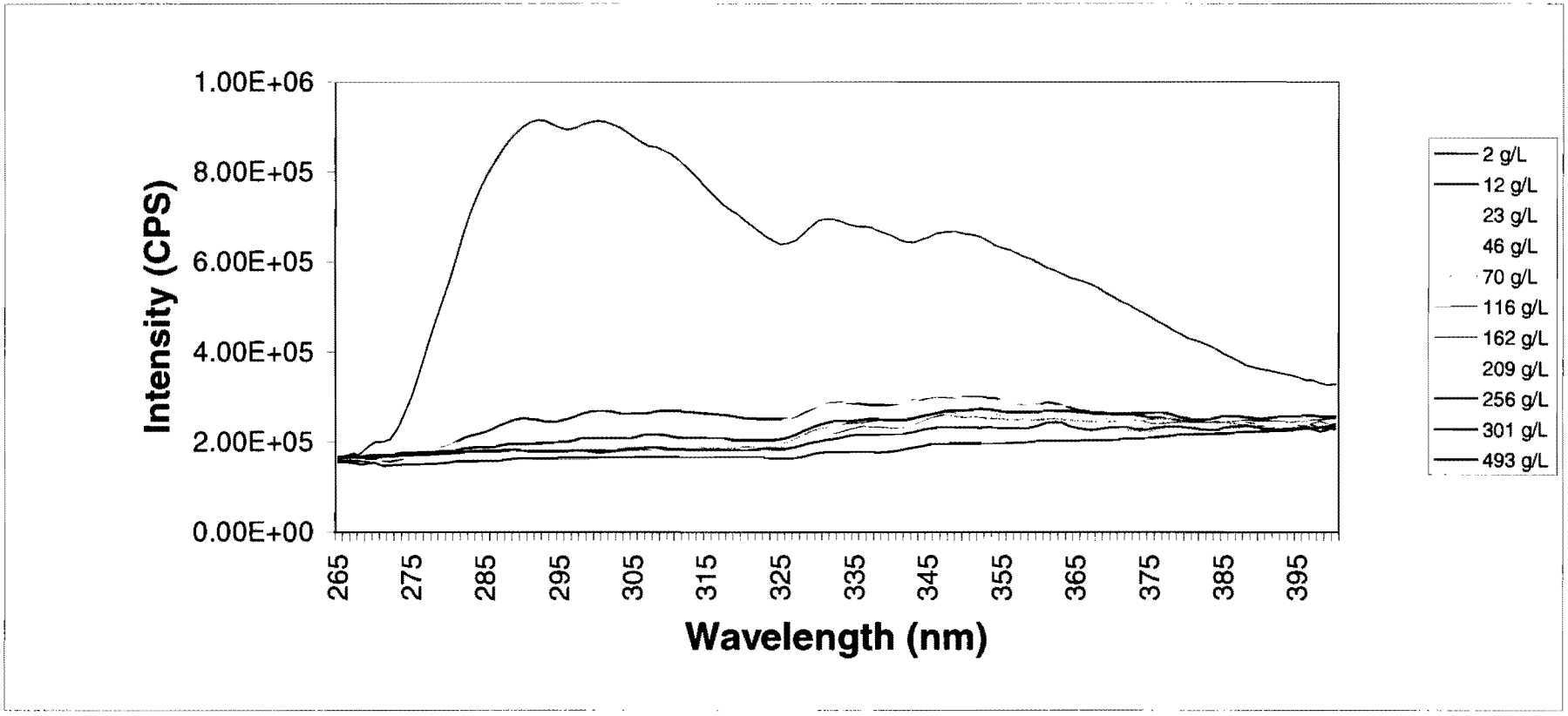

Figure 45. Fluorescence emission spectra for several concentrations of 1,3,5 tri-t-butyl benzene in decalin at 20°C with the excitation monochromator set to 250 nm. The band at 295 nm is attributed to monomer emission and the band at 350 nm is attributed to excimer emission.

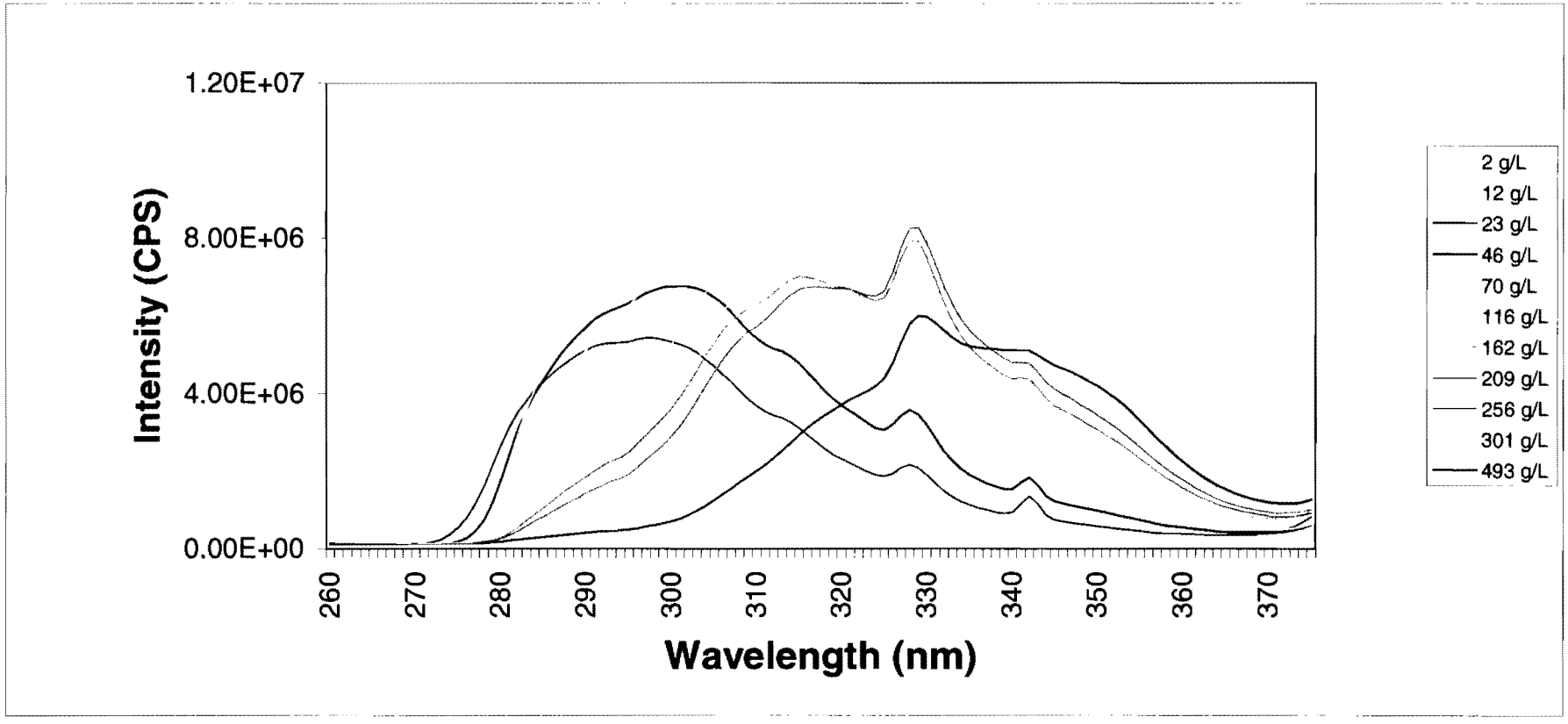

Figure 46. Fluorescence excitation spectra for several concentrations of 1,3,5 tri-t-butyl benzene in decalin at 20°C with the emission monochromator set to 380 nm. The band at 328 nm is due to dimer complex excitation.

means of decreasing the intensity was needed. To accomplish this, the emission monochromator was set 30 nm from the excimer λ_{max} of 350 to 380 nm. The resulting spectra are shown in Figure 46. The band that appears at 328 nm at higher concentrations is attributed to the formation of dimer complexes. Therefore, the bulky t-butyl groups are not able keep the benzene rings far enough apart to prevent the formation of excimers at high concentrations. It is possible that at high concentrations the t-butyl groups on neighboring chromophores can stagger and allow the rings to get close enough to interact with each other thereby forming dimer cornplexes.

A plot of the uncorrected dimer complex intensity for 1,3,5 tri-t-butyl benzene in decalin vs. concentration is shown in Figure 47. At concentrations below 116 g/L, this plot is similar to the polystyrene in decalin results where the points increase somewhat linearly with concentration. At concentrations above 116 g/L the intensity increases only slightly with concentration and forms a plateau until the concentration reaches approximately 256 g/L. This plateau is due to bulky t-butyl groups keeping the benzene rings apart and hindering the formation of dimer complexes even at relatively high concentrations. However, above 256 g/L the intensity begins to increase more dramatically which is attributed to the t-butyl groups staggering on neighboring rings thereby allowing the rings to get close enough to interact at high concentration. These interactions allow the formation of dimer complexes. The decreased intensity at 493 g/L is attributed to self-absorbance by the 1,3,5 tri-t-butyl benzene in highly concentrated yellow solution.

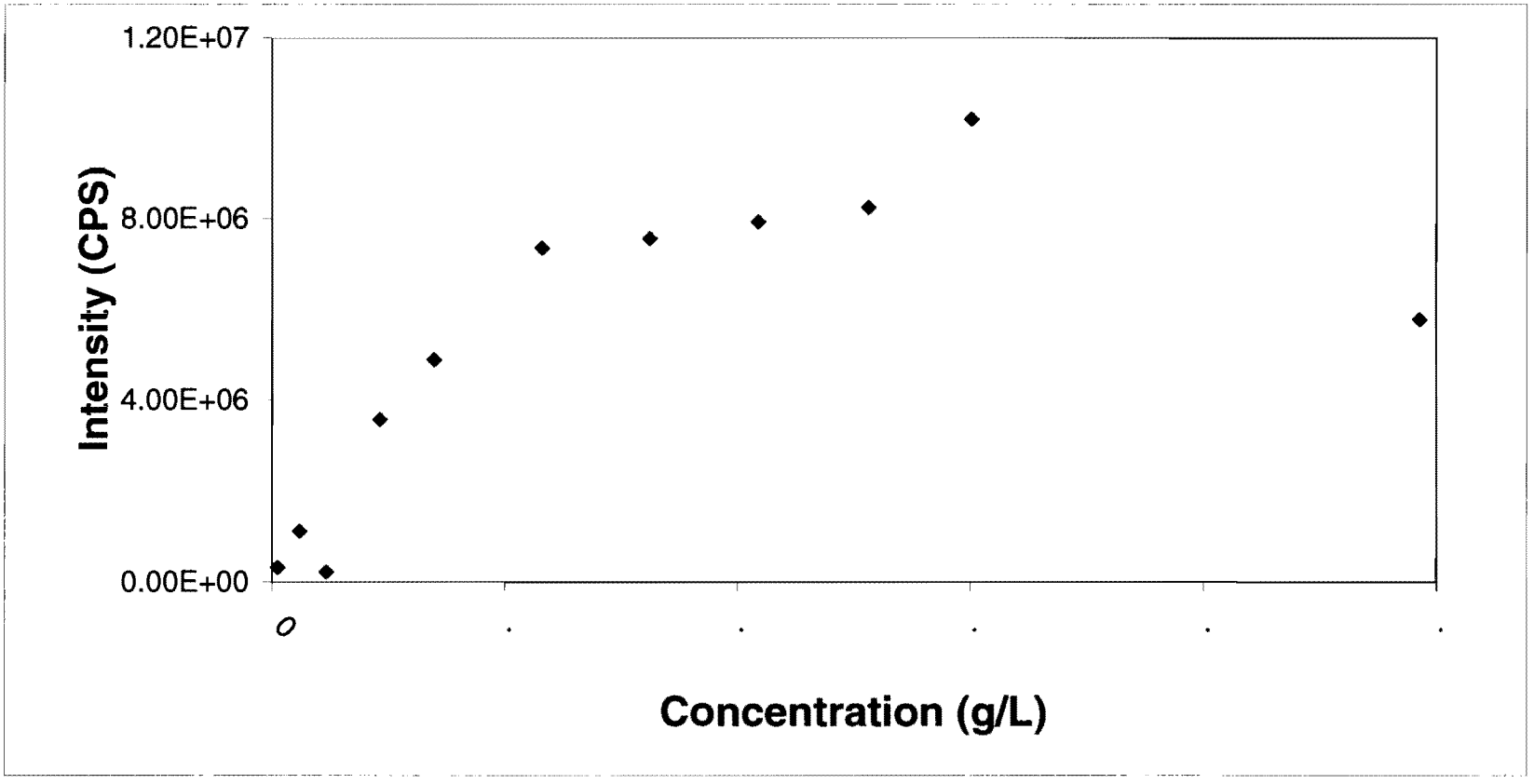

Figure 47. A plot of the uncorrected dimer complex intensity vs. concentration for 1,3,5 tri-t-butyl benzene in decalin at 20°. Below 116 g/L the uncorrected dimer complex intensity increases linearly with concentration. The plateau between 116 g/L and 256 g/L is attributed to decreased dimer complex formation due to the bulky t-butyl groups. The decrease at 493 g/L is attributed to self-absorbance at high concentrations.

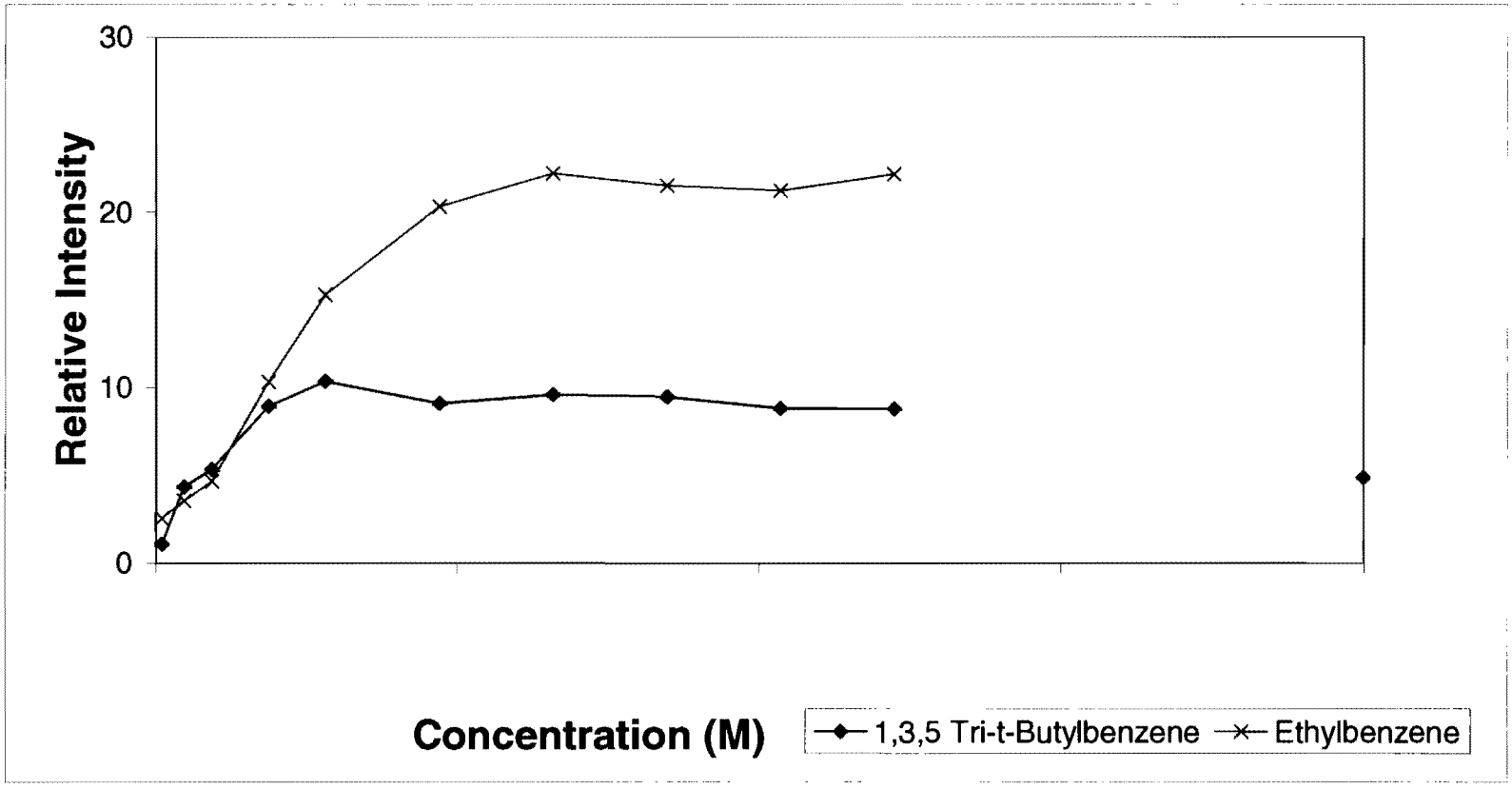

Figure 48. A plot of the corrected dimer complex intensity vs. concentration for 1,3,5 tri-t-butyl benzene and ethylbenzene in decalin at 20°. The increase in corrected dimer complex intensity above 1M for ethylbenzene corresponds to the transition from dilute to semi-dilute concentrations and is not apparent for 1,3,5 tri-t-butyl benzene. Concentrations converted to molarity to correct for differences in molecular weights. Error in the relative intensity is ± 0.5. Lines connecting points are for ease of interpretation only.

Figure 48 shows the corrected dimer complex intensity for both 1,3,5 tri-t-butyl benzene and ethylbenzene in decalin at 20°C. Concentrations converted to molarity to correct for differences in the molecular weights. The ethylbenzene data points show the transition between dilute and semi-dilute concentrations above 1 M. However, the 1,3,5 tri-t-butyl benzene data does not show the increase in corrected dimer complex intensity above 1 M which was noted with ethylbenzene. Although the t-butyl groups are not able to completely eliminate the formation of dimer complexes, this data shows they are able to hinder the formation of dimer complexes at concentrations where the positive control, ethylbenzene, could not.

C. Fluorescence of Polycarbonate in Dichloromethane

To determine the flexibility of this method, three molecular weights of poly(bisphenol A) carbonate in dichloromethane were also studied at 25°C. With the chromophores located in the backbone of the polymer as opposed to the pendant chromophores of polystyrene, it is expected that interactions between the phenol rings and hence the formation of dimer complexes, should be more difficult. Using fluorescence emission spectroscopy with the excitation monochromator set to 250 nm for poly(bisphenol A) carbonate (M_w = 24,400) in dichloromethane at 25°C, a monomer emission band was located at 290 nm and an excimer emission band at 350 nm as shown in Figure 49. This is a notable

red shift from the polystyrene in decalin samples where the monomer emission band was located at 283 nm and the excimer emission band at 332 nm. This red shift is the result of the para-substitution of the benzene rings for poly(bisphenol A) carbonate vs. the mono-substitution for polystyrene. This di-substitution lowers the energy requirement of the ring system and causes the fluorescence of the monomer as well as the excimer to occur at lower energy than with polystyrene. The greater red shift for the excimer emission (18 nm) vs. the monomer emission (7 nm) is observed because the excimers for poly (bisphenol A) carbonate are the result of four rings interacting instead of two benzene rings interacting as with polystyrene.

Because the monomer peak is very intense at lower concentrations, it causes the excimer peak to be difficult to read at higher concentrations. Figure 50 shows the fluorescence emission spectra of the more concentrated samples of poly(bisphenol A) carbonate in dichloromethane to better discern the excimer peak at 350 nm. These signals appear more noisy than Figure 49 because of the lower intensity of the signal and hence lower signal to noise ratio.

The fluorescence excitation spectra for poly(bisphenol A) carbonate in dichloromethane with the emission monochromator set to the excimer peak at 350 nm shows excessive fluorescence intensity at higher concentrations. To avoid saturating the quantum counter, the fluorescence excitation spectra for poly(bisphenol A) carbonate was performed with the emission monochromator set to 360 nm, 10 nm from the excimer λ_{max}. Poly(bisphenol A) carbonate (M_w = 24,400) was the first studied and shows a strong dimer complex band at 307 nm

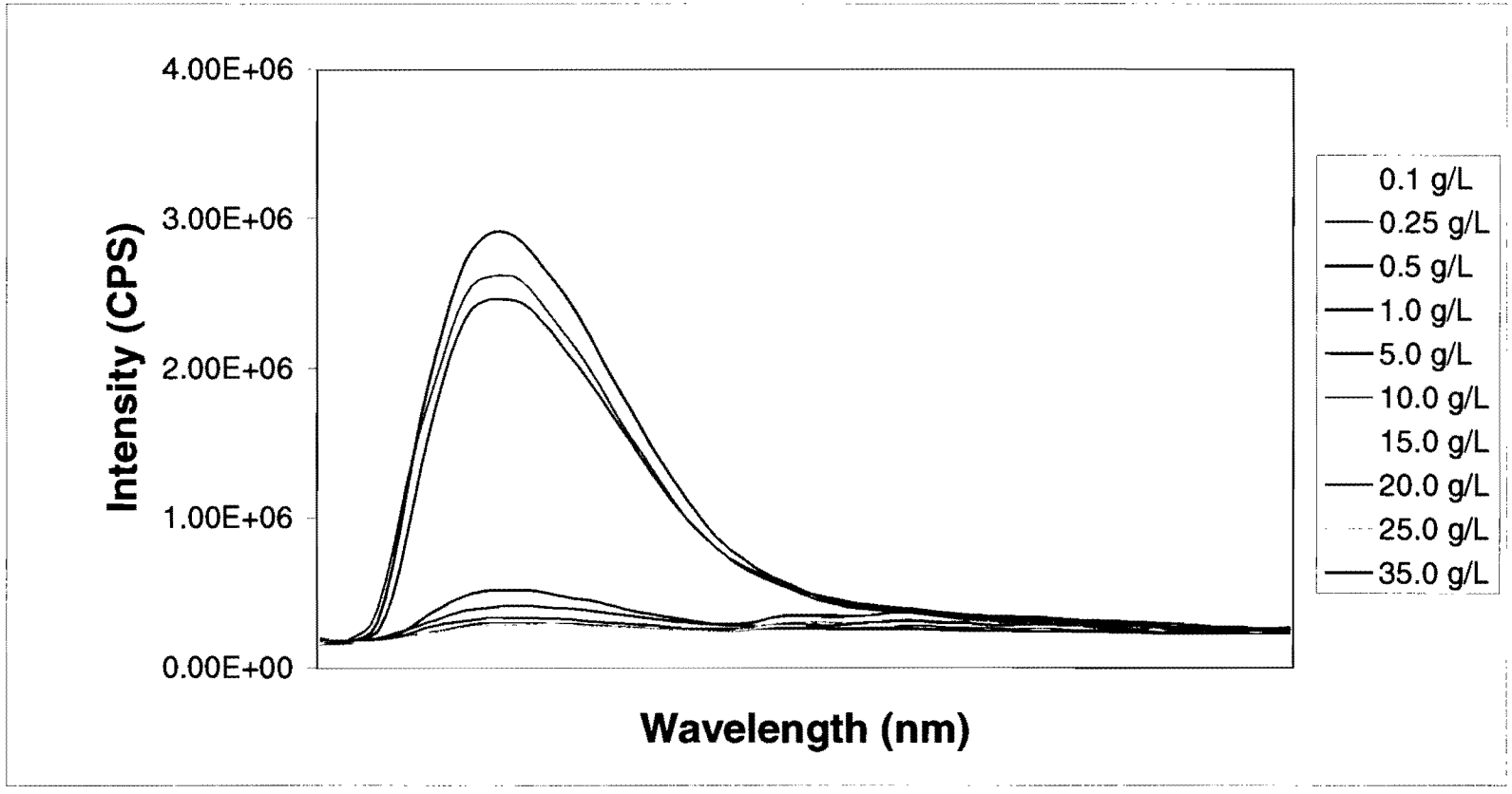

Figure 49. Fluorescence emission spectra for several concentrations of poly (bisphenol A) carbonate (M_w = 24,400) in dichloromethane at 25°C with the excitation monochromator set to 250 nm. The band at 290 nm is due to monomer emission while the band at 350 nm is due to excimer emission.

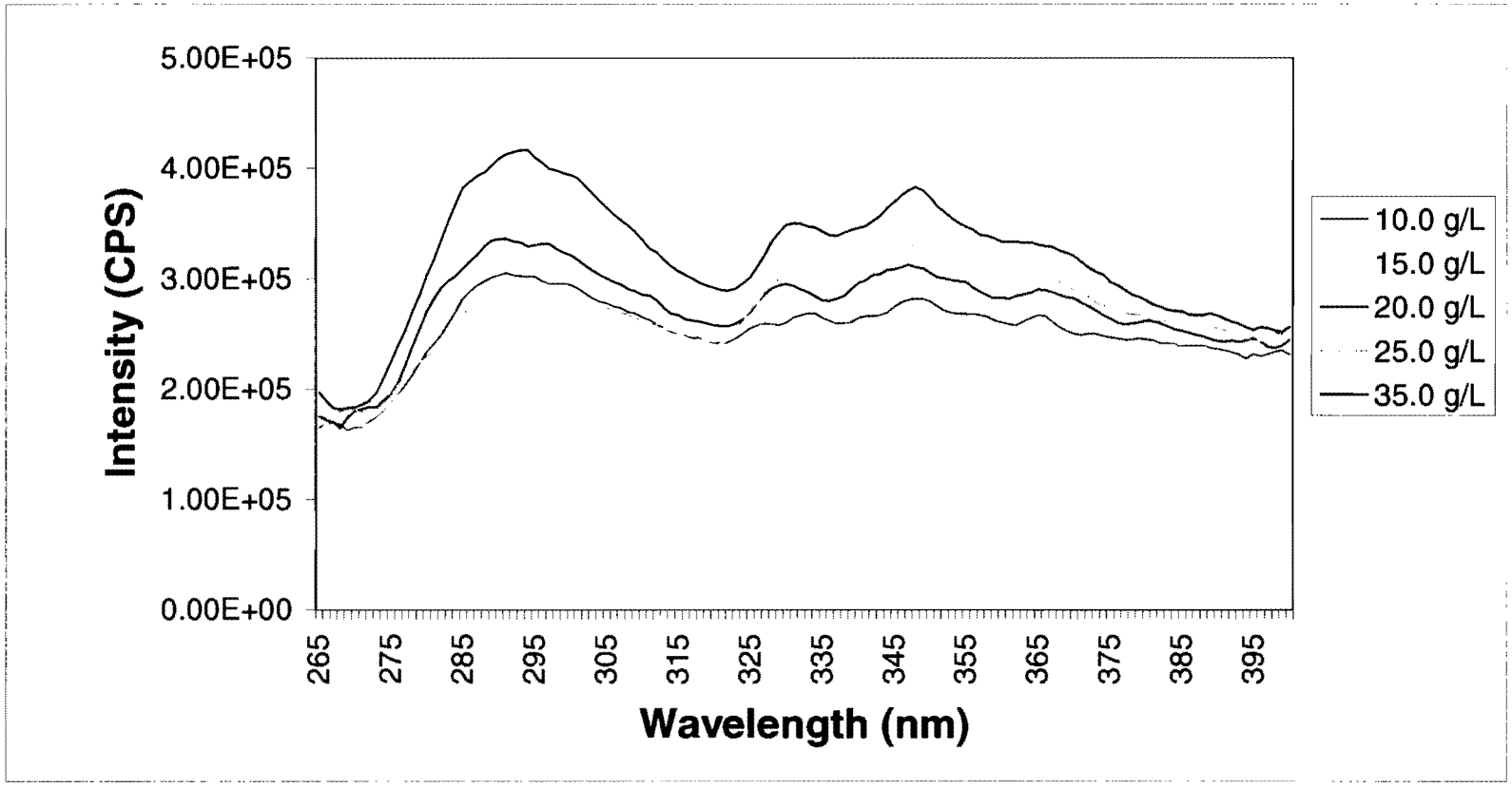

Figure 50. Fluorescence emission spectra for higher concentrations of poly (bisphenol A) carbonate (M_w = 24,400) in dichloromethane at 25°C with the excitation monochromator set to 250 nm. The band at 290 nm is due to monomer emission while the band at 350 nm is due to excimer emission.

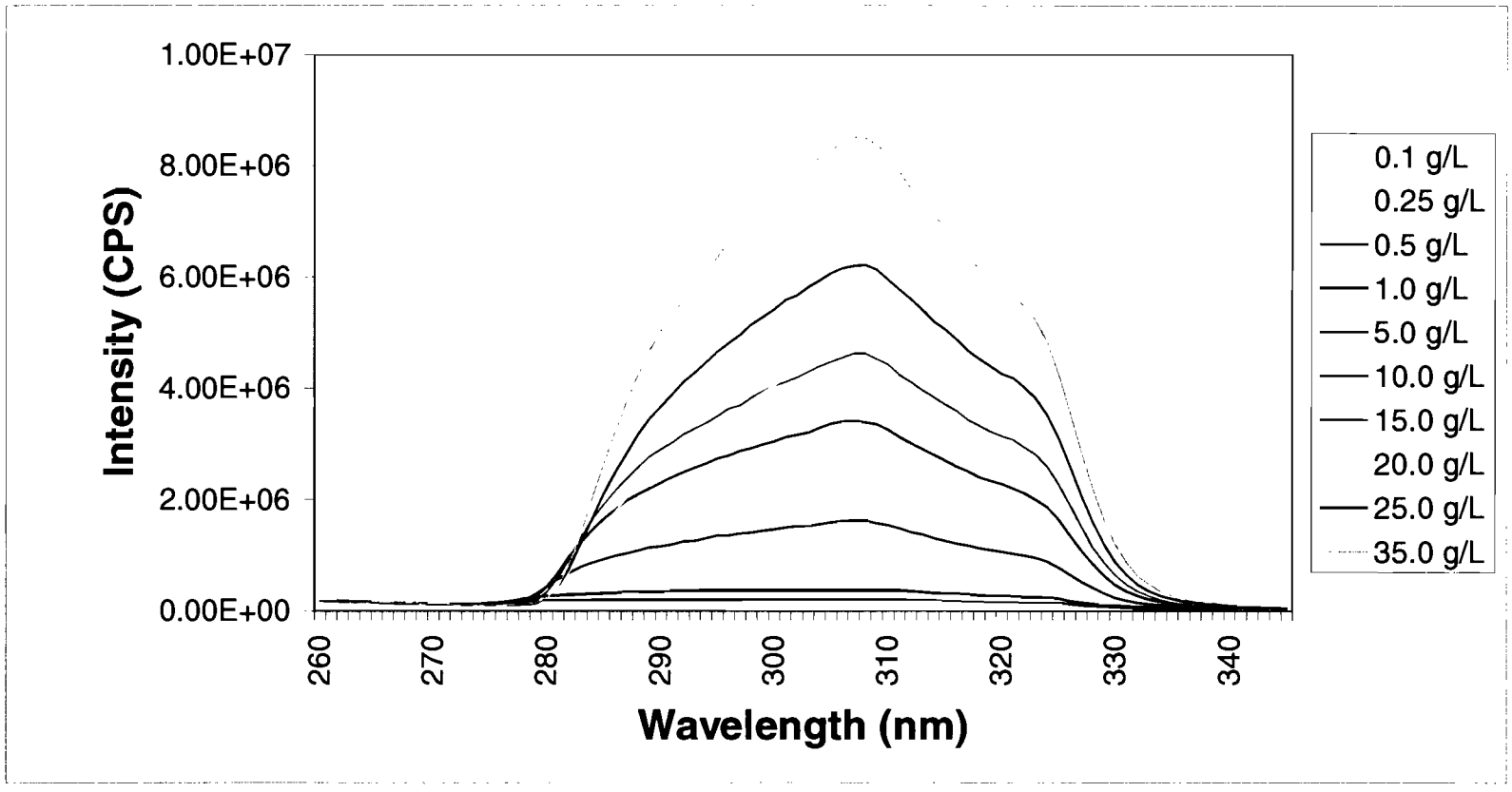

Figure 51. Fluorescence excitation spectra for several concentrations of poly (bisphenol A) carbonate (M_w = 24,400) in dichloromethane at 25°C with the emission monochromator set to 360 nm. The band at 307 nm is due to dimer complex excitation.

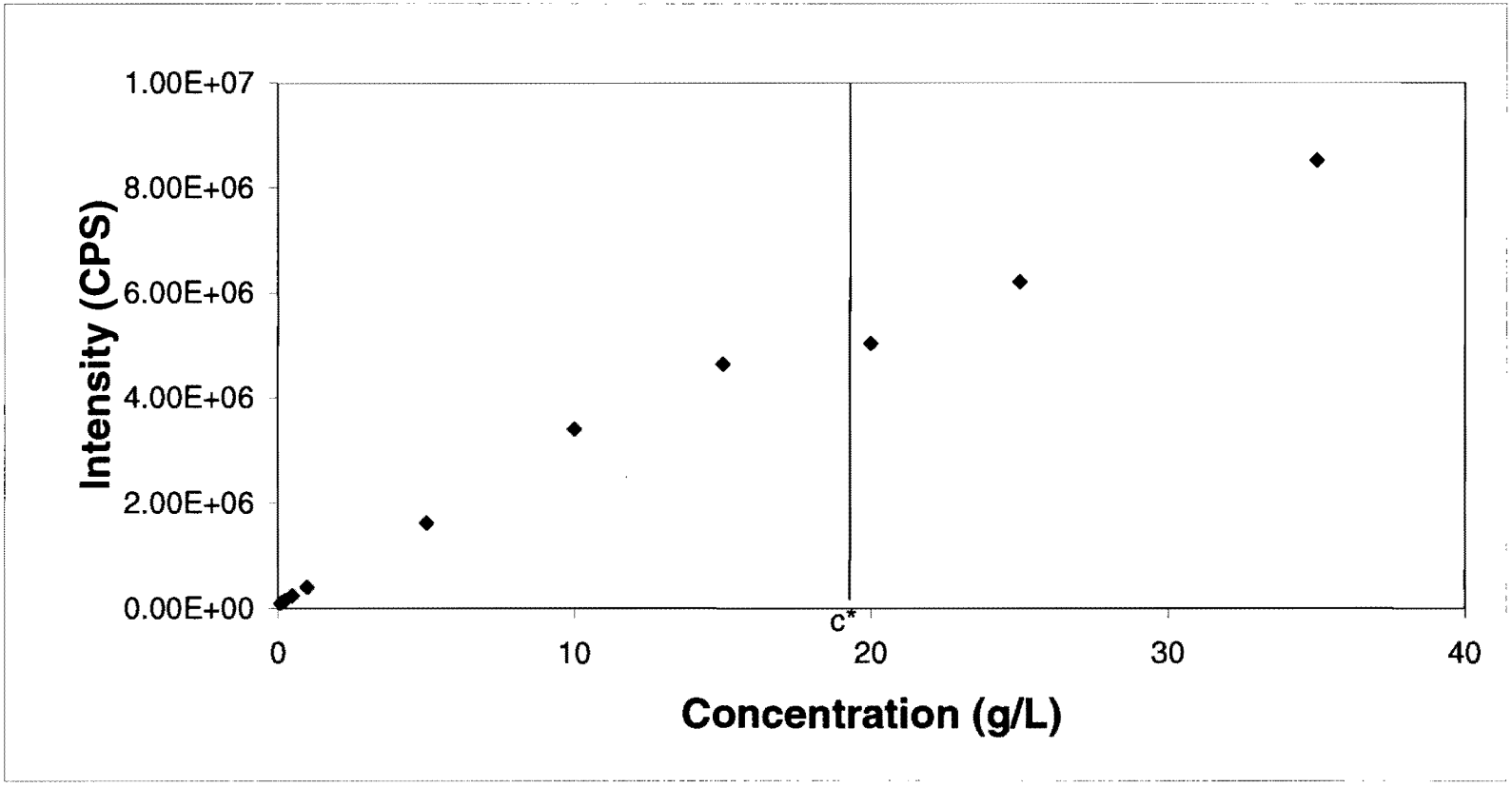

Figure 52. A plot of the uncorrected dimer complex intensity (I_{307}) vs. concentration for poly (bisphenol A) carbonate (M_w = 24,400) in dichloromethane at 25°C. The uncorrected dimer complex intensity increases with concentration but shows no change above the Mark-Houwink calculated c* value of 19 g/L. Measurement error is ± 1E+4 CPS.

as shown in Figure 51. Because there is no emission due to excimer formation at 339 nm, that wavelength was used as a baseline to correct the dimer complex data for scattering effects.

The uncorrected dimer complex fluorescence emission vs. concentration plot for poly(bisphenol A) carbonate (M_w = 24,400) in dichloromethane is shown in Figure 52. These results are similar to the polystyrene in decalin results discussed earlier with the uncorrected dimer complex emission increasing with concentration but showing little change above the Mark-Houwink calculated c* value of 19 g/L.

The plot of the corrected dimer complex fluorescence emission vs. concentration for poly(bisphenol A) carbonate (M_w = 24,400) in dichloromethane is shown in Figure 53. The dimer complex fluorescence is corrected for scattering by dividing the dimer complex band at 307 nm with the baseline at 339 nm. These results are also similar to the polystyrene results presented earlier with the corrected intensity increasing with concentration at lower concentrations followed by a plateau. At 20 g/L, the corrected dimer complex intensity begins to increase at a more significant rate. This is due to the increased inter and intramolecular interactions which occur above c*. Therefore, this plot shows the fluorescence derived c* for polycarbonate (Mw = 24,400) in dichloromethane at 25°C to be between 20 and 25 g/L.

Figure 54 shows the fluorescence excitation spectra for several concentrations of poly(bisphenol A) carbonate (M_w = 30,900) in dichloromethane at 25°C. As with the lower molecular weight polycarbonate, the emission

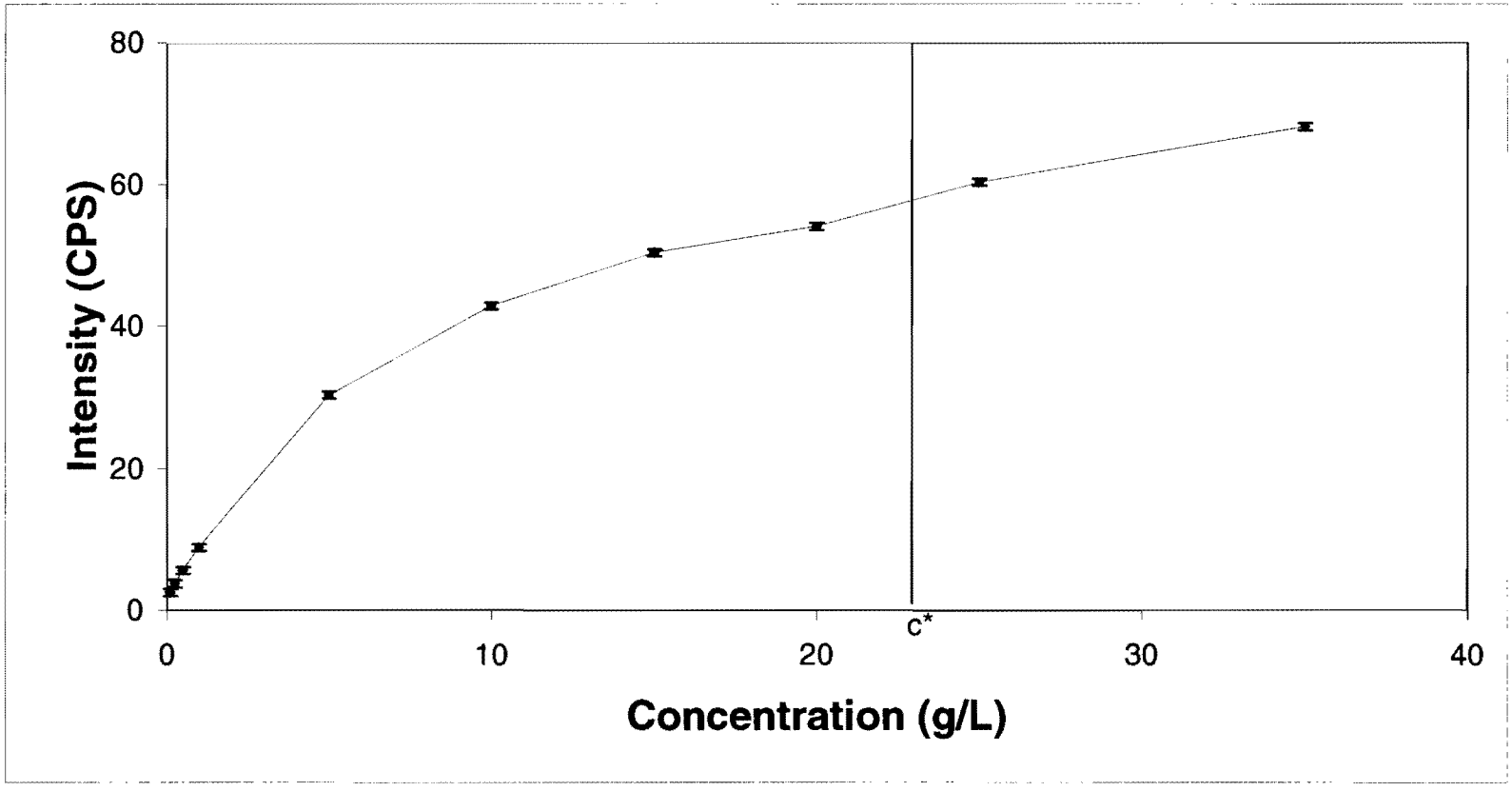

Figure 53. A plot of the corrected dimer complex intensity (I_{307}/I_{339}) vs. concentration for poly (bisphenol A) carbonate (M_w = 24,400) in dichloromethane at 25°. The increase in corrected dimer complex intensity above 20 g/L is attributed to the transition between dilute and semi-dilute concentrations. Lines connecting points are for ease of interpretation only.

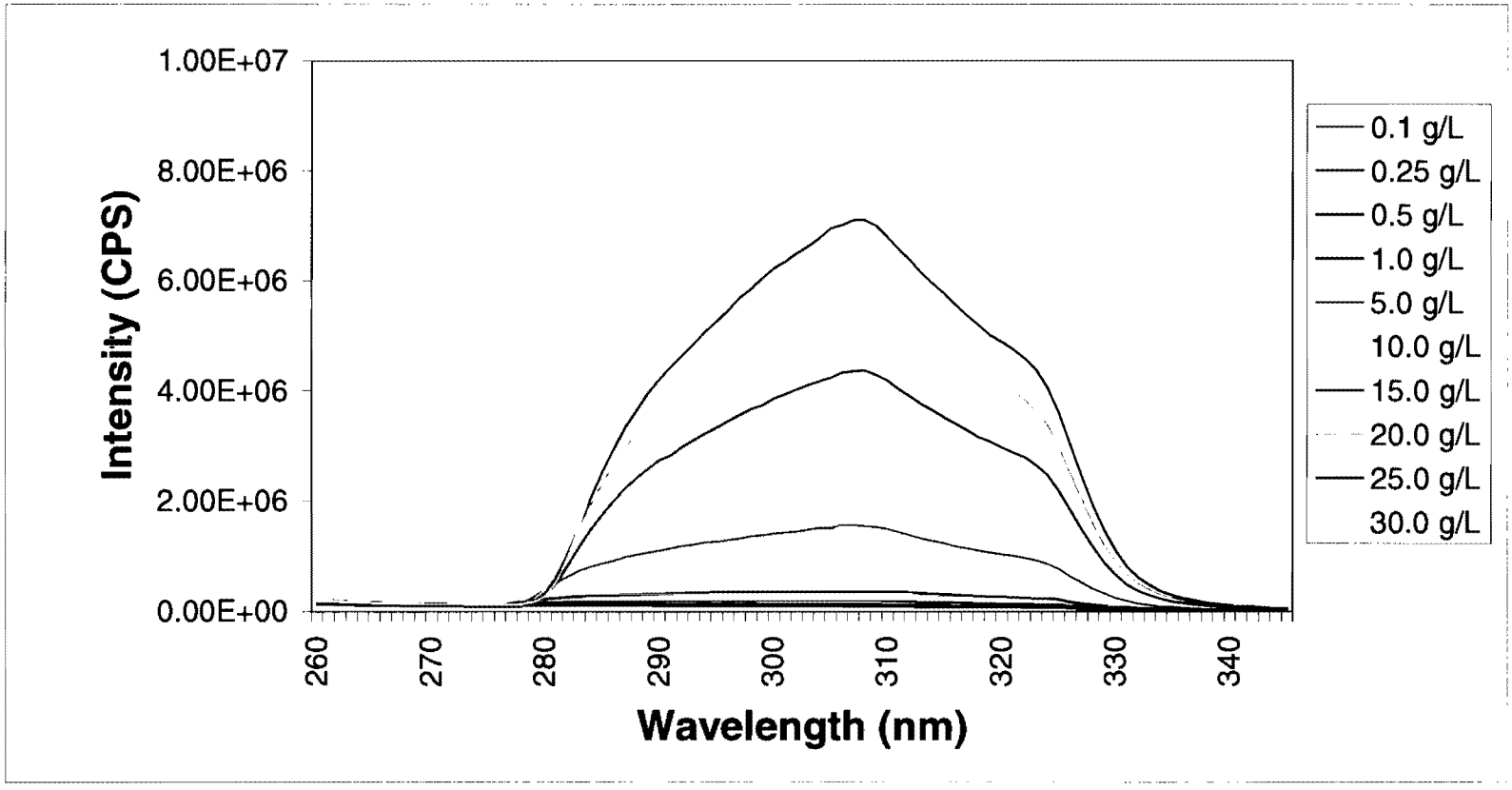

Figure 54. Fluorescence excitation spectra for several concentrations of poly (bisphenol A) carbonate (M_w = 30,900) in dichloromethane at 25°C with the emission monochromator set to 360 nm. The band at 307 nm is due to dimer complex emission.

monochromator was set to 360 nm to decrease the dimer complex fluorescence intensity and the spectra show the fluorescence emission due to the formation of dimer complexes at 307 nm and baseline at 339 nm. Figure 55 shows the uncorrected dimer complex fluorescence for poly(bisphenol A) carbonate (M_w = 30,900) in dichloromethane at 25°C as a function of concentration. As with previous results, the uncorrected dimer complex fluorescence increases with concentration with no significant change above the Mark-Houwink calculated c* value of 15.9 g/L.

The corrected dimer complex fluorescence for poly(bisphenol A) carbonate (M_w = 30,900) in dichloromethane at 25°C vs. concentration is shown in Figure 56. This plot shows the characteristic shape of the previous results with c* apparent between 20 and 25 g/L.

Figure 57 shows the fluorescence excitation spectra for several concentrations of poly(bisphenol A) carbonate (Mw = 36,600) in dichloromethane at 25°C with the emission monochromator set to 360 nm. The spectra are similar to the lower molecular weight samples of polycarbonate previously discussed with the dimer complex band located at 307 nm and baseline at 339 nm. The dimer complex intensity and scattering intensity increase with concentration.

Figure 58 shows a plot of the uncorrected dimer complex intensity as a function of concentration for poly(bisphenol A) carbonate (M_w = 36,600) in dichloromethane at 25°C. The intensity of the uncorrected dimer complex intensity increases with concentration with little change as the concentration increases above the Mark-Houwink calculated c* value of 14 g/L.

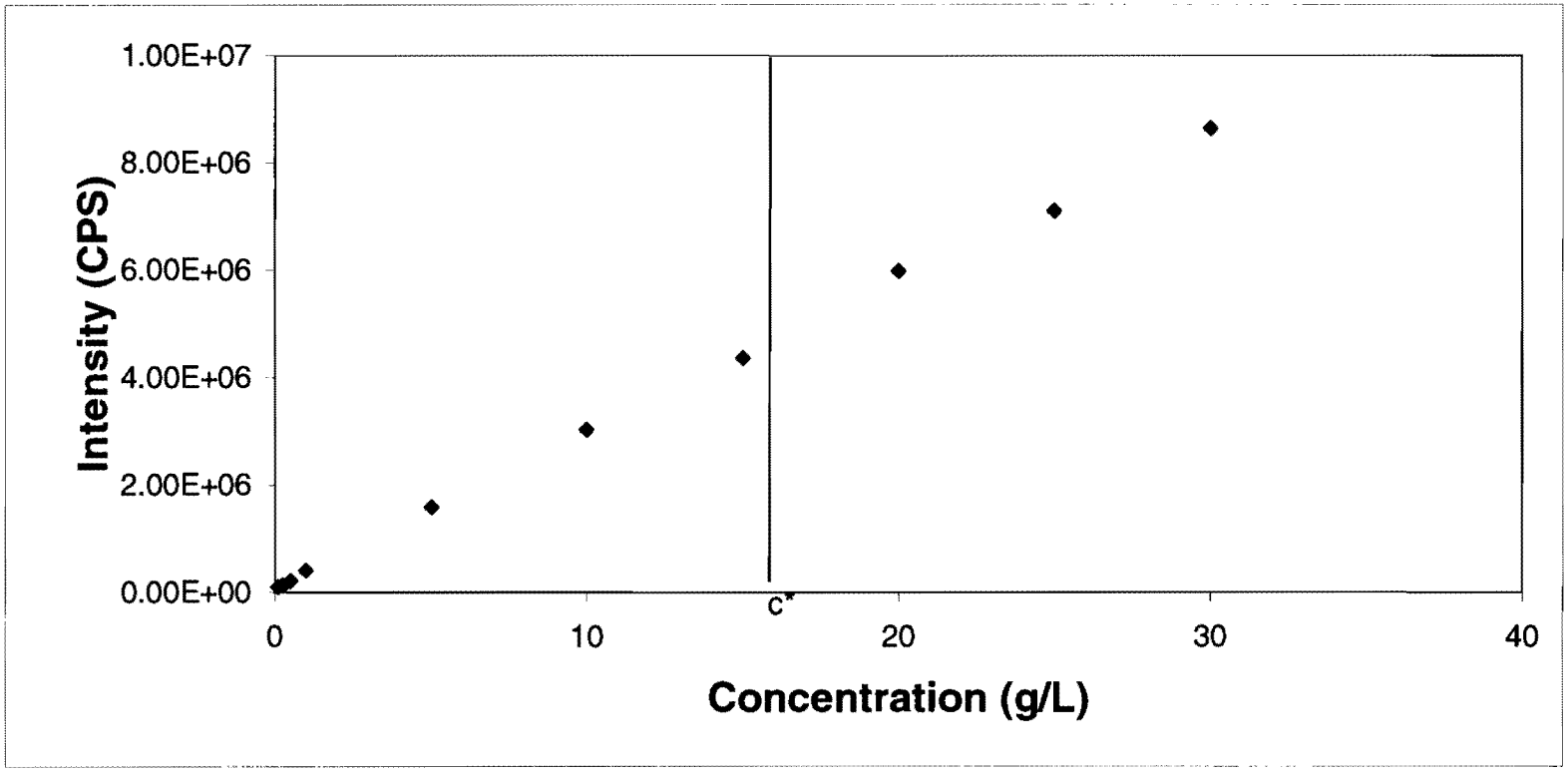

Figure 55. A plot of the uncorrected dimer complex intensity (I_{307}) vs. concentration for poly (bisphenol A) carbonate (M_w = 30,900) in dichloromethane at 25°C. The uncorrected dimer complex intensity increases with concentration but shows no change above the Mark-Houwink calculated c* value of 15.9 g/L. Measurement error is ± 1E+4 CPS.

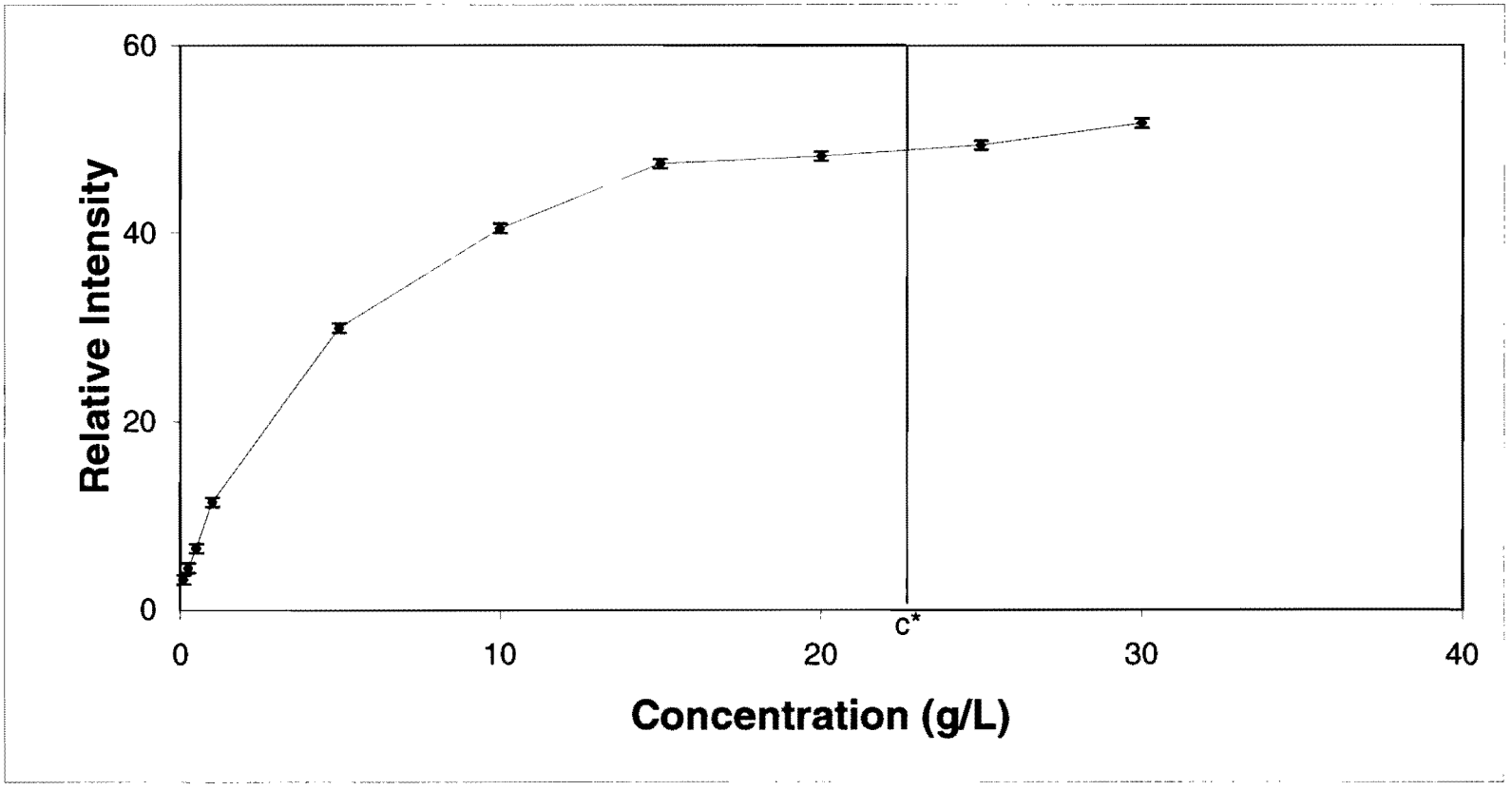

Figure 56. A plot of the corrected dimer complex intensity vs. concentration for poly (bisphenol A) carbonate (M_w = 30,900) in dichloromethane at 25°. The increase in corrected dimer complex intensity above 20 g/L is attributed to the transition between dilute and semi-dilute concentrations. Lines connecting points are for ease of interpretation only.

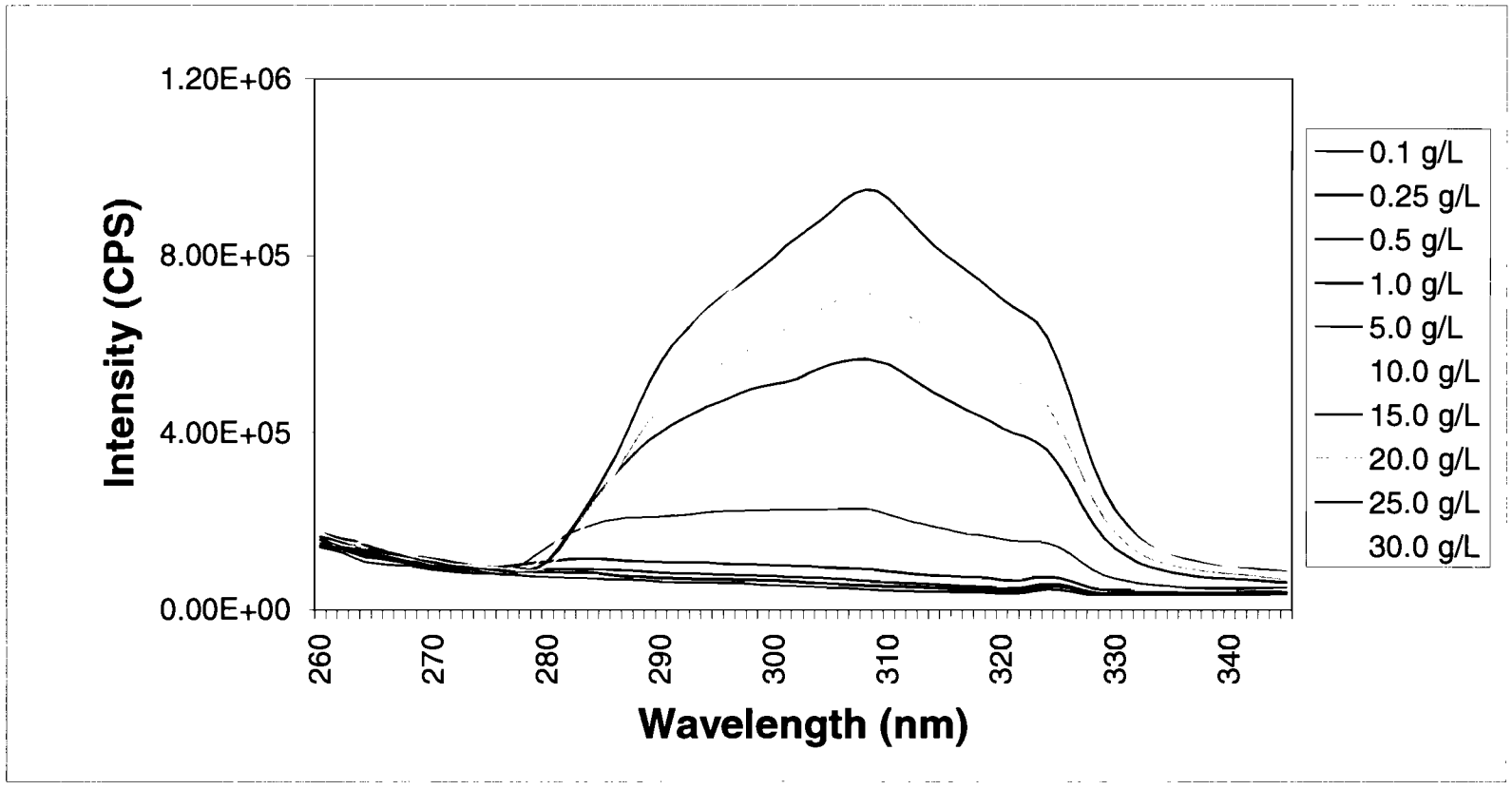

Figure 57. Fluorescence excitation spectra for several concentrations of poly (bisphenol A) carbonate (M_w = 36,600) in dichloromethane at 25°C with the emission monochromator set to 360 nm. The band at 307 nm is due to dimer complex excitation.

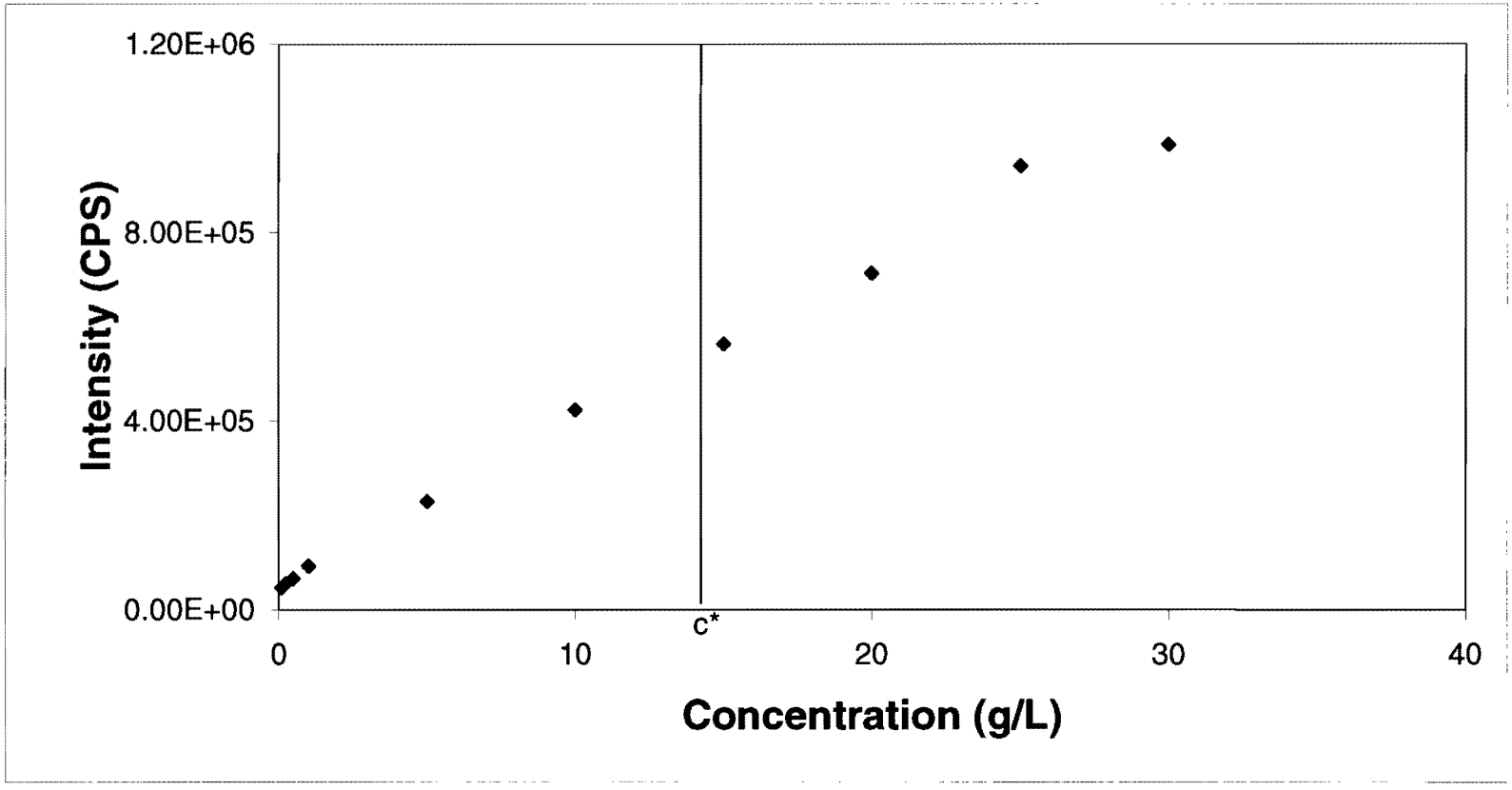

Figure 58. A plot of the uncorrected dimer complex intensity (I_{307}) vs. concentration for poly (bisphenol A) carbonate (M_w = 36,600) in dichloromethane at 25°C. The uncorrected dimer complex intensity increases with concentration but shows no change above the Mark-Houwink calculated c* value of 14 g/L. Measurement error is ± 1E+4 CPS.

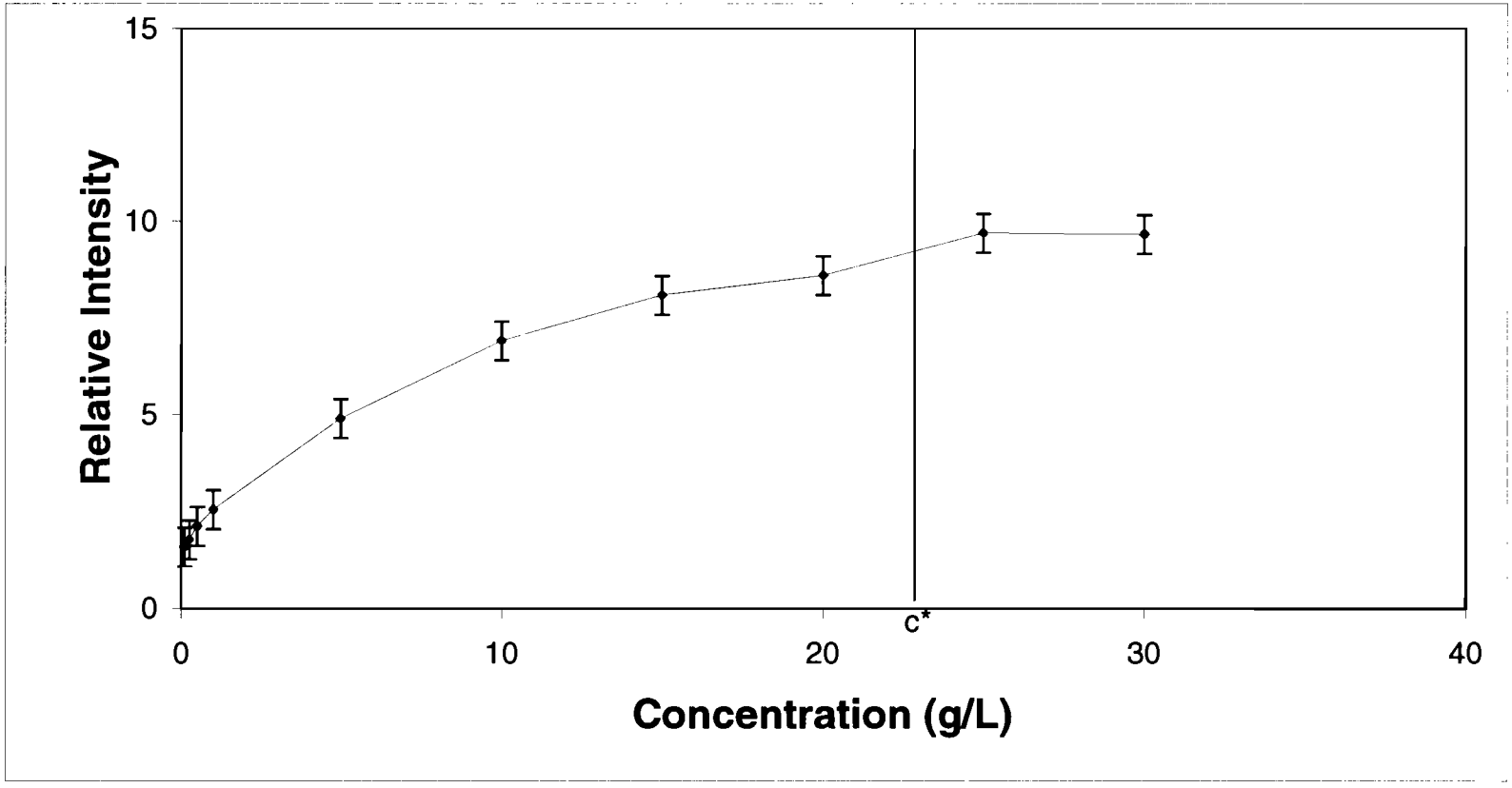

Figure 59. A plot of the corrected dimer complex intensity vs. concentration for poly (bisphenol A) carbonate (M_w = 36,600) in dichloromethane at 25°. The increase in corrected dimer complex intensity above 20 g/L is attributed to the transition between dilute and semi-dilute concentrations. Lines connecting points are for ease of interpretation only.

A plot of the corrected dimer complex intensity for poly(bisphenol A) carbonate (M_w = 36,600) in dichloromethane at 25°C is shown in Figure 59. This plot shows the characteristic shape of the previous corrected dimer complex vs. concentration plots. The increase in corrected intensity between 20 and 25 g/L is attributed to the increased intra and intermolecular interactions due to crossing from dilute to semi-dilute concentrations, also known as c*.

D. Light Scattering

To corroborate the fluorescence derived c* values, light scattering experiments were also performed. Light scattering is an accepted method for determining c*. When light scattering data is plotted as a Zimm or Debye plot, information such as the z-average radius of gyration and weight average molecular weight can be obtained. The radius of gyration is inversely related to c* because as the radius of gyration increases, there is more crowding within the solution at a given concentration and therefore c* occurs at a lower concentration. The radius of gyration can be used to calculate c* using Equation 1.7.

The light scattering data was collected for each molecular weight at several dilute concentrations at the specified temperature. The data were then analyzed using the best fitting model (Debye or Zimm plot) to obtain the radius of gyration. When fitting the data to a model, it was necessary to eliminate data

that deviated excessively from the model. These deviations can be caused by several factors such as imperfections in the scintillation vials or foreign particulates in the sample.

Light scattering studies were first performed on the polystyrene in decalin samples. Figure 60 shows the Zimm plot for five concentrations ranging from 0.1 to 1 g/L of polystyrene (M_w = 223,200 D) in decalin at 20°C. Detectors that were not used in this plot are the low angle detectors at 23°, 28°, and 32° due to excessive noise in the signal. This plot was fit with first-degree angle fit and zero-degree concentration fit. The z-average radius of gyration was calculated as 15.0 ± 1.5 nm which yields a c* value of 28.0 ± 8.0 g/L that is comparable to the Mark-Houwink c* value of 27.5 g/L.

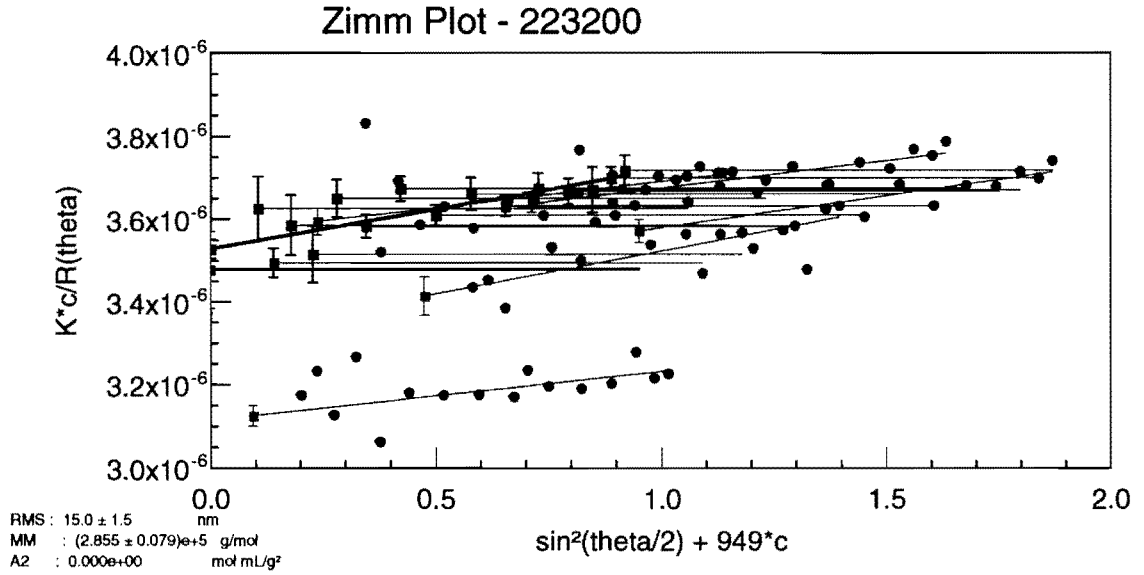

Figure 60. Zimm plot for polystyrene (M_w = 223,300) in decalin at 20°C.

Figure 61 shows the Zimm plot for four concentrations ranging from 0.25 to 1 g/L of polystyrene (M_w = 560,900 D) in decalin at 20°C. Detectors that were not used in this plot are the low angle detectors at 23°, 28°, and 32° due to excessive noise in the signal. This plot was fit with first-degree angle fit and zero-degree concentration fit. The z-average radius of gyration was calculated as 22.4 ± 3.1 nm which yields a c* value of 22.0 ± 9.0 g/L that is comparable to the Mark-Houwink c* value of 17.3 g/L.

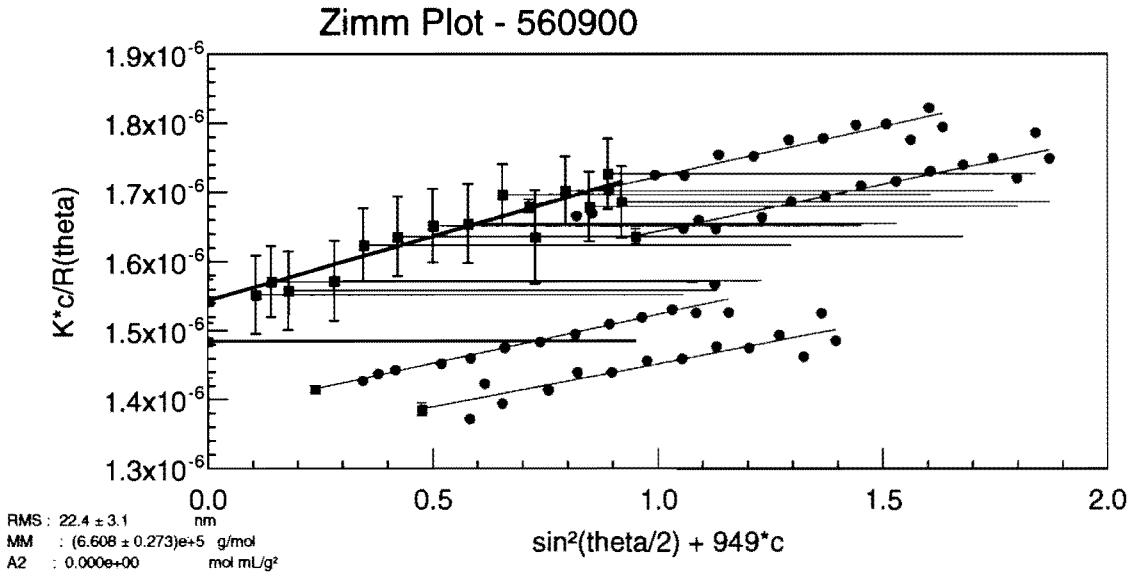

Figure 61. Zimm plot for polystyrene (M_w = 560,900 D) in decalin at 20°C.

Figure 62 shows the Zimm plot for four concentrations ranging from 0.25 g/L to 1 g/L of polystyrene (M_w = 1,015,000 D) in decalin at 20°C. Detectors that were not used in this plot are the low angle detectors at 23° and 28° as well as

38° and 44° due to excessive noise in the signal. This plot was fit with first-degree angle fit and first-degree concentration fit. The z-average radius of gyration was calculated as 30.8 ± 0.8 nm which yields a c* value of 13.8 ± 1.0 g/L that is comparable to the Mark-Houwink c* value of 12.9 g/L .

Figure 63 shows the Zimm plot for four concentrations ranging from 0.25 g/L to 1 g/L of polystyrene (M_w = 1,571,000 D) in decalin at 20°C. Detectors that were not used in this plot are the low angle detectors 23° and 28° due to excessive noise in the signal. This plot was fit with first-degree angle fit and zero-degree concentration fit. The z-average radius of gyration was calculated as 36.3 ± 1.2 nm which yields a c* value of 13.1 ± 1.3 g/L that is slightly higher than the Mark-Houwink c* value of 10.4 g/L.

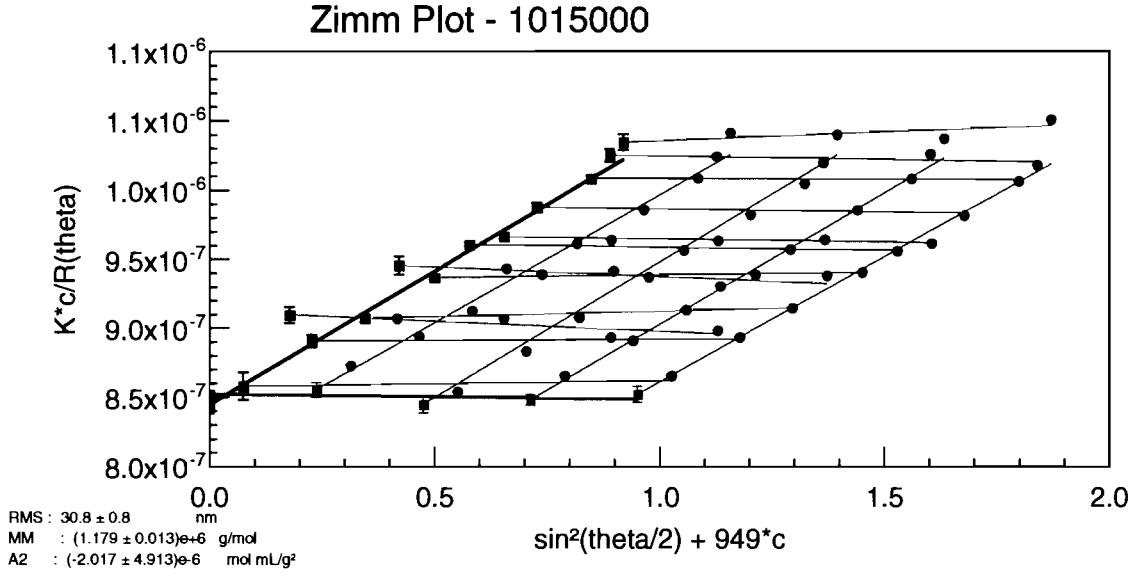

Figure 62. Zimm plot for polystyrene (M_w = 1,015,000 D) in decalin at 20°C.

Figure 64 shows the Zimm plot for four concentrations ranging from 0.25 g/L to 1 g/L of polystyrene (M_w = 223,200 D) in decalin at 30°C. Detectors that were not used in this plot are the low angle detectors at 23°, 28°, 32°, and 38° due to excessive noise in the signal. This plot was fit with first-degree angle fit and zero-degree concentration fit. The z-average radius of gyration was calculated as 15.4 ± 1.1 nm which yields a c* value of 25.0 ± 5.0 g/L. As mentioned earlier, Mark-Houwink c* values are not available for polystyrene in decalin at 30°C.

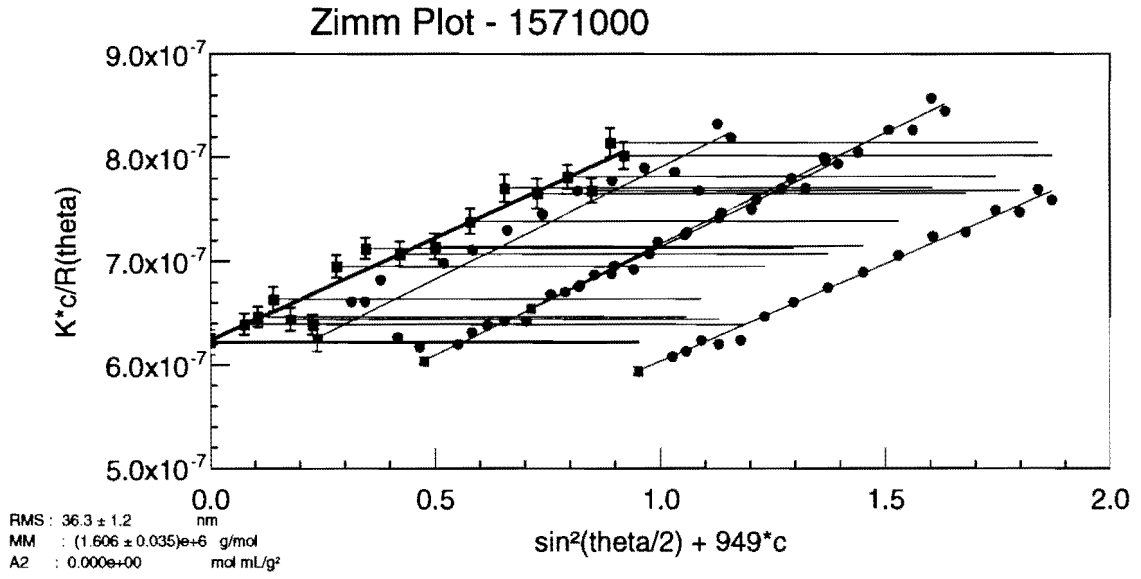

Figure 63. Zimm plot for polystyrene (M_w = 1,571,000 D) in decalin at 20°C.

Figure 65 shows the Zimm plot for four concentrations ranging from 0.25 g/L to 1 g/L of polystyrene (M_w = 560,900 D) in decalin at 30°C. Detectors that

were not used in this plot are the low angle detectors at 23° and 28° due to excessive noise in the signal. This plot was fit with first-degree angle fit and zero-degree concentration fit. The z-average radius of gyration was calculated as 27.2 ± 2.9 nm which yields a c* value of 11.3 ± 3.2 g/L.

Figure 66 shows the Zimm plot for four concentrations ranging from 0.25 g/L to 1 g/L of polystyrene (M_w = 1,015,000 D) in decalin at 30°C. Detectors that were not used in this plot are the low angle detectors at 23° and 28° as well as 147° due to excessive noise in the signal. This plot was fit with first-degree angle fit and zero-degree concentration fit. The z-average radius of gyration was calculated as 32.2 ± 0.5 nm which yields a c* value of 12.0 ± 0.5 g/L.

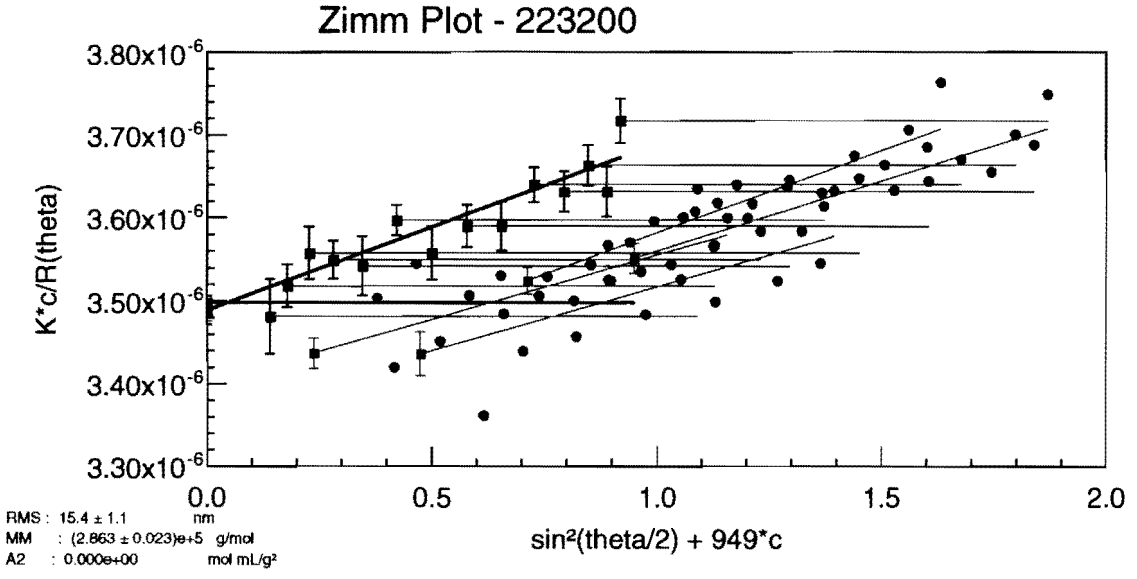

Figure 64. Zimm plot for polystyrene (M_w = 223,200 D) in decalin at 30°C.

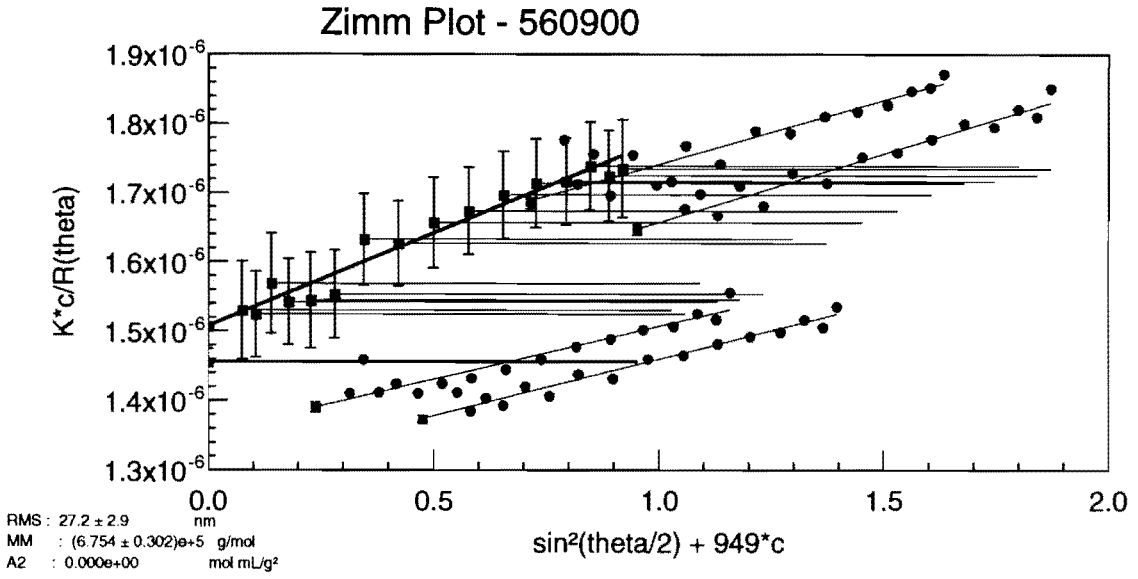

Figure 65. Zimm plot for polystyrene (M_w = 560,900 D) in decalin at 30°C.

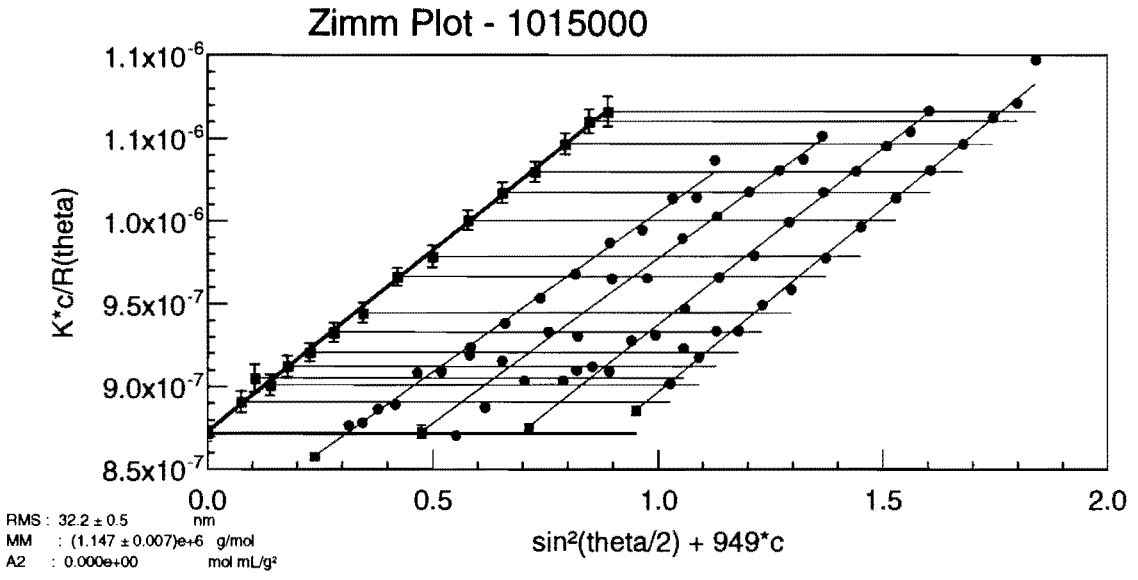

Figure 66. Zimm plot for polystyrene (M_w = 1,015,000 D) in decalin at 30°C.

Figure 67 shows the Zimm plot for four concentrations ranging from 0.25 g/L to 1 g/L of polystyrene (M_w = 1,571,000 D) in decalin at 30°C. Detectors that were not used in this plot are the low angle detectors at 23° and 28° due to excessive noise in the signal. This plot was fit with first-degree angle fit and zero-degree concentration fit. The z-average radius of gyration was calculated as 40.3 ± 0.7 nm which yields a c* value of 9.5 ± 0.5 g/L.

Table 3.1 shows a comparison of Mark-Houwink and light scattering c* values for polystyrene in decalin at 20°C and 30°C. Light scattering c* values at 20°C show good agreement with the Mark-Houwink c* values and light scattering c* values at 30°C show the expected lower values than corresponding c* values at 20°C.

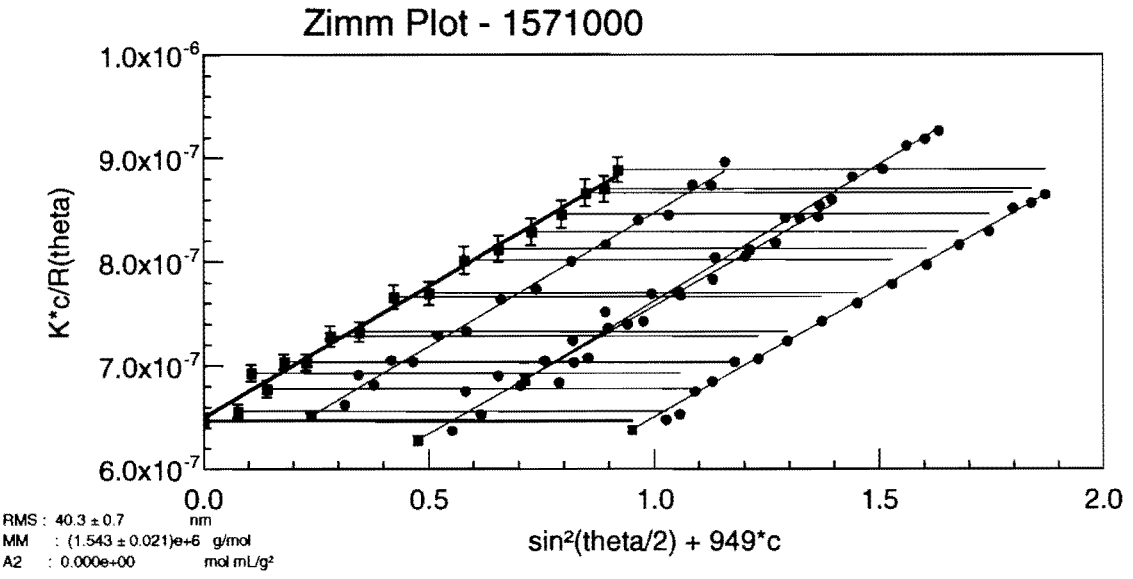

Figure 67. Zimm plot for polystyrene (M_w = 1,571,000 D) in decalin at 30°C.

Table 3.1. Light Scattering Critical Concentration (c*) Values for Polystyrene in Decalin at 20°C and 30°C.

PS MW	c* (g/L) Mark-Houwink (18°C)[a]	c* (g/L) Light Scattering (20°C)[b]	c* (g/L) Light Scattering (30°C)[b]
223,200 D	27.5	28 ± 8	25 ± 5
560,900 D	17.3	22 ± 9	11 ± 3
1,015,000 D	12.9	14 ± 1	12.0 ± 0.5
1,571,000 D	10.4	13 ± 1	9.5 ± 0.5

a. Calculated using equation 4.1 and data from reference.[44]

b. Calculated from R_g derived from light scattering data using equation 1.7.

The poly(bisphenol A) carbonate in dichloromethane at 25°C samples were analyzed using light scattering. This data fit best using a Debye model fit to a Zimm plot. Due to the large polydispersity of these samples, the data was noisy which caused excessive error in the radius of gyration calculations and was more difficult to fit to a Zimm plot than the narrow molecular weight polystyrene samples.

Figure 68 shows a Debye fit to a Zimm plot for two concentrations (0.5 and 1 g/L) of poly(bisphenol A) carbonate (M_w = 24,400) in dichloromethane at 25°C. Detectors that were not used in this plot are the low angle detectors at 23°

and 28° due to excessive noise in the signal. This plot was fit with first-degree angle fit and zero-angle concentration fit. The z-average radius of gyration was calculated as 16.2 ± 10.1 nm which yields a c* value of 20.6 ± 20.0 g/L that is comparable to the Mark-Houwink c* value of 19.0 g/L.

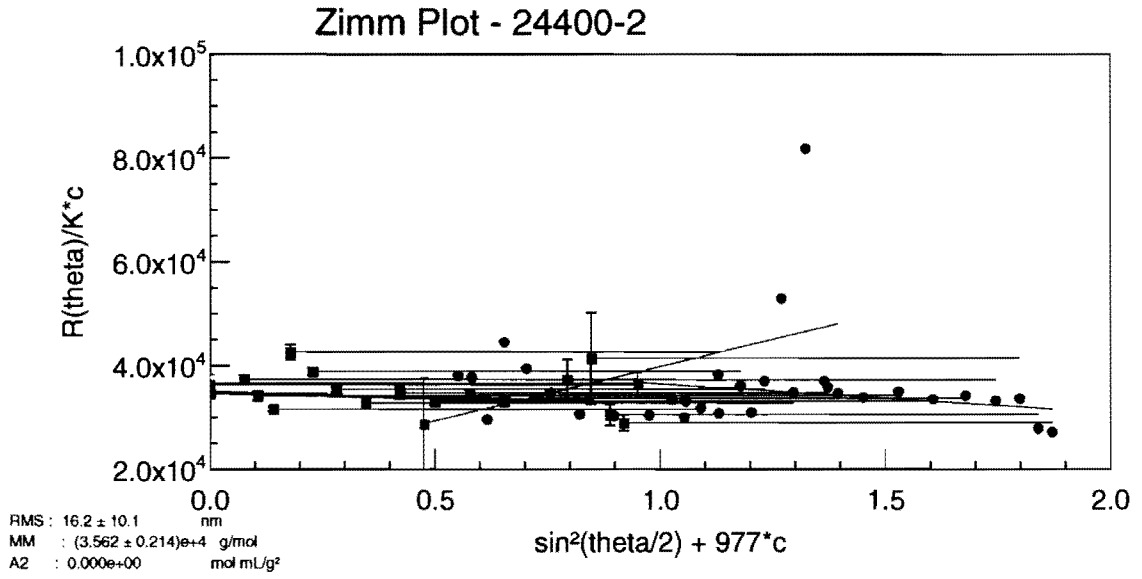

Figure 68. Zimm plot for poly(bisphenol A) carbonate (M_w = 24,400) in dichloromethane at 25°C.

Figure 69 shows a Debye fit to a Zimm plot for two concentrations (0.25 and 0.5 g/L) of poly(bisphenol A) carbonate (M_w = 30,900) in dichloromethane at 25°C. Detectors that were not used in this plot are the detectors at 23°, 28°, 32°, 38°, 44°, and 50° due to excessive noise in the signal. This plot was fit with first-degree angle fit and zero-degree concentration fit. The z-average radius of

gyration was calculated as 11.7 ± 3.7 nm which yields a c* value of 13.7 ± 10.3 g/L which is comparable to the Mark-Houwink c* value of 15.9 g/L.

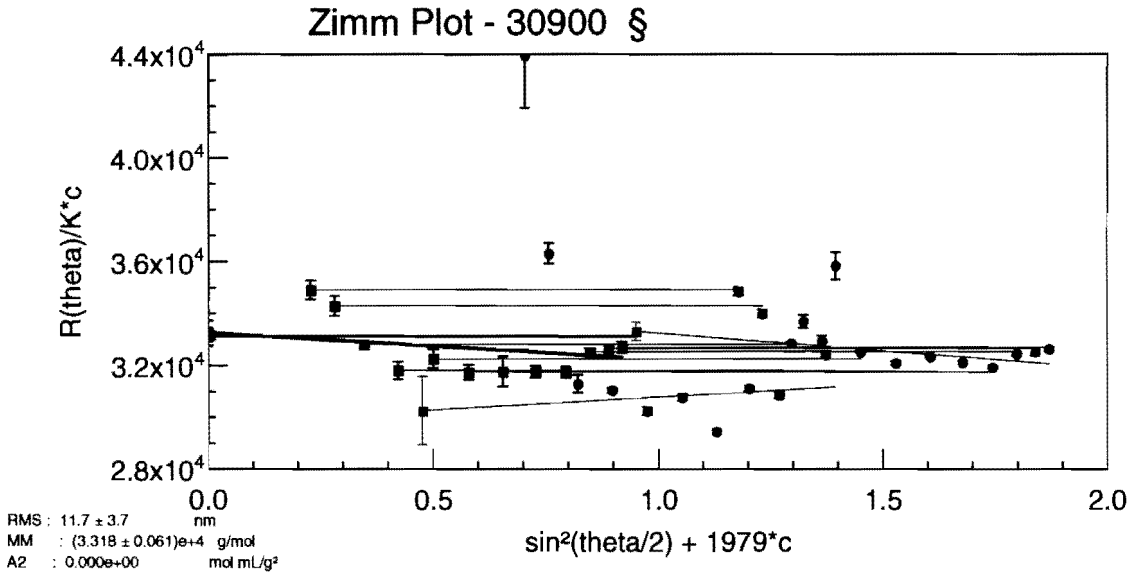

Figure 69. Zimm plot for poly(bisphenol A) carbonate (M_w = 30,900) in dichloromethane at 25°C.

Figure 70 shows a Debye fit to a Zimm plot for three concentrations (0.25, 0.5, and 1 g/L) of poly(bisphenol A) carbonate (M_w = 36,600) in dichloromethane at 25°C. Detectors that were not used in this plot are the detectors at 23°, 28°, 32°, 38°, 44°, 50°, 57°, 64°, 72°, and 147° due to excessive noise in the signal. This plot was fit with first-degree angle fit and zero-degree concentration fit. The z-average radius of gyration was calculated as 10.8 ± 3.7 nm which yields a c* value of 22.7 ± 17.9 g/L which is comparable to the Mark-Houwink c* value of 14.0 g/L.

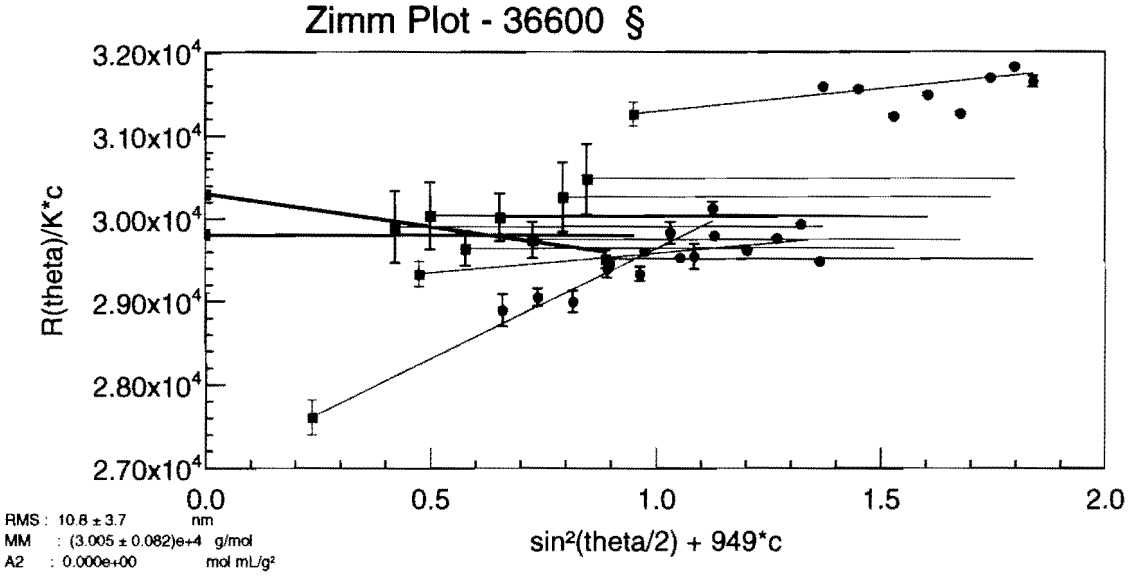

Figure 70. Zimm plot for poly(bisphenol A) carbonate (M_w = 36,600) in dichloromethane at 25°C.

Table 3.2 shows a comparison of Mark-Houwink and light scattering c* values for poly(bisphenol A) carbonate at 25°C. Although the Mark-Houwink c* values show decreasing c* values with increasing molecular weight, the c* values derived from light scattering do not change within experimental error. This is a consequence of the small range of molecular weights available for poly(bisphenol A) carbonate , thereby giving small changes in c* values. The large error of the light scattering c* values is attributed to the large polydispersity of the polycarbonate samples.

Table 3.2. Light Scattering Critical Concentration (c*) Values for Poly(bisphenol A) Carbonate in Dichloromethane at 25°C.

MW	c* (g/L) Mark-Houwink (25°C)[a]	c* (g/L) Light Scattering (25°C)[b]
24,400	19.0	21 ± 20
30,900	15.9	14 ± 10
36,600	14.0	23 ± 18

a. Calculated using equation 4.1 and data from reference.[44]

b. Calculated from R_g derived from light scattering data using equation 1.7.

Chapter 4

Discussion Section

The study of polymer solutions, including the critical concentration, has been of interest for many years. The critical concentration is interesting because it is the concentration when a physical change begins to occur to the polymers chains. c* is the concentration where polymer chains are forced into contact with each other and hence polymer-polymer interactions begin to occur. As the concentration is increased above the critical concentration, the polymer chains can no longer behave as solid spheres and must either intertwine with its neighbors or the radius of gyration must decrease. Knowledge of the critical concentration also allows calculation of the radius of gyration using equation 1.7. However, the accepted methods for determining c* use equipment which is not common to most laboratories and require difficult and time-consuming sample preparation. Therefore, a method that uses more common laboratory equipment with easier sample preparation would allow more research groups to have the ability to determine c* and R_g.

In order to determine c* from fluorescence data, the polymer of interest must contain fluorophores. Polystyrene, the first polymer evaluated using this method, was chosen because it contains fluorophores (the phenyl side chains), has been extensively studied by numerous methods (including fluorescence), and can be made with a narrow molecular weight distribution. As discussed in

the introduction, polystyrene is known to form intermolecular excimers at high concentrations due to interactions between neighboring benzene rings when the rings are in close proximity.[25-31] Fluorescence excitation spectroscopy was performed on four molecular weights of polystyrene ranging from approximately 200,000 to 1,500,000 at both 20°C and 30°C in decalin. These results were then compared to a c* value calculated using the Mark-Houwink equation and also a c* value derived from light scattering. The results of this study will prove the validity of the fluorescence method for determining c* of polystyrene.

It would also be beneficial to extend the usefulness of this method of determining c* for polymers other than polystyrene. In contrast to polystyrene which has the chromophores pendant to the polymer backbone, poly(bisphenol A) carbonate has the chromophores as part of the polymer backbone. It is expected that this configuration will prove more difficult in allowing the benzene rings to become close enough to interact and form excimers. Fluorescence excitation spectroscopy was performed on three molecular weights of poly(bisphenol A) carbonate in dichloromethane ranging from approximately 24,000 to 37,000 at 25°C. These results were then compared to a c* value calculated using the Mark-Houwink equation and also c* value derived from light scattering. Therefore, these results will prove the validity of this method for determining c* of poly(bisphenol A) carbonate, and suggest the wider applicability for this method.

Before performing fluorescence work, it was necessary to have an estimate of c* to allow measurements to be conducted in the correct

concentration range. One method of generating c* for a polymer/solvent system is to determine the intrinsic viscosity [η], the inverse of which is theoretically equivalent to c*.[44] The intrinsic viscosity can also be calculated using the Mark-Houwink equation:

$$c^* = \frac{1}{KM^a} = \frac{1}{[\eta]} \qquad (4.1)$$

were M is the weight-average molecular weight of the polymer and K and a are constants specific to a given polymer-solvent system. ($K=77 \times 10^{-3}$ mL/g and a=0.50 for polystyrene in decalin at 18°C and $K=29.9 \times 10^{-3}$ mL/g and a=0.74 for poly(bisphenol A) carbonate in dichloromethane at 25°C).[44] This method of calculating c* is known to typically underestimate the actual value.[28] The constants for the Mark-Houwink equation were found in literature and were originally determined using viscometry measurements at several concentrations.[44] These relative viscosity measurements were then plotted vs. concentration and the line extrapolated to infinite dilution yielding the intrinsic viscosity. The equation of this line was used to determine K and a for each polymer/solvent system.[44]

To minimize self-absorbance by the polymer, all fluorescence readings were taken from the front-face of the cell. As noted in previously published papers,[26-29] dilute concentrations of polystyrene exhibited a monomer band at 283 nm that was replaced at higher concentrations by an excimer band at 332 nm. Scheme 3 shows the pathways available for the formation of excimers.

Because excimers can form as the result of excited state interactions as well as ground state dimer interactions, studying excimer interactions will not necessarily provide the information required to accurately determine c*. However, by performing fluorescence excitation spectroscopy while observing the fluorescence of the excimer band, the resulting spectra reveal a band that appears at high concentrations. This band is attributed to a ground state dimer that is excited directly to become an excimer. These ground state dimers will be referred to as dimer complexes. When the concentration approaches c*, the polymers (and hence the chromophores) are forced close enough to interact with each other in the ground state and will show excimer fluorescence due to dimer complex formation. Therefore, fluorescence excitation spectroscopy should allow determination of c* by studying the intensity of the dimer complex band as a function of concentration.

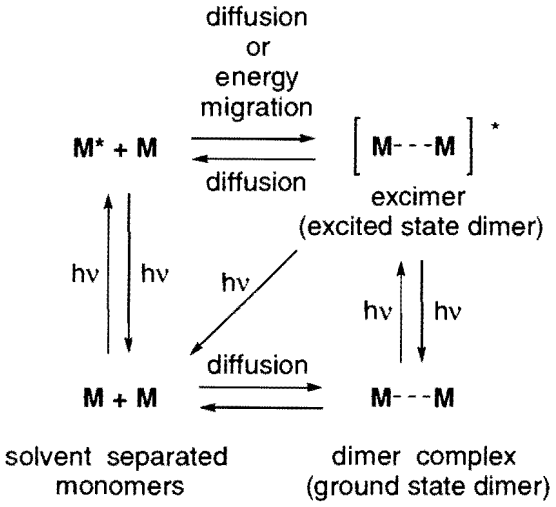

Scheme 3. Pathways for the formation and emission of excimers.

To establish the validity of determining c* using fluorescence excitation spectroscopy, the fluorescence derived c* values must be directly compared against an accepted method of determining c*. The results of the fluorescence derived c* values presented in this dissertation were compared against two accepted methods of determining c*. The first accepted method which was used to determine c* was to use the Mark-Houwink equation (equation 4.1) to calculate the intrinsic viscosity, the inverse of which is c*.[44] However, this method tends to under-estimate the true value of c*[28] and the variables are not available for all polymer/solvent systems at all temperatures. The second accepted method of determining c* which was used for comparison in this paper was laser light scattering.[13] Polymer solutions were placed in scintillation vials and the scattering observed at several angles. When light scattering data for several concentrations has been obtained, the data can be plotted using a Zimm or Debye plot to give information about the polymer/solvent system such as the z-average radius of gyration of the polymer.[13] The radius of gyration is inversely related to c* and can be used to calculate c* using equation 1.7.[19]

Several concentrations of two polymer/solvent systems, each at a variety of molecular weights, were evaluated using fluorescence excitation spectroscopy and multi-angle laser light scattering. Polystyrene was chosen because it is an extensively studied polymer and also contains chromophores which are pendant to the polymer backbone. Polystyrene was studied in decalin and was evaluated

at both 20°C and 30°C to prove the versatility of this method at different temperatures and to show the effects of temperature on c*.

A second polymer/solvent system, poly(bisphenol A) carbonate in dichloromethane, was also evaluated at 25°C to prove the versatility of this method for a polymer system with the chromophores as part of the polymer backbone. It was anticipated that having the chromophores as part of the backbone of the polymer should hinder interactions between neighboring rings more than for a polymer with pendant chromophores such as polystyrene which have a larger degree of flexibility. Therefore, if c* can be determined for polycarbonate using fluorescence excitation spectroscopy, this technique should work for most polymer systems that contain chromophores.

Table 4.1 shows the comparison of c* values for four different molecular weight polystyrene samples in decalin at 20°C. Unfortunately, the variables for the Mark-Houwink equation for polystyrene in decalin are only available at 18°C, not at the 20°C testing conditions. Therefore, these calculated c* values are expected to be lower than what is anticipated at the 20°C testing conditions (due to less swelling of the polymer at lower temperatures) in addition to the typical under-estimation associated with this calculation. These results show the c* values derived from fluorescence are comparable to the c* values calculated using equation 4.1, with some of the calculated c* values slightly lower as expected. The fluorescence derived c* values also correlate well with the light scattering derived c* values. It should be noted that if the fluorescence experiments were conducted with more concentrations around c*, the error in the

c* values could be reduced even further due to less spacing between corrected dimer complex fluorescence values thereby giving a more accurate c* value. These further experiments were not completed due to limited polymer availability and time constraints. These results show fluorescence excitation spectroscopy can be used to determine c* for polystyrene in decalin at 20°C. The results are equivalent to two accepted methods of determining c*, calculated c* values using the Mark-Houwink equation and also laser light scattering derived c* values.

Table 4.I. Critical Concentration (c*) Values for Polystyrene in Decalin at 20°C.

PS MW	c* (g/L) Calculated (18°C)[a]	c* (g/L) Fluorescence[b]	c* (g/L) Light Scattering[c]
223,200 D	27.5	33 ± 3	28 ± 8
560,900 D	17.3	18 ± 3	22 ± 9
1,015,000 D	12.9	12.5 ± 0.5	14 ± 1
1,571,000 D	10.4	14 ± 2	13 ± 1

a) Calculated using equation 4.1 and data from reference.[44]

b) Calculated from fluorescence excitation spectra as described in the text.

c) Calculated from R_g derived from light scattering data using equation 1.7.

Increasing the temperature of the system causes the polymer chains to expand which, theoretically, causes c* to occur at a lower concentration. c* values for four different molecular weights polystyrene samples in decalin at 30°C using fluorescence and light scattering are shown in Table 4.2. No Mark-Houwink calculated c* values are listed in this table because the variables are not available for polystyrene in decalin at 30°C. However, it was anticipated the corresponding c* values would be lower at 30°C than at 20°C. The fluorescence c* values show good agreement with the light scattering c* values and these results are lower than the corresponding 20°C results. Again, it is possible to reduce the error in the fluorescence derived c* value by conducting experiments on more concentrations around c*. These results show fluorescence excitation spectroscopy can be used to determine c* for polystyrene in decalin at 30°C with results that are equivalent to the light scattering derived c* values.

To extend the versatility of this method of determining c* to polymers other than polystyrene, poly(bisphenol A) carbonate was evaluated. Table 4.3 contains fluorescence derived c* values along with a calculated c* value and light scattering c* values for three different molecular weight poly(bisphenol A) carbonate samples in dichloromethane. The Mark-Houwink calculated c* value using equation 4.1 shows decreasing c* values with increasing molecular weight, as expected, because the radius of gyration increases with increasing molecular weight. However, the fluorescence derived c* values did not change within experimental error with increasing molecular weight

Table 4.2. Critical Concentration (c*) Values for Polystyrene in Decalin at 30°C.

PS MW	c* (g/L) Fluorescence[a]	C* (g/L) Light Scattering[b]
223,200 D	23 ± 3	25 ± 5
560,900 D	13 ± 3	11 ± 3
1,015,000 D	11 ± 1	12.0 ± 0.5
1,571,000 D	9 ± 1	9.5 ± 0.5

a) Calculated from fluorescence excitation spectra as described in the text.

b) Calculated from R_g derived from light scattering data using equation 1.7.

Several factors contribute to this phenomenon. First, only a small range of molecular weights are available for poly(bisphenol A) carbonate, which provide only small changes in c* values. Second, because poly(bisphenol A) carbonate cannot be made via an anionic polymerization (the method used to generate narrow molecular weight polystyrene), these polymers have a broader molecular weight distribution than polystyrene. This would make c* a less distinct transition and tend to increase the error. The large polydispersity of the samples probably explains the large errors in the light scattering c* values as well. Even though these results do not show as much precision as the polystyrene results do, the polycarbonate results show that this type of polymer does form dimer complexes

and excitation data can be used to obtain c*. However, these samples were not sufficiently differentiated for changes in c* to be readily distinguished by either fluorescence or light scattering.

Table 4.3. Critical Concentration (c*) Values for Poly(bisphenol A) Carbonate in Dichloromethane at 25°C.

MW	c* (g/L) Calculated (25°C)[a]	c* (g/L) Fluorescence[b]	c* (g/L) Light Scattering[c]
24,400	19.0	23 ± 3	21 ± 20
30,900	15.9	23 ± 3	14 ± 10
36,600	14.0	23 ± 3	23 ± 18

a) Calculated using equation 4.1 and data from reference.[44]

b) Calculated from fluorescence excitation spectra as described in the text.

c) Calculated from R_g derived from light scattering data using equation 1.7.

To prove the observations from the fluorescence excitation spectra are due to ground state dimer complex formation, both a positive control and a negative control were evaluated. For this type of experiment, the positive control is a compound known to form excimers and ground state dimer complexes without the constraints of the polymer backbone hindering the formation. Ideally, it should be a monomeric component of one of the polymers tested to support the data presented in this dissertation. The negative control is a compound that

would not allow the formation of excimers nor ground state dimer complexes. One way this can be accomplished is by keeping the chromophores far enough apart to prevent the formation of ground state dimer complexes, thereby minimizing the formation of excimers.

Ethylbenzene in decalin was chosen as the positive control because it is known to form excimers[27] and it also mimics the building blocks of polystyrene, therefore it should give results similar to polystyrene except there is no chance of intra-molecular interactions occurring. This data was treated the same as the polystyrene in decalin data. The excitation spectra for ethylbenzene is similar to the polystyrene spectra with the appearance of a dimer complex band at 291 nm at high concentrations. The plot of the corrected dimer complex intensity vs. concentration shows an analogous condition to c* occurring between 110 g/L and 130 g/L.

1,3,5 tri-t-butyl benzene was chosen as the negative control because the bulky t-butyl groups on the 1,3, and 5 positions of the ring should provide enough steric hindrance to prevent the benzene rings from getting close enough to interact and form excimers. However, the fluorescence emission spectroscopy results show that 1,3,5 tri-t-butyl benzene does form excimers at high concentrations. It appears the t-butyl groups on neighboring molecules may be able to stagger and allow the rings to get close enough to interact and form excimers. However, the analogous condition to c* as noted with ethylbenzene, does not occur under the conditions tested (up to 2M or almost 500 g/L). Therefore, while 1,3,5 tri-t-butyl benzene does form excimers at high

concentrations, the t-butyl groups are able to hinder the formation of the ground state dimer complex formation at concentrations where formation occurs for ethylbenzene.

Chapter 5

Conclusion

This dissertation has demonstrated a novel way of determining the critical concentration, c*, of aromatic polymers using excitation fluorescence spectroscopy. This method was able to successfully determine c* for several different molecular weights of a polymer with pendant aromatic chromophores (polystyrene) at 20°C and 30°C. The versatility of this method was shown by demonstrating the fundamental principles of the method on a polymer with the aromatic chromophores in the polymer backbone (poly(bisphenol A) carbonate) at 25°C. These results have been compared against two accepted methods of determining c*. The first accepted method, the Mark-Houwink equation, shows good agreement with the fluorescence derived c* values. The second accepted method, light scattering, also shows good agreement with the fluorescence derived c* values with approximately equivalent error. An additional benefit of this method is the ability to calculate the radius of gyration from c* using equation 1.7 and solving for R_g. To demonstrate the validity of these results, a positive (ethyl benzene) and a negative control (1,3,5 tri-t-butyl benzene) were evaluated. The positive control proved the ground state dimer cornplexes observed for the polymers were the result of intermolecular and not intramolecular interactions. The negative control was able to hinder the formation of these dimer complexes at concentrations where these complexes were able to form with the positive control. This shows the results are not an artifact of the instrument and are the result of the formation of ground state dimer complexes occurring. Therefore, fluorescence excitation spectroscopy allows for a quantitative determination of c*

and R_g for aromatic polymers by a method which has easier sample preparation and uses more common laboratory instrumentation than either light scattering or osmometry.

References

1. a) Sperling, L. H. *Introduction to Physical Polymer Science*, 2nd ed.; John Wiley & Sons: New York, 1992. b) Schafer, L. *Excluded Volume Effects in Polymer Solutions*; Springer: Berlin, 1999.
2. Elias, H. *An Introduction to Polymer Science;* VCH: New York, 1997.
3. Richards, E.G. *An Introduction to Physical Properties of Large Molecules in Solvent*, Cambridge University Press: New York, 1980.
4. de Gennes, P.G. *Scaling Concepts in Polymer Physics;* Cornell University Press: Ithaca, New York, 1979.
5. Schüler, C.; Caruso, F. *Biomacromolecules* **2001,** *2*, 921-926.
6. Wyatt, P. J. *Anal. Chim. Acta* **1993,** *272*, 1-40.
7. Zirnm, B. H. *J. Chem. Phys.* **1948**, *16*, 1093.
8. Zimm, B. H. *J. Chem. Phys.* **1948**, *16*, 1099.
9. Debye, P. *J. Phys. Coll. Chem.* **1947**, *51*, 18.
10. Nagasawa, M.; Takahaski, A. *Light Scattering from Polymer Solutions*; Huglin, M. B., Ed.; Academic Press: London, 1972.
11. Flory, P. J. *Principles of Polymer Chemistry*; Cornell University Press: New York, 1953.
12. Privalko, V. P.; Lipatov, Y. S. *Makromol. Chem.* **1972**, *175*, 641.
13. *Light Scattering Principles and Development*; Brown, W., Ed.; Oxford University Press: New York, 1996.
14. Flory, P. J. *Faraday Discuss. Chem. Soc.* **1979**, *68*, 14.

15. Gedde, U.W. *Polymer Physics;* Chapman and Hall: London, 1995.

16. Daoud, M.; Jannink, G. *J. Phys. (Paris)* **1976**, *37*, 973.

17. Grosberg, A. Y.; Khokhlov, A. R. *Giant Molecules*; Academic Press: San Diego, 1997.

18. Strobl, G. *The Physics of Polymers 2nd Ed.; Springer:* Berlin, 1997.

19. Noda, I.; Kato, N.; Kitano, T.; Nagasawa, M. *Macromolecules* **1981**, *14*, 668.

20. a) Barltrop, J.A.; Coyle, J.D. *Principles of Photochemistry;* Wiley: New York, 1978. b) Guillet, J. *Polymer Photophysics and Photochemistry;* Cambridge University Press: Cambridge, 1985. c) Phillips, D. ed. *Polymer Photophysics;* Chapman and Hall: New York, 1985.

21. Parker, C. A.; Joyce, T. A. *Chem. Commun.* **1968**, 749.

22. Lakowicz, J. R. *Principles of Fluorescence Spectroscopy*; Plenum Press: New York, 1986.

23. Eisinger, J.; Flores, J. *Anal. Biochem.* **1979**, *94*, 15.

24. Forster, T.; Kasper, K. *Z. Phys. Chem. (N.F.)* **1954**, *1*, 275.

25. Basile, L. J. *J. Chem. Phys.* **1962**, *36*, 2204.

26. Vala, M. T.; Haebig, J.; Rice, S. A. *J. Chem. Phys.* **1965**, *43*, 886.

27. Hirayama, F. *J. Chem. Phys.* **1965**, *42*, 3163.

28. Torkelson, J. M.; Lipsky, S.; Tirrell, M.; Tirrell, D. A. *Macromolecules* **1981**, *14*, 1601.

29. Frank, C. W.; Harrah, L. A. *J. Chem. Phys.* **1974**, *61*, 1526.

30. Kloppfer, W. *Chem. Phys. Lett.* **1969**, *4*, 193.

31. Chandross, E. A.; Dempster, C. J. *J. Am. Chem. Soc.* **1970**, *92*, 3586.

32. Wolff, C. *Eur. Polym. J.* **1977**, *13*, 739.

33. Phillips, D. *Polymer Photophysics*; Chapman and Hall: London, 1985.

34. Lindsell, W. E.; Robertson, F. C.; Soutar, I. *Eur. Polym. J.* **1981**, *17*, 203.

35. Nishihara, T.; Kaneko, M. *Makromol. Chem.* **1969**, *124*, 84.

36. Roots, J.; Nystrom, B. *Eur. Polym. J.* **1979**, *15*, 1127.

37. Torkelson, J. M.; Lipsky, S.; Tirrell, M.; Tirrell, D. A. *Macromolecules* **1983**, *16*, 326.

38. Roots, J.; Nystrom, B. *Poly. Comm.* **1984**, *25*, 166.

39. Nicolai, T.; Brown, W. *Macromolecules* **1990**, *23*, 3150.

40. Lee, C.; Waddell, W. H.; Casassa, E., F. *Macromolecules* **1981**, *14*, 1021.

41. Destor, C.; Langevin, D.; Rondelez, F. *J. Polym. Sci., Polym. Lett. Ed.* **1978**, *16*, 229.

42. Yeung, A. S.; Frank, C. W. *Polymer* **1990**, *31*, 2101.

43. Pethrick, R. A. *Macromolecules* **1991**, *24*, 5141.

44. *Polymer Handbook*; Brandrup, J.; Immergut, E. H., Eds.; Wiley: New York, 1975.